

**STUDIA**  
**UNIVERSITATIS BABEŞ-BOLYAI**

**PHYSICA**

**1**

**1992**

**CLUJ-NAPOCA**

**REDACTOR ȘEF: Acad. prof. I. HAIDUC**

**REDACTORI ȘEFI ADJUNCȚI: Prof. I. MAGYARI, prof. I. MARGA, prof.  
I. A. RUS**

**COMITETUL DE REDACȚIE AL SERIEI FIZICA: Prof. E. BURZO (redactor coordonator), prof. O. COZAR, prof. E. TĂTARU, conf. A. NEDA, conf. S. ȘIMON, cercet. șt. I I. ARDELEAN, cercet. șt. II S. CÔLDEA (secretar de redacție)**

# STUDIA UNIVERSITATIS BABEŞ-BOLYAI

## PHYSICA

### 1

---

Redacția 3400 CLUJ-NAPOCA str M Kogălniceanu nr 1 ▶ Telefon 116101

---

#### SUMAR - CONTENTS - SOMMAIRE

##### MAGNETISM

N REZLESCU, F REZLESCU, G PAŞNICU, M L CRAUS, P D POPA, Nickel-Zinc Ferrites with Additives and Substitutions	3
M COLDEA, Magnetic Susceptibility of $Y_{1-x}Ce_xAl_2$	13
M COLDEA, D ANDREICA, I POP, G BUD, Magnetic Properties of $Ce_{1-x}Y_xCu_2$	25
P LUCACI, I LUPŞA, Exchange Enhancement Paramagnetism in U-Co-Al Systems	33
I LUPŞA, P LUCACI, The U-Co-Ni Behaviour in the Paramagnetic Range	39
M PETEANU, L COCIU, I ARDELEAN, The Influence of the Vitreous Matrix on the $Cu^{2+}$ EPR Absorption Spectra	47

##### SUPRACONDUCTIBILITY

A STEPĂNESCU, P MAZZETTI, A MASOERO, I POP, I STIRBAT, G CONE, Magnetic Field-related Hysteretic Effects in the 1/f Noise of the $YBa_2Cu_3O_{7-x}$ Bulk Superconductors	61
I POP, I STIRBAT, G CONE, I M POPESCU, A STEPĂNESCU, The Ginzburg-Landau Theory and Superconductivity at High Temperature	69
E BURZO, V POP, Magnetic Properties of $YBa_2(Cu_{1-x}Zn_x)_3O_7$ Superconducting Materials	81
N REZLESCU, R ANGHELACHE, P POPA, C BUZEA, The Thermal Treatment Influence on Some Characteristic Parameters of the $Y_{123}$ Superconductors	93
T R REDAC, Aspects of the Substitutions for Gallium in the YBaCuO System	103



## NICKEL-ZINC FERRITES WITH ADDITIVES AND SUBSTITUTIONS

N.REZLESCU\*, E.REZLESCU\*, C.PAȘNICU\*, M.L.CRAUS\*, P.D.POPA\*

Received: 26.10.1992

**ABSTRACT.** - The present paper describes the effect of additives and substitutions on the properties of sintered Ni-Zn ferrites used in high frequency. It was found that the choice of the additive or substitution may favourably influence the magnetic and electrical properties of ferrites. It is possible to obtain a good soft magnetic material for use in high frequency by optimally choosing the substitution or additive.

**1. Introduction.** In the first part of this paper is investigated the effect of addition of CaO, Na<sub>2</sub>O, ZrO<sub>2</sub>, Li<sub>2</sub>O, K<sub>2</sub>O, Sb<sub>2</sub>O<sub>3</sub> and the combined addition of these oxides on the properties of sintered ferrite Ni<sub>0.36</sub>Zn<sub>0.64</sub>Fe<sub>2</sub>O<sub>4</sub> used in magnetic recording heads. Particularly, the effect of additives on the porosity was investigated.

In the second part, the effect of Fe substitution by Ti and/or Ge ions on the properties of Ni<sub>0.7</sub>Zn<sub>0.3</sub>Fe<sub>2</sub>O<sub>4</sub> ferrite was studied.

A special attention has been given to the improvement of the magnetic and mechanical properties of Ni-Zn ferrites. The possibility to obtain a good soft magnetic material, without hot-pressing technique, by optimally choosing the additives or the substitutions is suggested.

**2. Experimental procedure.** By a conventional method were prepared Ni-Zn polycrystalline ferrites both with additives and with substitutions. The preparation has been described by us in [1].

---

\* Institute of Technical Physics, Iași, Romania

The composition  $\text{Ni}_{0.36}\text{Zn}_{0.64}\text{Fe}_2\text{O}_4$  with the simple and combined additives of  $\text{CaO}$ ,  $\text{Na}_2\text{O}$ ,  $\text{ZrO}_2$ ,  $\text{Li}_2\text{O}$ ,  $\text{K}_2\text{O}$  and  $\text{Sb}_2\text{O}_3$  was prepared. The additives were added over the stoichiometric composition, in a small quantity, of 0.05 - 0.3 wt%.

Also, it was prepared the  $\text{Ni}_{0.7}\text{Zn}_{0.3}\text{Fe}_2\text{O}_4$  ferrite, in which the Fe ions were substituted by Ge and/or Ti ions.

The porosity of sintered bodies was determined by measuring the Archimedes density and comparing the result with the theoretical density obtained by using precise X-ray diffraction data from polished sections.

The initial magnetic permeability and coercive force were measured at a frequency of 1 kHz by the bridge method and by an integrator fluxmeter. The measuring fields for initial permeability was of 5 mOe, and for coercive force it was of 10 Oe.

The specific saturation magnetization was measured at liquid nitrogen temperature by a vibrating sample magnetometer, in a field of 5 kOe.

By means of the temperature variation curves of the specific magnetization and of the initial permeability, the Curie temperatures were obtained.

The d.c. resistivity at room temperature was measured by the two contact method using silver paste contacts.

### 3. Results and discussion.

#### 3.1. $\text{Ni}_{0.36}\text{Zn}_{0.64}\text{Fe}_2\text{O}_4$ ferrite with additives.

When a polycrystalline ferrite is used for magnetic heads,

it is desirable for the ferrite to have a high density to enable it to form a mechanically strong magnetic gap. We tried to increase the density by the addition of  $\text{CaO}$ ,  $\text{Na}_2\text{O}$ ,  $\text{ZrO}_2$ ,  $\text{Li}_2\text{O}$ ,  $\text{K}_2\text{O}$  and  $\text{Sb}_2\text{O}_3$  and by the combined addition of these oxides. Also, we have studied the effect of these additives and upon another material parameters, as initial magnetic permeability  $\mu'$ , coercive force  $H_c$ , electrical resistivity  $\rho$ , specific saturation magnetization  $\sigma_s$ , Curie temperature  $T_c$ .

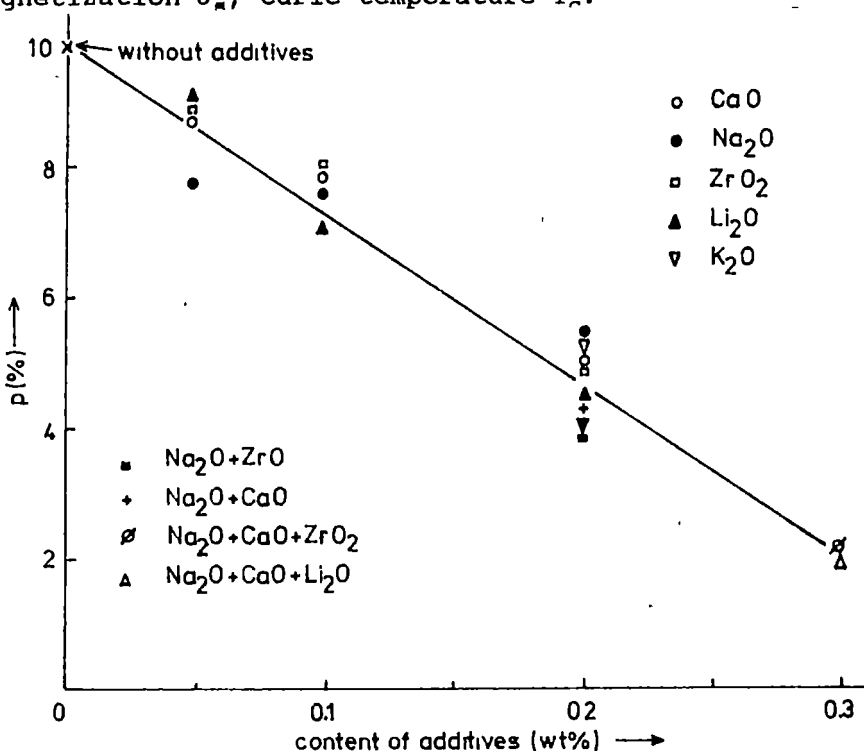


Fig.1. The variation of the porosity  $p$  as a function of the content of simple and combined additives.

The experimental results indicate that the Curie temperature, the specific saturation magnetization and the electrical resistivity were not affected practically by additives.

In Figure 1 the dependence of the porosity on the simple and combined additives content is presented. It is seen that the porosity decreases with increasing impurity content; the smallest value was obtained for a triple addition of  $\text{Na}_2\text{O}-\text{CaO}-\text{ZrO}_2$  and  $\text{Na}_2\text{O}-\text{CaO}-\text{Li}_2\text{O}$ .

Figure 2 exemplifies the dependence of initial permeability

and specific magnetization on the content of additives, for the samples with simple additives only. It is seen that the additives cause to decrease the permeability, excepting  $\text{Li}_2\text{O}$  additive. For the  $\text{Li}_2\text{O}$ ,  $\mu'$  increases continuously with increasing  $\text{Li}_2\text{O}$  content.

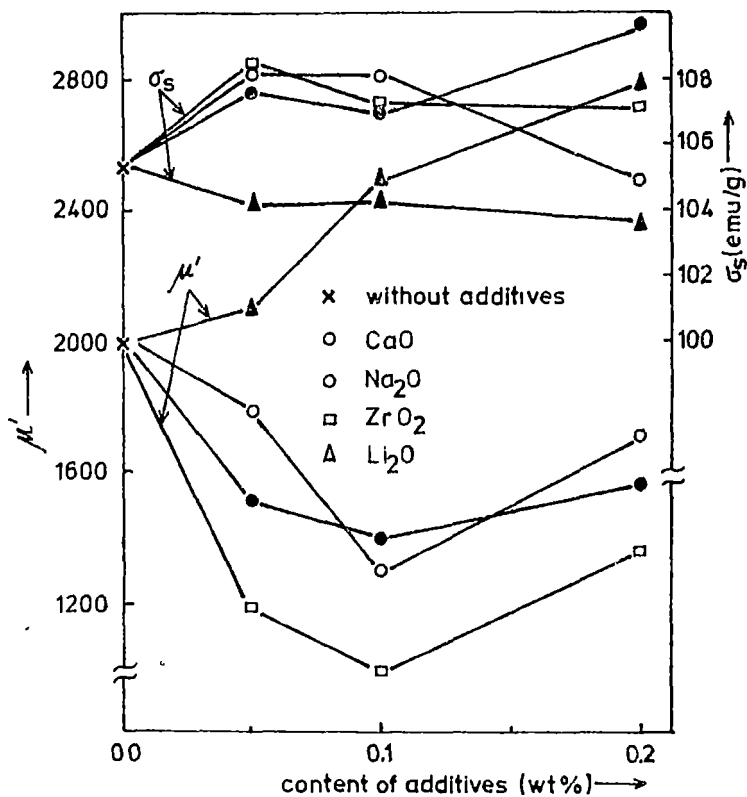
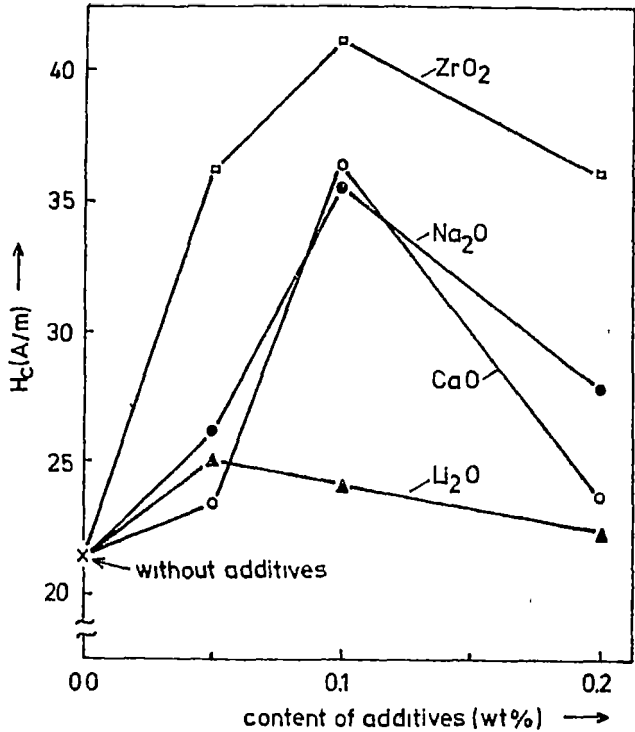


Fig.2. The variation of the specific saturation magnetization  $\sigma_s$  and of the initial magnetic permeability  $\mu'$  as a function of the quantity of impurity, for the samples with simple additives.



Coercivity is also affected by additives. In Fig.3 it is shown the variation of  $H_c$  as a function of simple additives content. The highest values of the  $H_c$  were obtained for  $ZrO_2$ . The  $Li_2O$  had a little effect on the  $H_c$ .



The results concerning the effect of additives on the magnetic permeability  $\mu'$  and coercive force  $H_c$  can be explained by a segregation of additives at the grain boundaries.

Fig.3. The variation of the coercive force  $H_c$  as a function of the content of additives for the samples with simple additions.

grain boundaries is hindered and the further crystal growth is stemmed [2], [3]. For a small additive content (0.05 - 0.1 wt%), in the sintered body there will be both grains stopped by the segregated additives and a certain percentage of large crystals increased freely, with inside pores. It is known that the action of inside pores on the magnetic domain walls displacement is important enough [4]. For a large amount of additives (0.2 - 0.3

wt%), because the number of the crystals inhibited during their growth will be much higher, it was obtained a smaller average grain size, with a reduced inside porosity. This phenomenon should contribute to an increase in initial permeability and a decrease in coercive force. The higher value of  $H_c$  at the samples with  $ZrO_2$  can be explained by a nonuniform segregation of  $ZrO_2$  which results in a coalescence of grains (discontinuous grain growth) in accordance with other experiments [3], [5].

Judging from the point of view of magnetic and mechanical characteristics acceptable for magnetic heads, the best results were obtained by the combined of  $Na_2O-CaO-ZrO_2$  or  $Na_2O-CaO-Li_2O$ .

### 3.2. $Ni_{0.7}Zn_{0.3}Fe_2O_4$ ferrite with Ti-Ge substitutions

Ti and Ge ions substitute the Fe ions in a constant proportion of 4 mol%. We choose as mixed substitution  $(GeO_2)_x(TiO_2)_{0.04-x}$ , where  $Ge^{4+}$  ions prefer tetrahedral sites and  $Ti^{4+}$  ions, octahedral sites.

Fig.4 shows the dependence of the specific magnetization measured at 77 K and the Curie temperature on the substitute composition, where  $x = 0.00, 0.01, 0.02, 0.03$  and  $0.04$ . One can remark that, by introducing germanium instead of titanium,  $\sigma_s$  increases and it attains the highest value for 3 mol%  $GeO_2$  - 1 mol%  $TiO_2$ . This dependence may be explained taking into account the fact the  $Ge^{4+}$  ions with cation radius of  $0.53\text{\AA}$  prefer the A sites, while  $Ti^{4+}$  ions with the cation radius of  $0.68\text{\AA}$  [6] prefer the B sites.

By introducing  $GeO_2$  instead of  $TiO_2$   $\sigma_s$  will increase due to

the decrease of the tetrahedral lattice magnetization. At high  $\text{GeO}_2$  concentration ( $x > 0.03$ )  $\sigma_B$  decreases slowly because of the  $\text{GeFe}_2\text{O}_4$  nonmagnetic solid phase which appears probably at higher Ge content.

The variation of the Curie temperature may be attributed to the modification of the A - B exchange

interaction due to the transition from Ti substitution to Ge one. In this case of the substitution of tetrahedral iron as compared with the substitution of an octahedral iron ( $\text{Fe}_B^{3+}$ ) the weakening of the A - B exchange interaction is more pronounced. This fact explains a certain decrease of the  $T_C$  when  $\text{Ti}^{+4}$  ions are substituted by  $\text{Ge}^{+4}$  ions.

Fig.5 shows the dependence of the d.c. resistivity  $\rho$  and of the porosity  $p$  on the substitute composition. One can remark that by introducing  $\text{GeO}_2$  instead of  $\text{TiO}_2$ ,  $\rho$  increases and reaches a maximum value for  $x = 0.03$ . This value is about two orders of magnitude higher than that for  $x = 0$ . Satbir and coworker [7] suppose that the introducing of  $\text{Me}^{4+}$  ions, like Ge or Sn, could generate a certain amount of  $\text{Fe}^{2+}$  ions. Also, it is known that

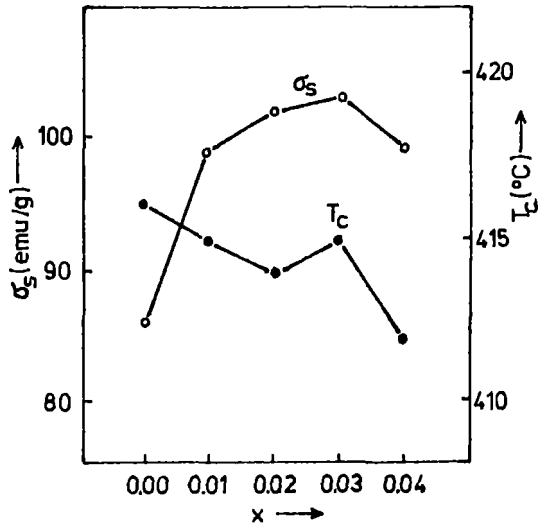


Fig.4. Specific magnetization  $\sigma_B$  and Curie temperature  $T_C$  as a function of the substitute composition  $(\text{GeO}_2)_x(\text{TiO}_2)_{0.04-x}$ .

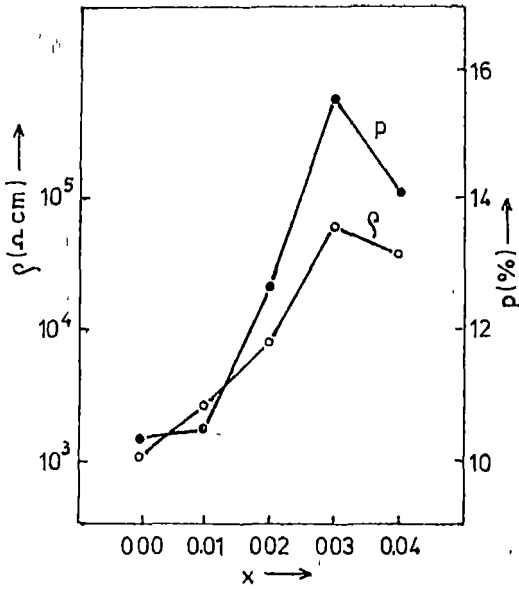


Fig.5. Resistivity  $\rho$  and porosity  $p$  as a function of the substitute composition  $(\text{GeO}_2)_x(\text{TiO}_2)_{0.04-x}$ , measures at room temperature.

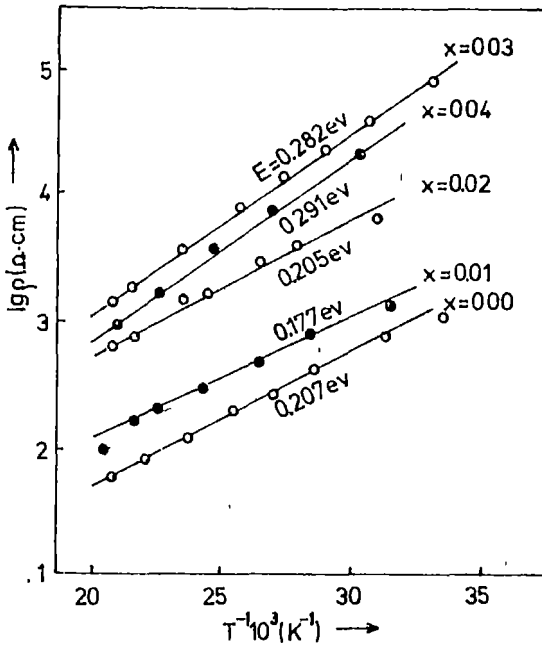


Fig.6. Resistivity  $\rho$  as a function of reciprocal temperature and the values of the activation energy for the studied ferrites.

the electronic conduction in ferrites consists in the electronic exchange  $Fe^{3+} \leftrightarrow Fe^{2+}$  on octahedral sites only [8], [9]. In this case, the  $Ti^{4+}$  substitution will increase the number of  $Fe^{2+}$  ions on octahedral sites, resulting in a decrease of the resistivity. But the  $Ge^{4+}$  ions will generate the  $Fe^{2+}$  ions on tetrahedral sites which do not participate in the conduction process. They will form stable with covalent bonds  $Ge^{4+}$  ions, i.e. the  $Ge^{4+} - Fe^{2+}$  pair [7]. Consequently, the resistivity will increase with increasing  $GeO_2$  amount in the mixed substituent. The obtained values of the activation energy (between 0.177 and 0.281 eV) (Fig.6) confirm the above mentioned idea.

Regarding to the porosity (Fig.5), the curve  $p = f(x)$  is similar to that of the resistivity. The results we obtained are in agreement with those obtained in [10] for Ni-Zn ferrites too, where it is shown that the resistivity is mainly determined by the porosity of the samples.

In conclusion, we found that the choice of the substitution composition or the additive may favourably influence the magnetic and electrical properties of ferrites, and, therefore, it is possible to obtain a good magnetic material by optimally choosing the substitution or additive.

R E F E R E N C E S

1. Rezlescu E., Rezlescu N., Pasnicu C., Craus M.L. and Popa D.P., *The influence of additives on the properties of Ni-Zn ferrite used in magnetic heads in JMMM* (to be published).
2. Paulus M., *Influence des pores et des inclusions sur la croissance des cristaux de ferrite* in "Phys. Stat. Sol.", 2, 1325 (1962).
3. Hirota K., Fujimoto Y., Watanabe K. and Sugimura M., *High B and  $\mu$  Mn-Zn ferrite with improved mechanical strength*, Private communication, Central Research Laboratory, Matsushiba Electric Industrial Co., Ltd, Kadoma, Osaka, Japan (1986).
4. Globus A., *Influence de la structure granulaire sur la dispersion de la*

- perméabilité des ferrites*, Thesis, Université de Paris, 1963.
5. Simonet W. and Hermosin A., *Soft Li-Li-Zn ferrites with resistivity > 10<sup>8</sup> Ω.cm* in "JEER Trans. MAG-14", 903 (1978).
  6. Kleber W., *Einführung in die Kristallographie*, VEB Verlag Technik, Berlin, 1959, p.139.
  7. Satbir S., Tripathi R.B. and DAS B.K., *Dissaccomodation in GeO<sub>2</sub>/SnO<sub>2</sub> doped Ni-Zn ferrites* in *Phys. Stat. Sol. (a)*, 100, k185 (1987).
  8. Smit J. et Wijn H.P.J., *Les Ferrites*, Dunod, Paris, 1961.
  9. Rezlescu N., Rezlescu E., Ioan C. and Luca E., *Time variation of the electrical conductivity in spinal ferrites* in *Phys. Stat. Sol.(a)* 11, 351 (1972).
  10. Dietzmann G., Krötzsch M. und Wolf S., *Elektrische Leitfähigkeit und Porosität von Ni-Zn Ferriten* in *Phys. Stat. Sol.*, 2, 1762 (1962).

## MAGNETIC SUSCEPTIBILITY OF $Y_{1-x}Ce_xAl_2$

M. COLDEA\*

Received: 16.10.1992

**ABSTRACT.** - A continuous transition from Kondo state ( $x > 0.30$ ) to intermediate valence (IV) state ( $x < 0.30$ ) of Ce ions in  $Y_{1-x}Ce_xAl_2$  is revealed. The magnetic susceptibility of  $Y_{1-x}Ce_xAl_2$  in the IV state is analysed in terms of the concept of characteristic - energy behaviour. The results pointed out a substantial suppression of the spin - fluctuation effects in  $Y_{0.98-x}Ce_xGd_{0.02}Al_2$  compared to pure  $Y_{1-x}Ce_xAl_2$ , and confirmed the intrinsic nature of the magnetic susceptibility increase at lower temperatures for  $Y_{1-x}Ce_xAl_2$  compounds in the IV state.

1. **Introduction.** The cubic Laves - phase compounds  $Y_{1-x}Ce_xAl_2$  form a very interesting system to study the continuous passage from trivalent spin fluctuation (Kondo behaviour) to IV state [1-3]. In this system Kondo interactions compete with RKKY exchange interactions and the Kondo temperature  $T_K$  has been shown to increase rapidly with Y content [1].

The spin fluctuation rates  $1/\tau_c \approx 3 \times 10^{12} s^{-1}$  of the Ce ions in  $Y_{1-x}Ce_xAl_2$  for  $x \geq 0.3$  were estimated from  $Gd^{3+}$  - ESR measurements by Coldea et al. [3].

Due to the presence of the magnetic impurities in compounds containing Ce in the IV state there is much confusion about the intrinsic susceptibility at low temperatures. In  $CePd_3$  an intrinsic increase of the susceptibility at low temperatures is established, which is not present in  $CeSn_3$  [4].

It is the aim of this paper to study: (i) the temperature dependence of the magnetic susceptibility of  $Y_{1-x}Ce_xAl_2$  both in the Kondo state and in the IV state and (ii) the effect of Gd

---

\* "Babeş-Bolyai" University, Faculty of Physics, 3400 Cluj-Napoca, Romania

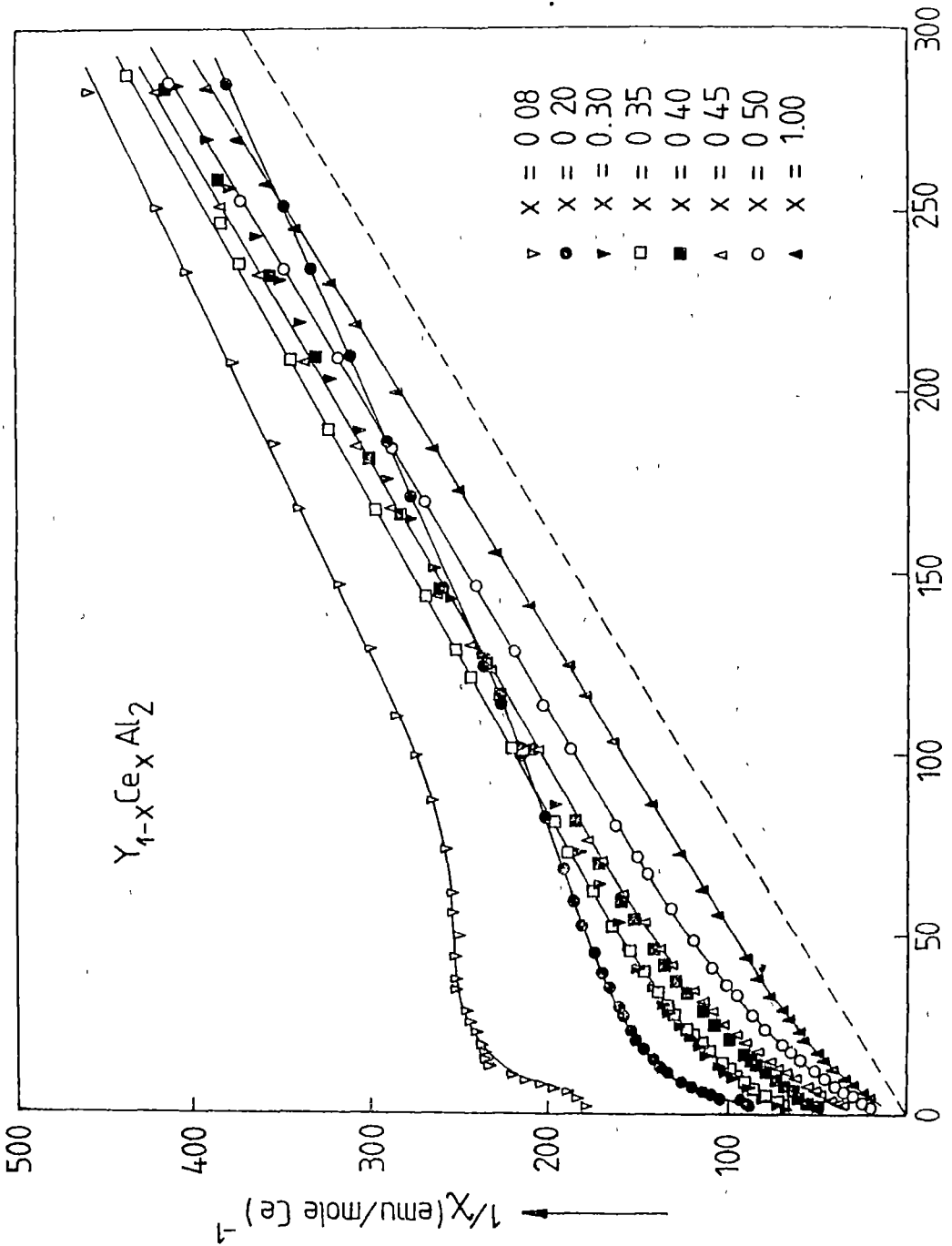


Fig.1. Temperature dependence of the reciprocal magnetic susceptibility of  $Y_{1-x}Ce_xAl_2$ . The dashed line gives the theoretical Curie law for free  $Ce^{3+}$  ions ( $\mu = 2.54\mu_B$ ).



magnetic impurities on the Ce susceptibility and to estimate (iii) the spin fluctuation time  $\tau_c$  of Ce ions in the IV state.

**2. Experimental.** The samples  $Y_{1-x-y}Ce_xGd_yAl_2$  ( $0.08 \leq x \leq 1.0$ ,  $0 \leq y \leq 0.02$ ) were prepared in a cold crucible induction furnace under a purified argon atmosphere. The purity of the starting materials was 99.99% for Ce and Y, 99.9% for Gd, and 99.9999% for Al. X-ray power diffraction measurements showed that all the compounds formed the C15 cubic Laves phase. The lattice parameters agree with those reported by Aarts et al. [1]. Susceptibility measurements were performed with a vibrating sample magnetometer between 2.6 and 290 K in a magnetic field of 10 kOe.

**3. Results and discussion.** Figure 1 shows the temperature dependence of the inverse magnetic susceptibility  $\chi_{Ce}^{-1}$ , i.e.  $(\chi(Y_{1-x}Ce_xAl_2) - \chi(YAl_2))^{-1}$ . The susceptibility of  $YAl_2$  is  $1.03 \cdot 10^{-4}$  emu/mole at room temperature and is almost temperature independent [5]. The susceptibility per Ce atom gradually decreases as the Y concentration increases and a marked change in the behaviour of  $\chi_{Ce}^{-1}(T)$  occurs at approximately  $x = 0.30$ . For  $x > 0.30$  the paramagnetic susceptibilities show crystal field effects and a Kondo behaviour, whereas for  $x \leq 0.20$ , they are typical for IV compounds. The magnetic susceptibility of  $Y_{0.92}Ce_{0.08}Al_2$  is almost constant for  $30 \text{ K} < T < 70 \text{ K}$ , increases at lower temperatures and turns again to a constant value as  $T \rightarrow 0 \text{ K}$  (Fig.2). The compound  $Y_{0.80}Ce_{0.20}Al_2$  has a similar behaviour

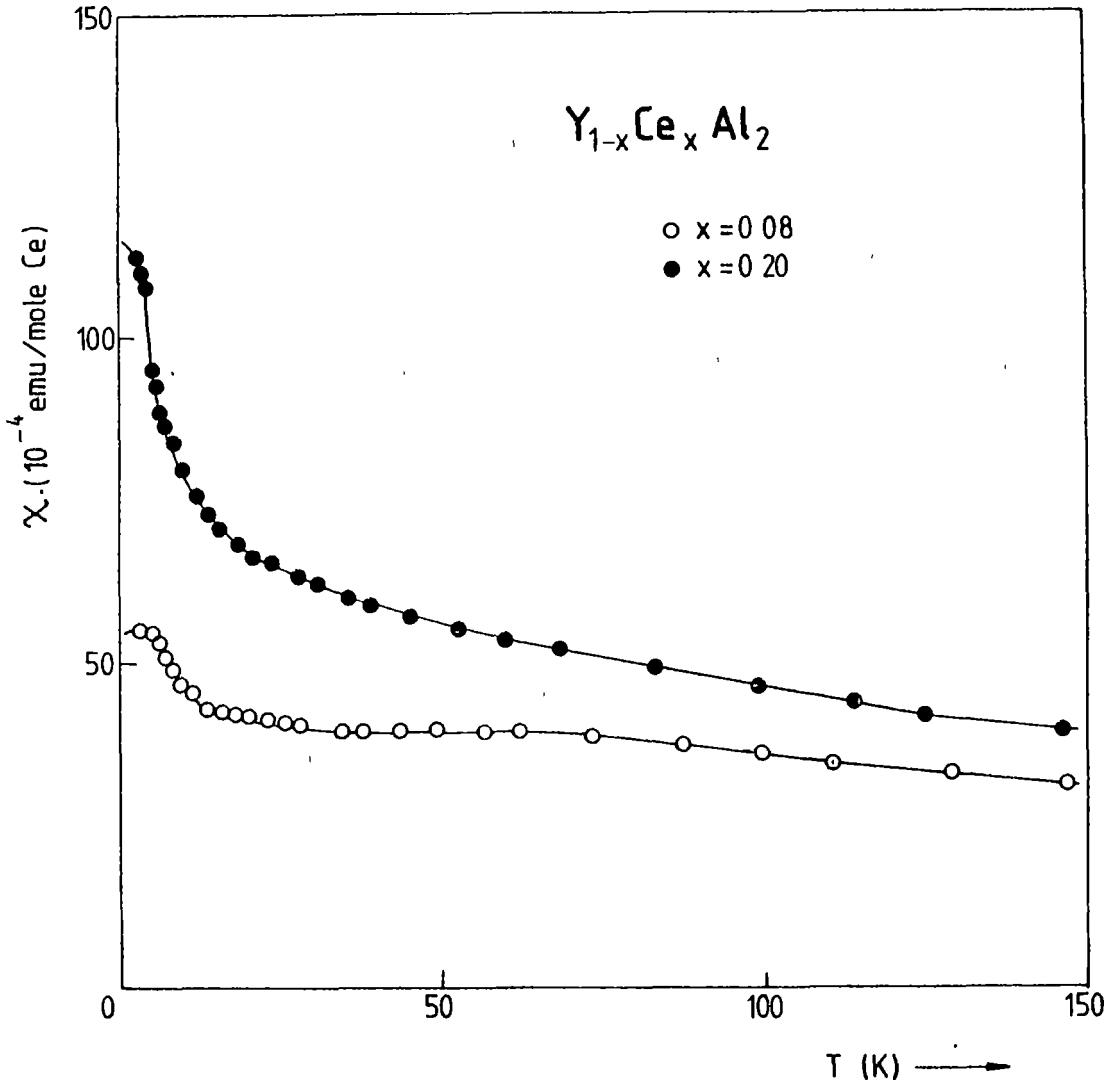


Fig.2. Temperature dependence of the magnetic susceptibility of  $Y_{0.92}Ce_{0.08}Al_2$  and  $Y_{0.80}Ce_{0.20}Al_2$ .

with - the only difference that the constant portion in  $\chi(T)$  curve is reduced to an inflexion near point  $T = 35$  K. A feature of the low - temperature susceptibility is that for  $x \leq 0.20$  one obtains a finite value at  $T = 0$  K. This shows that the upturn in the low-temperature susceptibility of  $Y_{1-x}Ce_xAl_2$  compounds in the mixed valent state is intrinsic.

In the analysis of the magnetic susceptibility of  $Y_{1-x}Ce_xAl_2$  compounds for  $x \geq 0.30$ , we considered the following three interactions: (i) the interaction of the Ce ions with the cubic crystal field, which gives rise to a splitting of the six degenerate states of  $Ce^{3+}$  ions into a  $\Gamma_7$  doublet ground state and a  $\Gamma_8$  quartet excited state with an energy separation  $\Delta$ ; (ii) the exchange interaction ( $J < 0$ ), between  $Ce^{3+}$  localized moments and conduction electrons (Kondo effect), which causes a negative paramagnetic Curie-Weiss temperature  $\theta_K$  ( $|\theta_K| = T_K$ ) and (iii) the indirect exchange interaction of  $Ce^{3+}$  ions via the RKKY interaction, which leads in our case to a positive paramagnetic Curie-Weiss temperature  $\theta_{RKKY}$ . In the whole temperature range ( $2.6$  K  $\leq T \leq 290$ K), the usual expression for the magnetic susceptibility of Ce ions in a cubic crystal field [6]

$$\chi(T) = \frac{C \cdot f(T, \Delta)}{T - \theta} \quad (1)$$

gives only an approximate description of the experimental data. In (1)  $C$  is the Curie constant,  $\theta = \theta_K + \theta_{RKKY}$  and the function

$$f(T, \Delta) = \frac{5 + 26 \exp(-\Delta/T) + 32T/\Delta \cdot [1 - \exp(-\Delta/T)]}{21 [1 + 2 \exp(-\Delta/T)]} \quad (2)$$

describes the crystal field splitting  $\Delta$  [7]. Deviations from (1)

are observed in all compounds where Ce is subjected to a crystal field [6, 8, 9]. However, in the low temperature region ( $T \leq 50$  K), the susceptibility data for  $x \geq 0.30$  are well described by (1). The fit yields magnetic moments per Ce atom which are about 10% smaller than the free  $Ce^{3+}$  ion value. This is in agreement with the theoretical value obtained by Krishana-Murthy et al, [10] for a Kondo ion in the symmetric Anderson model. The  $\theta$  value for  $CeAl_2$  ( $\sim 0.6$  K) indicates that  $\theta_K = -\theta_{RKKY}$ , thus confirming earlier findings [1]. This balance breaks down in the diluted compounds: namely,  $\theta_K$  decreases with Y concentration while  $\theta_{RKKY}$  also decreases as a result of magnetic dilution. The crystal field splitting  $\Delta$  in  $CeAl_2$  is 107 K but increases to about 200K in diluted compounds.

The magnetic susceptibility of  $Y_{1-x}Ce_xAl_2$  in the IV state ( $x < 0.30$ ) may be discussed in terms of the concept of characteristic-energy behaviour [11]. The phenomenology implies two energy scales to explain the susceptibility:

$$\chi(T) = \frac{C}{T+T_{sf}} \quad \text{for } T \gg T_{sf} \quad (3)$$

and

$$\chi(T) = \frac{C}{2T_{sf}} \quad \text{for } T \ll T_{sf} \quad (4)$$

The broad susceptibility maximum occurs at a temperature representing the crossover from low-temperature to high-temperature behaviour ( $T_{max} = T_{sf}/2$ ). Here  $C = 0.807$  emu K/mole is the Curie constant for free  $Ce^{3+}$  ion and  $T_{sf}$  is the spin fluctuation temperature. The intrinsic upturn in the measured

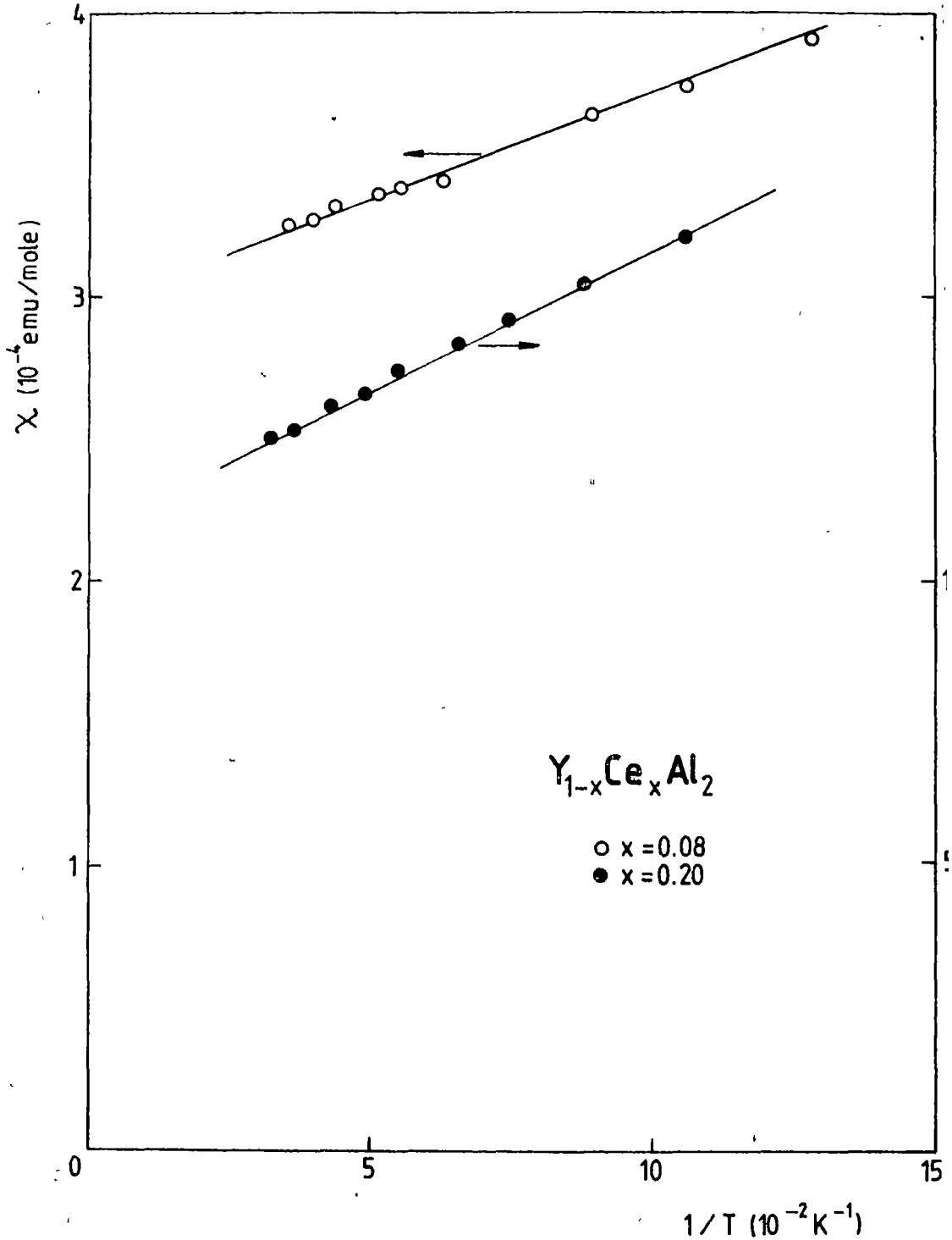


Fig.3. Low temperature susceptibility versus  $1/T$  for  $Y_{0.92}Ce_{0.08}Al_2$  and  $Y_{0.80}Ce_{0.20}Al_2$ .

low-temperature susceptibility of  $Y_{1-x}Ce_xAl_2$  in the IV state (Fig.2) can be described by

$$\chi(T) = \frac{C}{T} + \chi(0) \quad (5)$$

where  $\chi(0)$  is the zero temperature value of the susceptibility due to the Ce ions in the IV state. Figure 3 shows the low temperature susceptibility ( $6 \text{ K} < T < 30 \text{ K}$ ) versus  $1/T$  for  $Y_{0.92}Ce_{0.08}Al_2$  and  $Y_{0.80}Ce_{0.20}Al_2$ . From this plot results for the zero temperature susceptibility expressed per Ce atom the values  $\chi(0) = 36.87 \cdot 10^{-4}$  emu/mole Ce for  $x = 0.08$  and  $\chi(0) = 54.5 \cdot 10^{-4}$  emu/mole Ce for  $x = 0.20$ . The equation (4) yields  $T_{\text{sf}} = 109.4 \text{ K}$  and  $73.6 \text{ K}$  for  $Y_{0.92}Ce_{0.08}Al_2$  and  $Y_{0.80}Ce_{0.20}Al_2$ , respectively. From the alopes of these curves we obtained the average number of  $Ce^{3+}$  ions as "impurities" in two compounds at temperatures  $T \ll T_{\text{sf}}$ , namely 1.3% for  $x = 0.08$  and 6% for  $x = 0.20$  from the total number of rare-earth ions. The intrinsic upturn in the magnetic susceptibility is due to narrow 4f states near the Fermi level [12]. At present, we have no reliable theory of splin fluctuations valid for all temperatures. According to the multiorbital Anderson model the spin fluctuation time is related to the magnetic susceptibility  $\chi(0)$  at 0 K by [13]:

$$\tau_c(0)^{-1} = (g/\mu_B)^2 / \hbar \chi(0) \quad (6)$$

From this equation results for the spin fluctuation rates of Ce ions the values  $\tau_c^{-1}(0) = 6.6 \cdot 10^{12} \text{ s}^{-1}$  for  $x=0.20$  and  $\tau_c^{-1}(0) = 9.8 \cdot 10^{12} \text{ s}^{-1}$  for  $x = 0.08$ . These values are comparable to those derived directly from the Kondo temperature with the relation

$$\hbar/\tau_c = k_B T_K \quad (7)$$

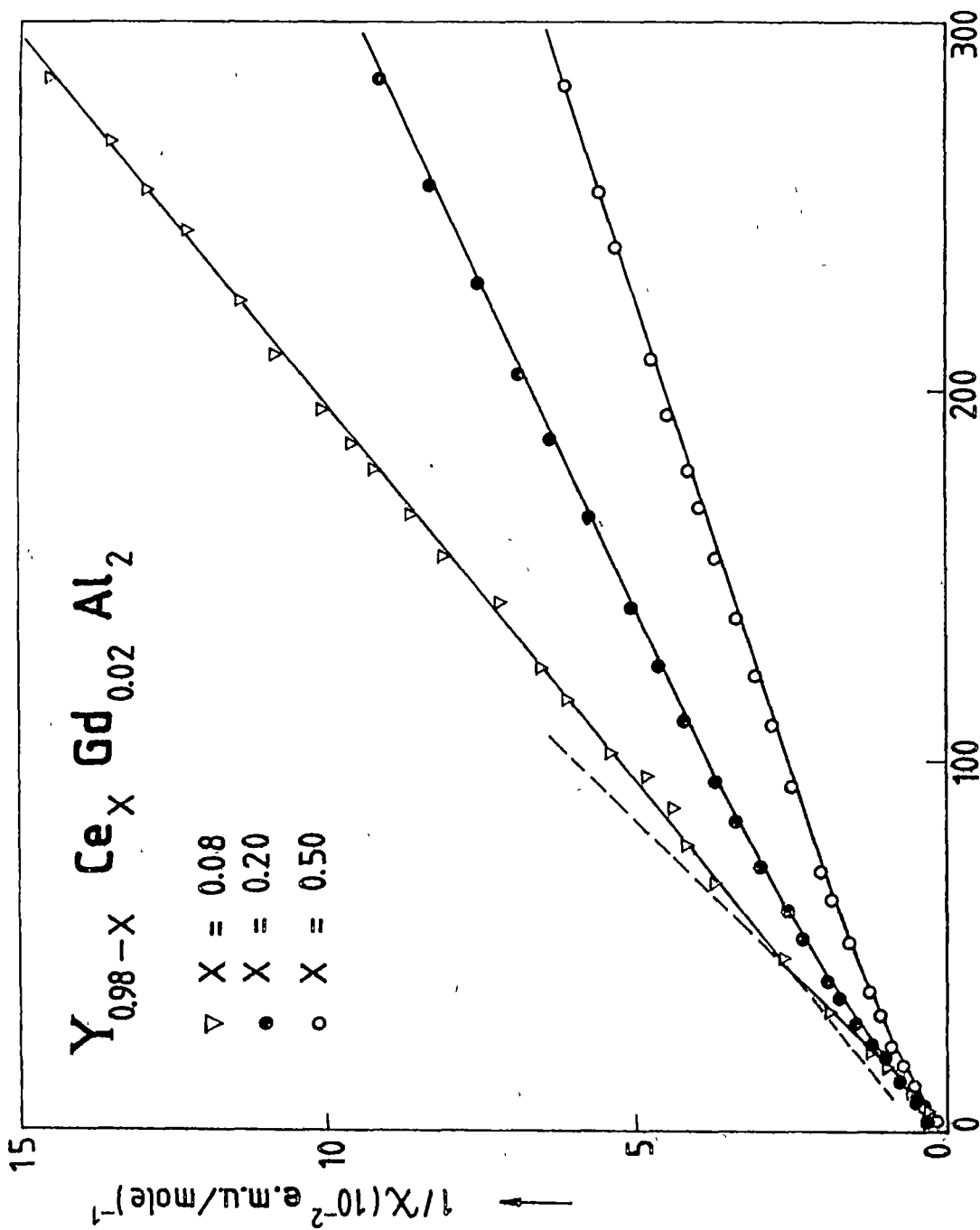


Fig. 4. Temperature dependence of the reciprocal magnetic susceptibility of  $Y_{0.98-x}Ce_xGd_{0.02}Al_2$ .

if we assume  $T_K \equiv T_{Bf}$ . Moshchalkov showed that all Ce-based intermediate valence compounds are concentrated Kondo systems with high  $T_K$  [14].

To explain the low-temperature susceptibility for these two compounds we considered also the effect of Gd impurities on the Ce susceptibility. The  $1/\chi(T)$  curves for some selected samples  $Y_{0.98-x}Ce_xGd_{0.02}Al_2$  are given in Fig.4. The main results of this investigation can be summarized as follows: (i) a change in the slope of  $1/\chi(T)$  dependence occurs at approximately  $T = 40$  K and 25 K for  $Y_{0.90}Ce_{0.08}Gd_{0.02}Al_2$  and  $Y_{0.78}Ce_{0.20}Gd_{0.02}Al_2$ , respectively; (ii) no Ce contribution to the effective moments per unit formula can be deduced from  $1/\chi(T)$  curves in the low-temperature region; (iii) the contribution of Ce ions in the measured susceptibility of the above mentioned compounds, i.e.  $\chi(Y_{0.98-x}Ce_xGd_{0.02}Al_2) - \chi(Gd)$ , presents no more an upturn in the low-temperature region. These findings reveal a substantial suppression of the spin-fluctuation effects in  $Y_{0.98-x}Ce_xGd_{0.02}Al_2$  compared to pure  $Y_{1-x}Ce_xAl_2$  and confirm the intrinsic nature of the magnetic susceptibility increase at lower temperatures for  $Y_{1-x}Ce_xAl_2$  compounds in the IV state.

**Acknowledgement.** The author wishes to express his thanks for the hospitality and technical assistance extended by the Institut für Festkörperphysik, TH Darmstadt, during his stay, and to the Alexander von Humboldt Foundation for financial support.



## R E F E R E N C E S

1. Aarts J., De Boer F.R., Horn F., Steglich F., Meschede D., Proc. of the Int. Conf. on Valence Fluctuations in Solids, Eds. L.M.Falicov, W.Hanke, M.P.Maple (Amsterdam, North-Holland) 1981, p. 301.
2. Schefzyk R., Heibel J., Steglich F., Felten R., Weber G., J.Magn. Magn. Mat. 47-48, 83 (1985).
3. Coldea M. Schaeffer H., Weissenberger V., Elschner B., Z. Phys. B68, 25 (1987).
4. Veenhuizen P.A., van Kalker G., Klaasse J.C.J., Menovsky A., Moleman A.C., de Boer F.R., Aarts J., J. Magn. Magn. Mat. 54-57, 425 (1986).
5. Van Daal H.J., Buschow K.H.J., Phys. Stat. Sol. (a) 3, 853 (1970).
6. Felsch W., Winzer K., v. Minnigerode G., Z.Physik B21, 151 (1975).
7. White J.A., Williams H.J., Wernick J.H., Sherwood R.C., Phys. Rev. 131, 1039 (1963).
8. Aarts J., de Boer F.R., de Chatel P.F., J. Magn. Magn. Mat. 49, 271 (1985).
9. Pierre J., Galera R.M., Siand E., J. Physique 46, 621 (1985).
10. Krishna-Murthy H.R., Wilson K.G., Wilkins J.W., Phys. Rev. Lett. 35, 1101 (1975).
11. Lawrance J., Phys. Rev. B20, 3770 (1979).
12. Torikachvili M.S., Yang K.N., Maple M.B., Meisner G.P., J. Appl. Phys. 57, 3137 (1985).
13. Mekata M., Ito S., Sato N., Satoh T., J. Magn. Magn. Mat. 54-57, 433 (1986).
14. Moshchalkov V.V., J. Magn. Magn. Mat. 47-48, 7 (1985).



MAGNETIC PROPERTIES OF  $Ce_{1-x}Y_xCu_2$

M. COLDEA\*, D. ANDREICA\*, I. POP\*, G. BUD\*

Received: 12.10.1992

**ABSTRACT.** - The magnetic susceptibility measurements in  $Ce_{1-x}Y_xCu_2$  pointed out a transition from trivalent spin fluctuation (Kondo behaviour) to intermediate valence state of Ce - ions at high Y concentration. A strong enhancement of the Pauli susceptibility in these compounds is also revealed.

1. **Introduction.** The Intermetallic compound  $CeCu_2$  orders antiferromagnetically at 3.5 K [1] and neutron diffraction experiments suggest a very long - range antiferromagnetic structure [2]. Resistivity measurements have shown that Kondo effect is present in this compound with  $T_K = 10$  K [3]. The compounds  $CeCu_2$  and  $YCu_2$  crystallize in the same orthorhombic  $CeCu_2$  structure (the space group  $D_{2h}^{28}$ ) with the lattice parameters  $a = 4.43$  Å,  $b = 7.05$  Å,  $c = 7.45$  Å [4] and respectively  $a = 4.305$  Å,  $b = 6.80$  Å,  $c = 7.315$  Å [5]. The substitution of Ce by Y leads to a lattice pressure on the Ce - ions in the  $Ce_{1-x}Y_xCu_2$  system.

In the similar compounds  $Ce_{1-x}Y_xAl_2$  (cubic Laves-phase) the specific heat and thermal expansion [6] and magnetic susceptibility [7] measurements pointed out a continuous transition from trivalent spin fluctuation (Kondo behaviour) to intermediate valence state of the Ce - ions with increasing X. In this system Kondo interactions compete with RKKY exchange interactions and the Kondo temperature  $T_K$  has been shown to increase rapidly with Y content.

---

\* "Babeș-Bolyai" University, Faculty of Physics, 3400 Cluj-Napoca, Romania

We have undertaken to study the evolution of the magnetic properties in the  $Ce_{1-x}Y_xCu_2$  series at high Y concentration (i.e. high lattice pressure) and we present the magnetic susceptibilities of  $Ce_{0.20}Y_{0.80}Cu_2$  and  $Ce_{0.10}Y_{0.90}Cu_2$  measured at various temperatures between 100 K and 600 K.

**2. Experimental.** The investigated compounds were prepared in an arc - melting furnace under a pure argon atmosphere. The purity of the starting elements was 99.99% for Cu and Y and 99.8% for Ce. X-ray investigations confirmed the existence of a single phase in the two compounds  $Ce_{0.20}Y_{0.80}Cu_2$  and  $Ce_{0.10}Y_{0.90}Cu_2$ . In the limit of the experimental errors, the lattice parameters for the two compounds verify the Vegard law.

The magnetic susceptibility was measured at 9450 Oe with a Faraday - type magnetic balance, having a sensitivity of  $10^{-8}$  emu/g.

**3. Results and discussion.** Fig.1 shows the temperature dependence of the inverse magnetic susceptibility of  $Ce_{0.20}Y_{0.80}Cu_2$  and  $Ce_{0.10}Y_{0.90}Cu_2$  compounds.

The experimental data fit a Curie-Weiss term plus a temperature independent one, according to

$$\chi = \frac{C}{T-\theta} + \chi_0 \quad (1)$$

The values of the magnetic moments per Ce atom and the Curie temperatures are  $2.53\mu_B$  and  $-68$  K for  $Ce_{0.20}Y_{0.80}Cu_2$  and  $2.32\mu_B$  and  $-23$  K for  $Ce_{0.10}Y_{0.90}Cu_2$ . The value of the magnetic moment is

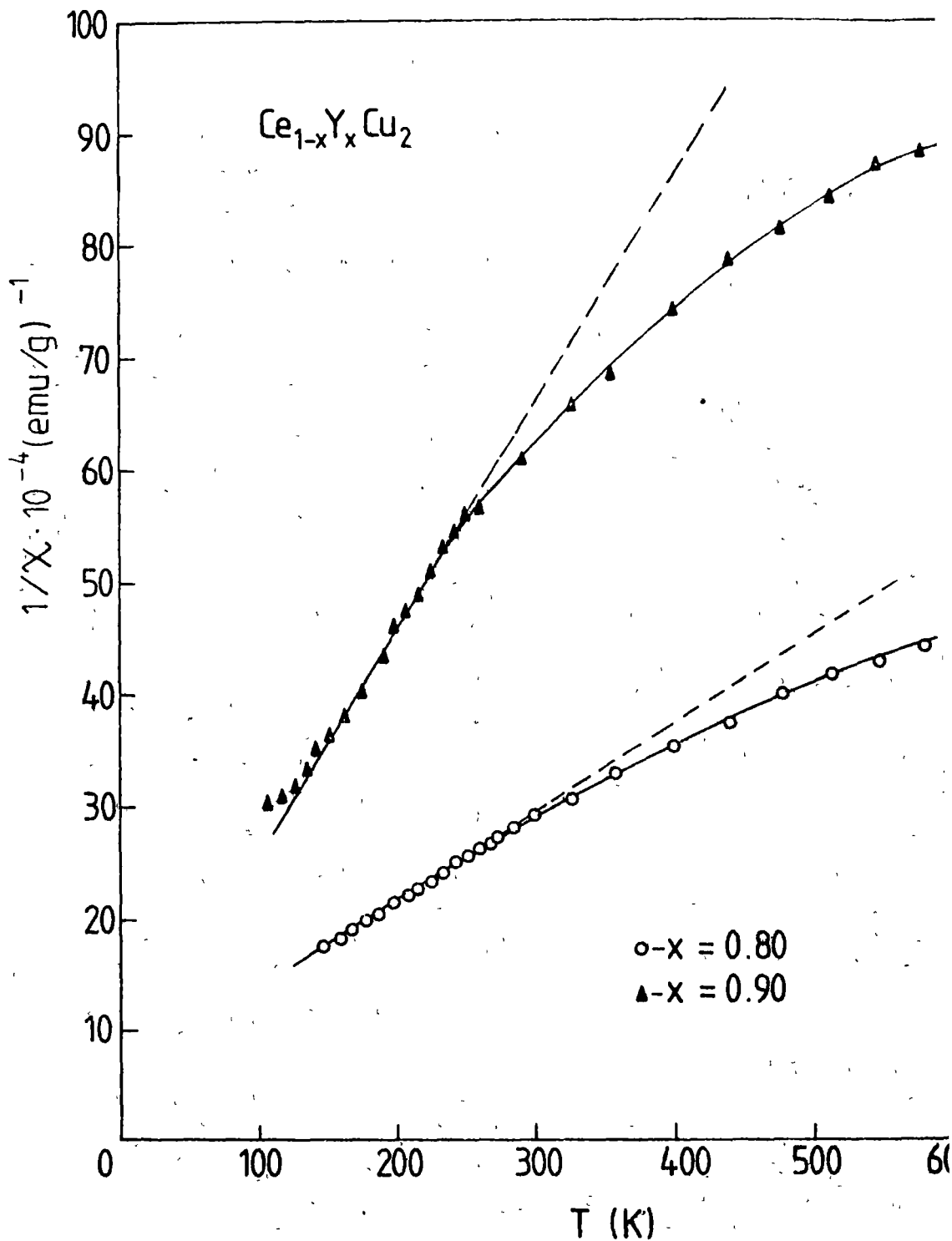


Fig. 1. Reciprocal magnetic susceptibility versus temperature for  $Ce_{0.20}Y_{0.80}Cu_2$  and  $Ce_{0.10}Y_{0.90}Cu_2$ .

very close to the free  $\text{Ce}^{3+}$  ion value of  $2.54\mu_B$  for  $x = 0.80$ , but is smaller with 10% for  $x = 0.90$ .

The susceptibility  $\chi$  plotted against  $(T-\theta)^{-1}$  gives for the temperature independent susceptibility the values  $\chi_0 = 1.10 \cdot 10^{-6}$  emu/g for  $\text{Ce}_{0.20}\text{Y}_{0.80}\text{Cu}_2$  and  $\chi_0 = 0.58 \cdot 10^{-6}$  emu/g for  $\text{Ce}_{0.10}\text{Y}_{0.90}\text{Cu}_2$ . The temperature-independent term may be expressed as

$$\chi_0 = f \cdot \chi_p^0 + \chi_{orb}^{5d^1} + \chi_{vv}^{4f} + \chi_L + \chi_{dia} \quad (2)$$

where  $\chi_p^0$  is the free electron Pauli paramagnetism,  $f$  is the enhancement factor of the Pauli paramagnetism,  $\chi_{orb}^{5d^1}$  is the orbital contribution of the  $5d^1$  electrons,  $\chi_{vv}^{4f}$  is the Van Vleck paramagnetism of the  $4f$  electrons,  $\chi_L$  is the Landau diamagnetism of the conduction electrons and  $\chi_{dia}$  is the diamagnetism of the Ce, Y and Cu atomic cores. All the contributions in the temperature - independent term, calculated in the same manner as for the  $\text{RCu}_6$  compounds [8], are given in Table 1.

Compound	$\chi_0$	$\chi_p^0$	$\chi_{orb}^{5d^1}$	$\chi_{vv}^{4f}$	$\chi_L$	$\chi_{dia}$	$f$
$\text{Ce}_{0.20}\text{Y}_{0.80}\text{Cu}_2$	226.23	32.59	38.8	45	-10.86	-37.6	5.85
$\text{Ce}_{0.10}\text{Y}_{0.90}\text{Cu}_2$	128.24	33.22	38.8	45	-11.07	-36.8	2.78

Table 1. The contributions in the temperature-independent susceptibility of  $\text{Ce}_{0.20}\text{Y}_{0.80}\text{Cu}_2$  and  $\text{Ce}_{0.10}\text{Y}_{0.90}\text{Cu}_2$  expressed in  $10^{-6}$  emu/mole.

When it is expressed per Ce atom, the factor  $f$  has approximately the same value for the two compounds. These values point out a

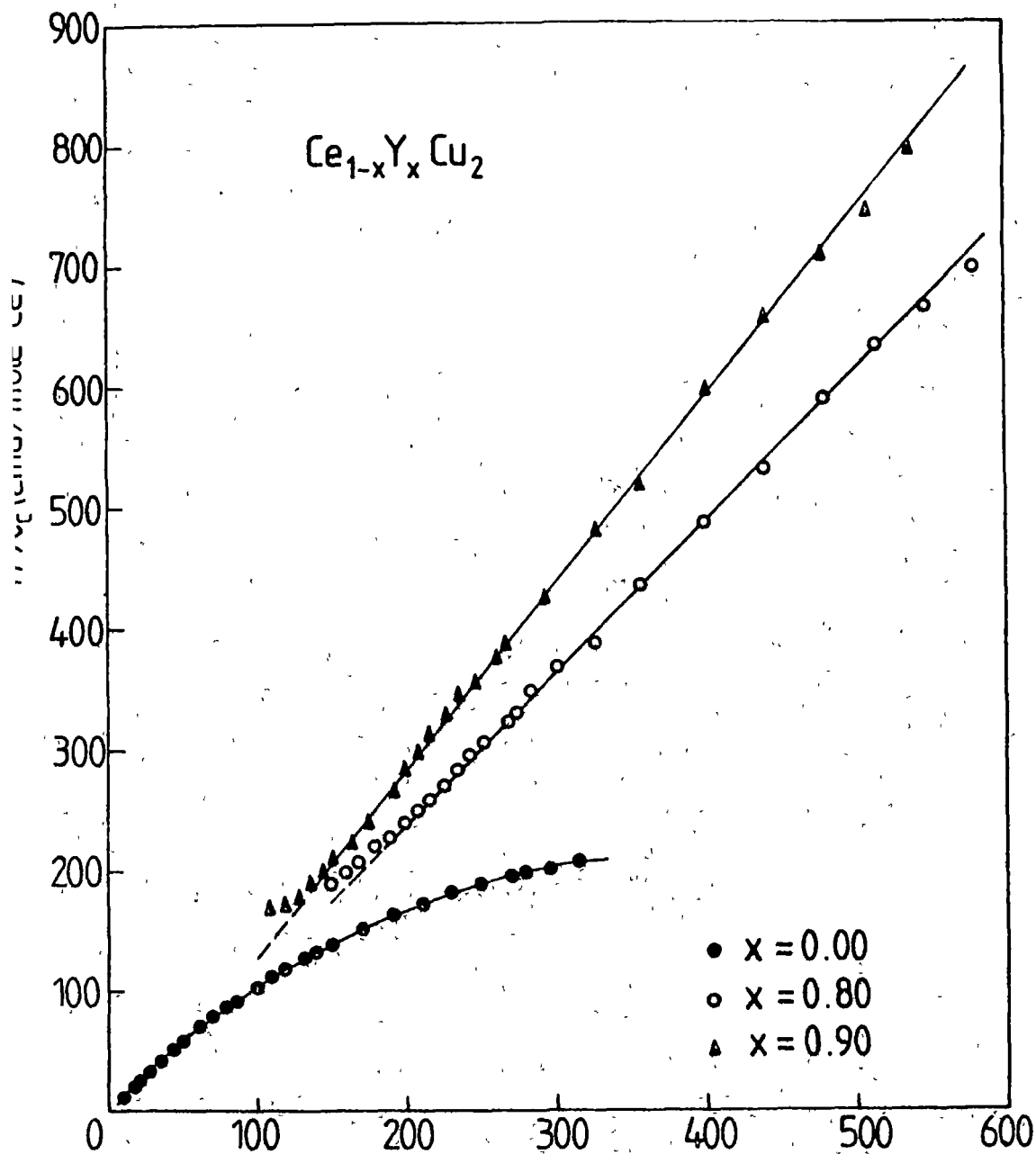


Fig. 2. Reciprocal magnetic susceptibility (corrected for independent term  $\chi_0$  and expressed per Ce atom) versus temperature for  $Ce_{0.10}Y_{0.90}Cu_2$ ,  $Ce_{0.20}Y_{0.80}Cu_2$  and  $CeCu_2$ .

strong enhancement of the Pauli susceptibility in the investigated compounds.

In order to see the evolution of the magnetic properties in  $Ce_{1-x}Y_xCu_2$  system, in Fig.2 are shown the temperature dependence of the corrected susceptibilities  $\chi_c$  (the Curie term) expressed per Ce atom for the two compounds together with that of  $CeCu_2$  measured by Hashimoto et al.[9].

Substitution of Ce by Y changes drastically the magnetic properties of  $CeCu_2$ . The susceptibility per Ce atom gradually decreases as the Y concentration increase and that reveals an increasing demagnetisation of the single Ce - ions with increasing magnetic dilution. Furthermore, from a susceptibility which shows crystal field effects for  $CeCu_2$  one passes in the compounds with Y to a susceptibility which tends to a broad maximum or a constant value at low temperatures. To confirm one of these assumptions, measurements at lower temperatures would be necessary. This behaviour is characteristic for intermediate valence (IV) compounds or for concentrated Kondo systems (CKS).

These results lead to the conclusion that in  $Ce_{1-x}Y_xCu_2$  system (for high Y concentration) a strong hybridization of the 4f states with the conduction electron band takes place. The strength of this hybridization is [3]

$$\Gamma = \Pi V^2 N(E_F) \quad (3)$$

where V is an appropriate average over the hybridization matrix element and  $N(E_F)$  is the density of states at the Fermi level. This mixing destabilizes the local 4f moments. The resulting nonmagnetic ground state at low temperatures is characterized by



an enhanced Pauli paramagnetism. The hybridization causes Abrikosov - Suhl - type scattering resonances  $E_R$  near the Fermi level  $E_F$  [10], leading to a virtual bound state of width  $\Gamma$  and an enhanced density of states at the Fermi level of the order of  $\Gamma^{-1}$ . In our case the enhanced density of states at the Fermi level can be observed from the value of the enhancement factor  $f$  of the Pauli susceptibility. In fact, as Moshchalkov showed [11], all Ce - based "IV" - are CKS with  $E_R > E_F$  and high  $T_K$ .

## R E F E R E N C E S

1. Onuki Y., Machii Y., Shimizu Y., Komatsubara T., Fujita T., J.Phys. Soc. Jpn., **54**, 3562 (1985).
2. Gratz E., Bauer E., Barbara B., Zemirli S., Steglich F., Brede C.D., Lieke W., J.Phys. F **15**, 1975 (1985).
3. Bauer E., Adv. Phys. **40**, 417 (1991).
4. Larson A.C., Cromer D.T., Acta Cryst. **14**, 73 (1961).
5. Storm A.R., Benson K.E., Acta Cryst. **16**, 701 (1963).
6. Schefzyk R., Heibel J., Steglich F., Felten R., Weber G., J.Magn. Magn. Mat. **47-48**, 83 (1985).
7. Coldea M., Schaeffer H., Weissenberger V., Elschner B., Z.Phys. **B68**, 25 (1987).
8. Coldea M., Pop I., Philos. Mag. **28**, 881 (1973).
9. Hashimoto Y., Fujii H., Fujiwara H., Okamoto T., J.Phys. Soc. Jpn. **47**, 73 (1979).
10. Schlottmann P., Phys. Rev. B **25**, 4815, 4828, 4838 (1982).
11. Moshchalkov V.V., J.Magn. Magn. Mat. **47-48**, 7 (1985).



EXCHANGE ENHANCEMENT PARAMAGNETISM IN U-Co-Al SYSTEMS

P. LUCACI\*, I. LUPȘA\*

Received: 10.06.1992

**ABSTRACT.** - The magnetic and structural properties of  $U(Co_xAl_{1-x})_3$  systems with  $x \geq 0.6$  were studied in the temperature range 4.2 and 700K and fields up to 70kOe. Their crystallographical structure is a hexagonal one. The systems present an exchange enhancement paramagnetism.

**1. Introduction.**  $UCo_3$  compound crystallizes in a hexagonal  $NbBe_3$  - type structure, having  $R\bar{3}m$  space group [1]. According to Turan [2,3],  $UCo_3$  is weakly paramagnet with a low-temperature upturn, connected probably with a small amount of magnetic ordered impurity. Their magnetic properties are dependent on stoichiometry.

As a part of an ongoing investigation of uranium intermetallic compounds, we analysed the magnetic properties of mixed  $UAl_3 - UCo_3$  systems with  $x \geq 0.6$ , where aluminium is gradually replaced by cobalt. In order to obtain accurate data, the influence of magnetic impurities was eliminated by analysing the field dependences of the magnetic susceptibilities.

**2. Experimental.** The samples were melted in an arc furnace, in purified argon atmosphere. In order to ensure a good homogeneity, the samples were remelted several times. The alloys were subsequent annealed in vacuum, at 850°C, for one week. The results of X-ray analysis shown in Fig.1 indicate an hexagonal structure for the compounds having  $x \geq 0.6$ .

---

\* Technical University, 3400 Cluj-Napoca, Romania

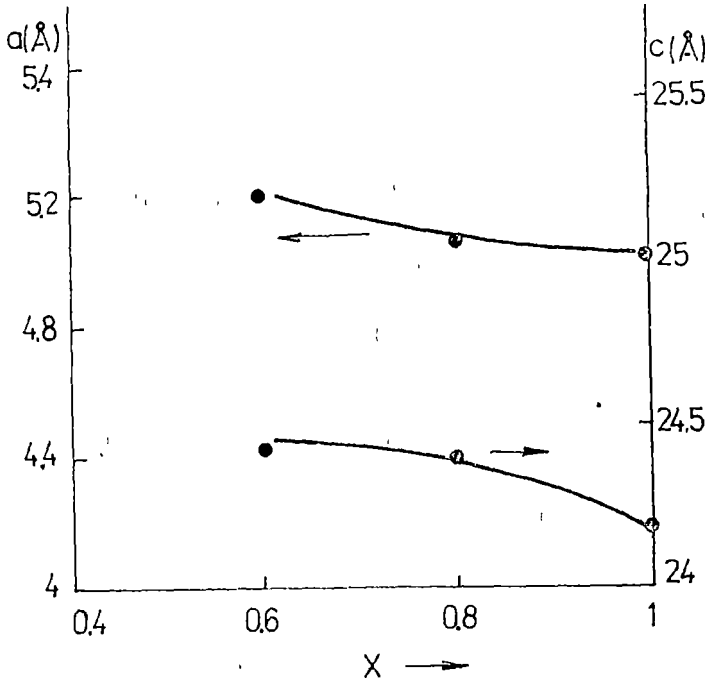


Fig.1. Composition dependence of lattice parameters

Magnetic measurements were performed in the temperature range 4.2-700 K and external fields up to 70 kOe.

The susceptibilities,  $\chi$ , were obtained from their field dependences, according to Honda-Owen plots [4]  $\chi_m = \chi + c M_s H^{-1}$ , by extrapolating to  $H^{-1} \rightarrow 0$ , respectively, By  $c$  is denoted a presumably content of a magnetic ordered impurity,  $M_s$  is their saturation magnetization and  $\chi_m$  is the measured susceptibility in a field  $H$ . By this method accurate values of magnetic susceptibilities were obtained.

3. Experimental results. As a general feature, we mention that  $U(Co_x, Al_{1-x})_3$  compounds are paramagnetic down to 4.2 K. The thermal variations of magnetic susceptibilities are plotted in Figure 2.

3. Experimental results. As a general feature, we mention that  $U(Co_x, Al_{1-x})_3$  compounds are paramagnetic down to 4.2 K. The thermal variations of magnetic susceptibilities are plotted in Figure 2.

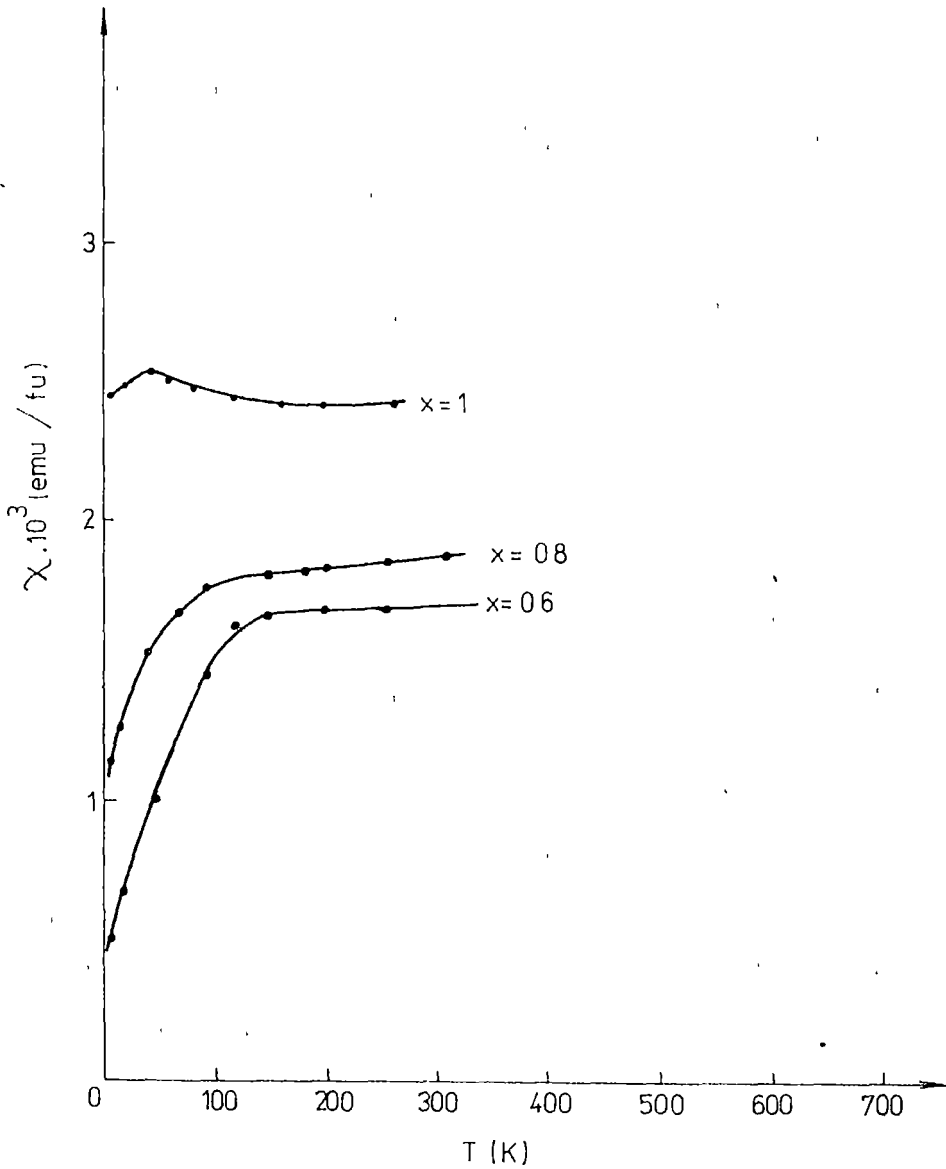


Fig.2. Thermal variations of magnetic susceptibilities in  $U(Co_xAl_{1-x})_3$  compounds with  $x \geq 0.6$

The magnetic susceptibilities of  $UAl_3$  increase, as a function of temperature and has a maximum  $T_m = 140$  K. Then the

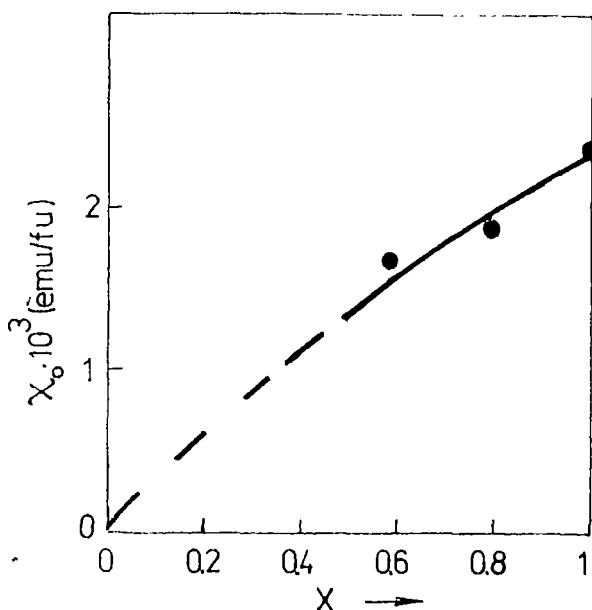
$\chi$  values decrease. Above the temperature corresponding to maximum, the susceptibility value decreases and shows at high temperatures a modified Curie-Weiss law. The effective magnetic moment determined from Curie constant is  $3.70 \mu_B$  being close to that previously reported in  $UAl_2$  [5,6].

The magnetic behaviour evidenced in compounds having composition  $x \geq 0.6$  shows that the magnetic susceptibility increases up to a temperature  $T_a$ . At higher temperatures than  $T_a$ , the  $\chi$  values are nearly constant. The temperatures  $T_a$  decrease from 140 K ( $x=0.6$ ) to 90K( $x=1$ ). In the addition, the low temperature variations of susceptibilities decrease, as the cobalt content increases. The susceptibilities  $\chi_q$ , determined at  $T > T_a$  increases as a function of cobalt content-

**4. Discussion.**  $UAl_3$  compound shows an interesting thermal variation of the magnetic susceptibility. The  $\chi$  values increase up to a temperature,  $T_m$ , followed, at high temperatures, by a Curie-Weiss type behaviour. This temperature dependence of  $\chi$  values is similar to that evidenced in  $YCo_2$  and  $LuCo_2$  compounds [7]. The above behaviour may be considered in the self-consistent renormalization (SCR) theory of spin fluctuations [8-11]. In this model the wave number dependent susceptibility,  $\chi_q$  has a large enhancement due to electron-electron interaction only for small  $q$  and the temperature dependence is significant only for those  $\chi_q$  with small  $q$ . The average amplitude of the local spin fluctuations  $\langle J_{loc}^2 \rangle = 3 k_B T \sum_q \chi_q$  is a temperature dependent quantity. The  $\langle J_{loc}^2 \rangle$  increases when increasing temperature, until

it reaches an upper limit determined by the charge neutrality condition, at a temperature  $T^* \approx 250$  K. Above  $T^*$ ,  $UAl_3$  behaves as having local moment. The effective moment determined experimentally in the high temperature range is close to that of  $U^{3+}$  ( $\mu_{\text{eff}} = 3.62 \mu_B$  [12]).

Fig. 3. Composition dependence of temperature independent contribution  $\chi_0$ .



The magnetic susceptibilities of compounds with  $x \geq 0.6$  having hexagonal structure, increase,

at low temperatures and above a characteristic temperature,  $T_a$ , the  $\chi$  values are nearly constant. The temperature variations of susceptibilities are smaller, when increasing the cobalt content. In addition the temperature independent contribution ( $T > T_a$ ) are higher. The low temperature increase of the susceptibilities, characteristic for spin fluctuations behaviour, is not followed by a Curie-Weiss behaviour at high temperatures. In these situations the spin fluctuations are nearly quenched, the predominant magnetic behaviour being the temperature independent

paramagnetism.

Finally, we conclude that  $UAl_3$  compound shows a spin fluctuations type behaviour. A gradual transition to a Pauli-type paramagnetism is evidenced, when aluminium is substituted by cobalt.  $UCo_3$  shows a small temperature dependence of the magnetic susceptibilities, at low temperatures. The maximum variation in the magnetic susceptibilities for  $T < 300K$  is smaller than 4%.

#### REFERENCES

1. A.E.Dwight, Acta cryst. B24(1968) 1395.
2. J.Turan, A.Zentko, J.Sternberk and J.Hrebik, Acta Phys. Slovaca 31 (1981) 143.
3. V.Šechovsky and L.Havela in Handbook of Ferromagnetic Materials, Vol.4, North Holland Publ. Company, 1988.
4. L.F.Bates, Modern Magnetism, Cambridge University Press, Cambridge, England, 1959 p.133.
5. R.J.Trainor, M.B.Brodsky and H.W Culbert, Phys. Rev. Lett. 34(1975) 1019.
6. E.Burzo and P.Lucaci, Solid State Commun, 72(1989) 305.
7. E.Burzo and R.Lemaire, Solid State Commun, 84(1992) 1145.
8. T.Moriya and A.Kawabata, J.Phys. Soc. Jpn. 34(1973) 636.
9. T.Moriya, Solid State Commun. 26(1978) 483.
10. V.Takahashi and T.Moriya, J.Phys. Soc. Jpn. 46(1979) 3451.
11. T.Moriya, J.Magn. Magn. Mat. 14(1979) 1
12. S.V.Vonsovski, Magnetizm, Moskva, Nauka, 1971.



THE U-Co-Ni BEHAVIOUR IN THE PARAMAGNETIC RANGE

I.LUPȘA\*, P.LUCACI\*

Received: 10.06.1992

**ABSTRACT.** - The magnetic properties of  $x\text{UCo}_{5.3}(1-x)\text{UNi}_5$  compounds were studied in the paramagnetic temperature range and fields up to 70kOe.  $\text{UNi}_5$  is a paramagnet. A peak in the temperature dependence of the susceptibility is evidenced at  $T = 20$  K. The compounds with  $x \geq 0.2$  are ferromagnetically ordered. Above the Curie temperatures, the reciprocal susceptibilities show a Curie-Weiss type behaviour. The experimental data are analysed in spin fluctuations model.

1. **Introduction.**  $\text{UCo}_{5.3}$  compound crystalizes in a rhombohedral structure which is a displacive of  $\text{CaCu}_5$  lattice. The unit cell consists of 2.5  $\text{CaCu}_5$  layers and an adopter layer occupied by cobalt atoms [1]. The crystal structure of  $\text{UNi}_5$  is cubic of  $\text{AuBe}_5$  type [2].

Magnetic measurements performed on  $\text{UNi}_5$  showed that this compound has a temperature independent susceptibility [3,4].  $\text{UCo}_{5.3}$  compound is ferromagnetically ordered at temperatures lower than  $T_c \approx 360$  K. The saturation magnetization per formula unit, extrapolated at absolute zero, is  $2.4 \mu_B$  [5]. The neutron diffraction measurements evidenced a magnetic moment of about  $0.6 \mu_B$  per cobalt atom, oriented parallel to trigonal axis.

2. **Experimental.** The  $x\text{UCo}_{5.3}(1-x)\text{UNi}_5$  samples were melted in an arc furnace, in purified argon atmosphere. They were thermally treated in vacuum, during one week, at 850 C. The X-ray analyses show the presence of  $\text{AuBe}_5$  type structure in the composition range  $x \leq 0.6$  and rhombohedral structure, of  $\text{UCo}_{5.3}$  type for

---

\* Technical University, 3400 Cluj-Napoca, Romania

$x \geq 0.8$ . In the composition range  $0.6 < x < 0.8$ , the samples consist from a mixture of the above phases.

The magnetic measurements above the Curie temperatures above the Curie temperatures, allowed to obtain the susceptibilities  $\chi$  from their field dependences, according to Honda-Owen plots

$$\chi_m = \chi + c M_s H^{-1} \quad (1)$$

by extrapolating to  $H^{-1} \rightarrow 0$ , respectively.

By  $c$  is denoted a presumably impurity content and  $M_s$  is their saturation magnetization.

This method allows to eliminate any influence of magnetic ordered impurities on susceptibility values. We estimated in paramagnetic range, in all cases, a magnetic impurity content lower than 0.1 mol %.

**3. Experimental results.** The thermal variation of  $\text{UNi}_5$  magnetic susceptibility indicates a maximum in the temperature dependence of  $\chi$  values is evidenced at  $T \approx 20$  K. Then, the susceptibilities decrease and for  $T > 140$  K, the  $\chi$  values are not temperature-dependent. A similar behaviour was previously evidenced in  $\text{ZrCo}_2$  compound at  $T < 600$  K [6]. The susceptibility value for  $\text{UNi}_5$  determined at  $T > 140$  K is only little smaller than previously reported data [2-4].

The compounds having  $x \geq 0.2$  are ferromagnetically ordered.

The thermal variations of reciprocal susceptibilities are plotted in Fig.1. The experimental data follow a Curie-Weiss type behaviour.

$$\chi = C/(T - \theta)^{-1} \quad (2)$$

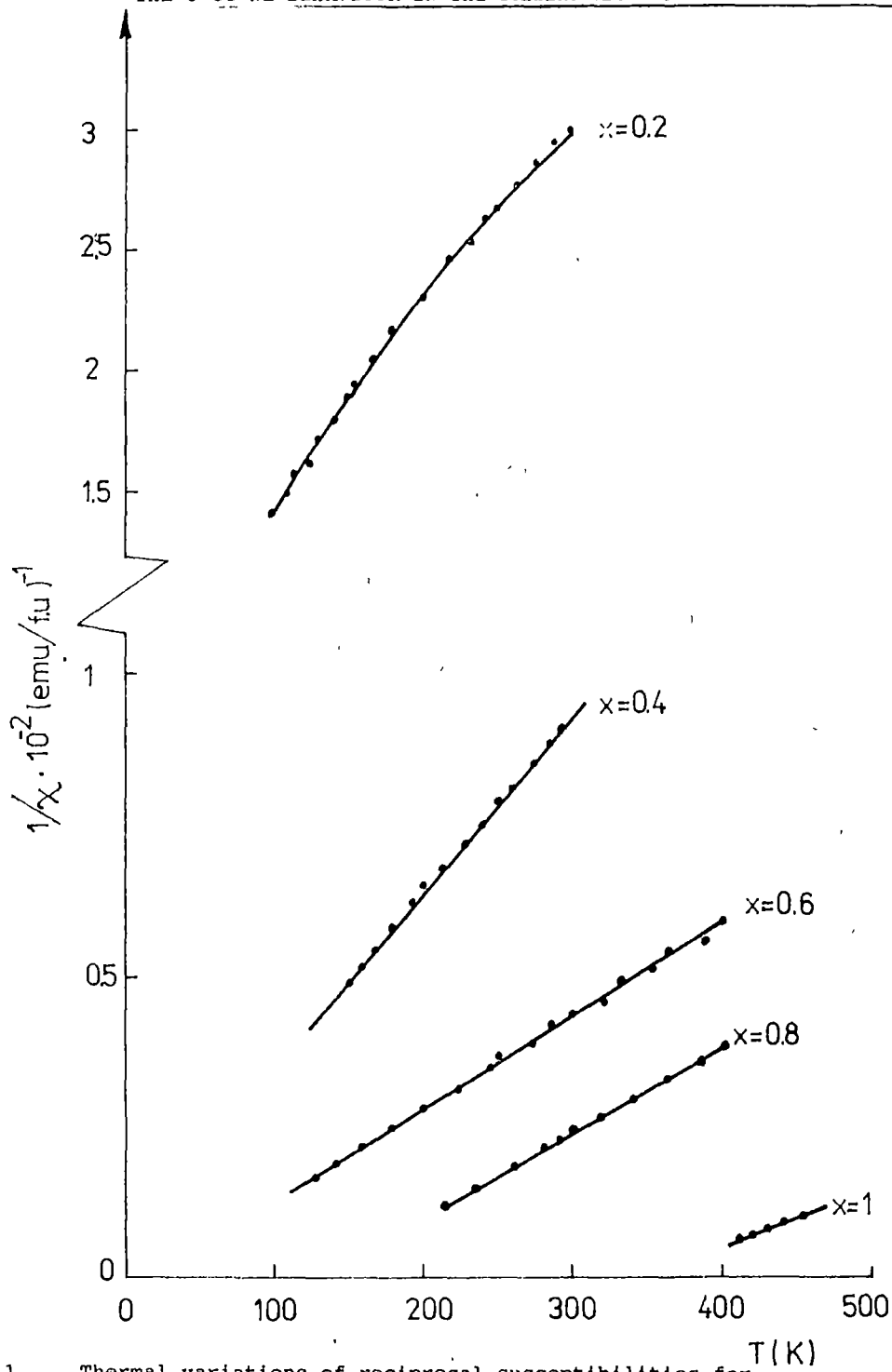


Fig.1. Thermal variations of reciprocal susceptibilities for  $x\text{UCo}_{53}(1-x)\text{UNi}_5$  compounds

By  $C$  is denoted the Curie constant and  $\theta$  is the paramagnetic Curie temperature.

The measurements show a sudden increase of the susceptibilities, for a characteristic temperature,  $T_t$ , which is dependent on composition. A similar behaviour was observed, for example, in  $R_2Fe_{14}B$  type compounds [7] and was ascribed to a structural phase transition. Due to above changes in  $\chi$  values, the paramagnetic data were obtained only in a limited temperature range above  $T_c$ , particularly for  $UCo_{5.3}$  compound.

The composition dependences of the paramagnetic Curie temperatures, Curie constants and effective cobalt moments are plotted in Fig.2. The  $\theta$  values are negative for compositions  $x \leq 0.5$  and become positive for higher cobalt content. The effective cobalt moments are  $\approx 3.9 \mu_B$  for  $x \leq 0.8$  and  $\approx 4.40 \mu_B$  for  $x = 1.0$ . The first value coincides with expected  $Co^{2+}$  effective moment supposing only spin contribution. An effective moment of  $Co^{2+}$  ion of the order of  $\approx 4.60 \mu_B$  is commonly determined in paramagnetic salts [8].

**4. Discussion.** In the temperature range  $T > 2$  K  $UNi_5$  compound is paramagnetic. Nickel is not magnetic in this compound. When nickel is replaced by cobalt, the compounds are ferromagnetically ordered. Admitting, as in  $UNi_5$ , that nickel has no magnetic contribution, the mean cobalt moments were determined. In the paramagnetic range, the effective cobalt moments are close to those expected for  $Co^{2+}$  ions.

The magnetic behaviour of  $xUCo_{5.3}(1-x)UNi_5$  may be analysed

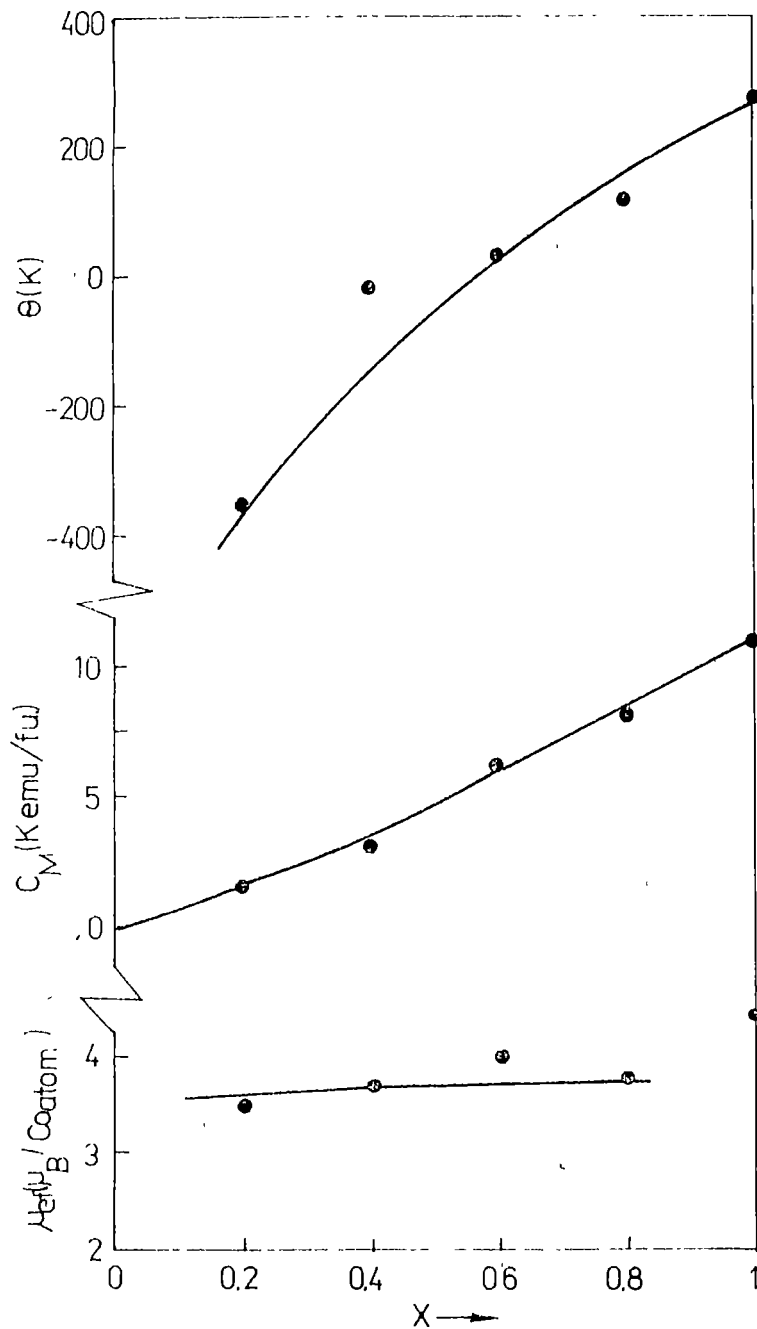


Fig.2. Composition dependences of the paramagnetic Curie temperatures, Curie constants and effective cobalt moments.

in the self consistent renormalization (SCR) theory of spin fluctuations for weakly ferromagnetic alloys [9]. In this model, at  $T > T_c$ , the wave number dependent susceptibility,  $\chi_q$ , has large enhancement due to electron-electron interaction, only for small  $q$ . Thus,  $\langle S_{loc}^2 \rangle = 3k_g T \sum_q \chi_q$  is a temperature dependent quantity. The  $\langle S_{loc}^2 \rangle$  may increase rapidly when increasing temperature until it reaches an upper limit determined by the charge neutrality condition, at a certain temperature  $T^*$  [10-12]. Above  $T^*$  the system would behave as if having local moment.

In  $x\text{UCo}_{5.3}(1-x)\text{UNi}_5$  the  $T^*$  temperature is only little greater than the Curie points, in the composition range  $x > 0.2$ . For the compound with  $x = 0.2$ , the saturation is obtained at higher temperatures ( $T^* = T_c + 100$ ) as compared to the Curie points as for other alloys (Fig. 1). If  $S_{loc}^2$  for cobalt is saturated, the charge neutrality condition would give the effective moment  $\mu_{eff}(\text{Co}) = g\sqrt{S(S+1)}\mu_B$ , if only spin contribution is considered. This behaviour is evidenced in  $x\text{UCo}_{5.3}(1-x)\text{UNi}_5$  compounds with  $x \leq 0.8$ , mainly having cubic structure. We note that the cubic Laves phase exchange enhanced paramagnets  $\text{ACo}_2$  ( $A = \text{Y, Lu, Sc}$ ) show at high temperature a Curie-Weiss behaviour. The effective cobalt moments coincide with the spin contribution, only [6,13].

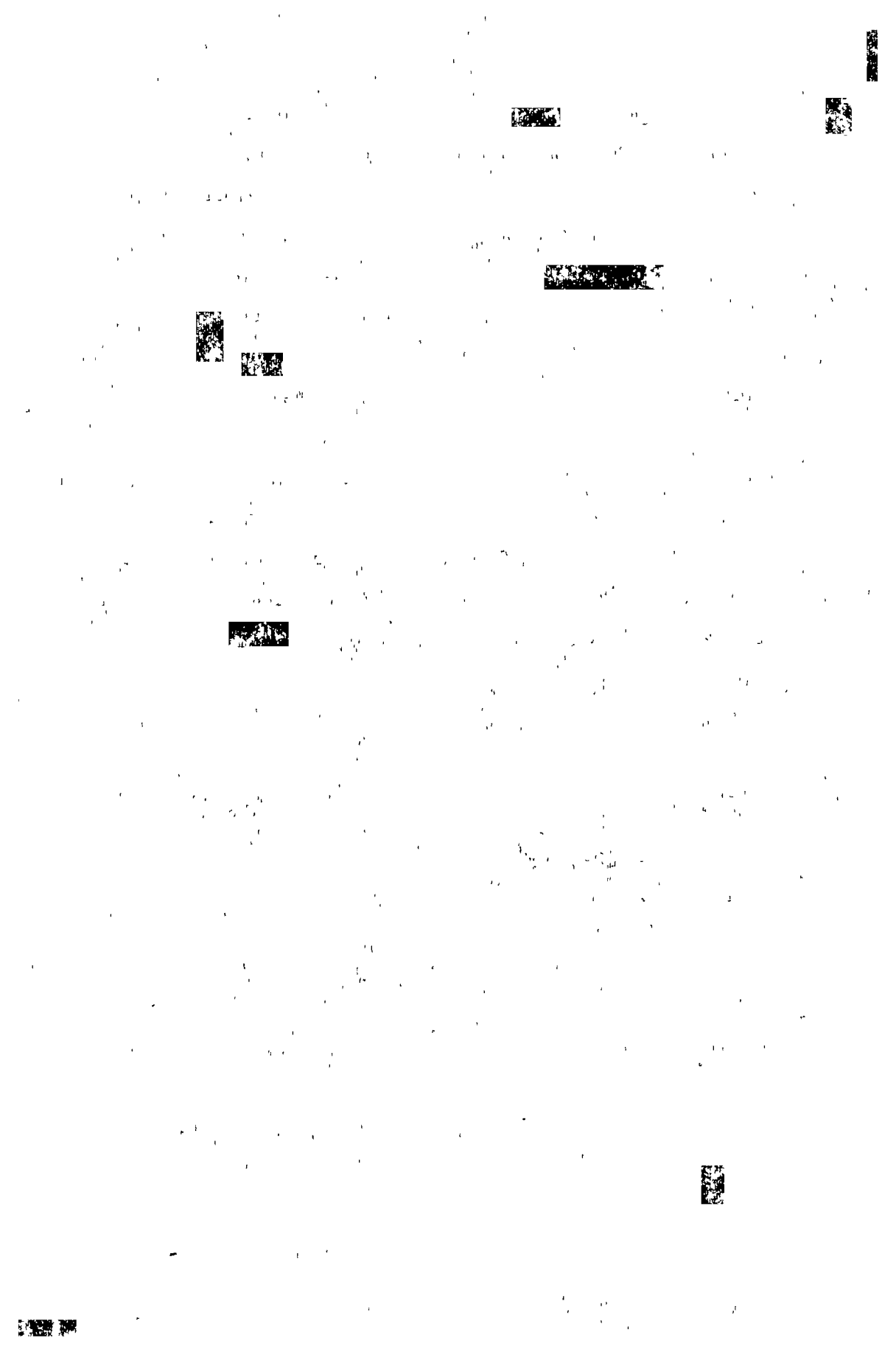
For  $\text{UCo}_{5.3}$ , the higher value of the effective cobalt moment suggests the presence of an orbital contribution. Taking into account a mean proportion of 20 % for orbital contribution, as in  $\text{YCo}_5$ , the effective cobalt moment of  $\approx 4.40 \mu_B$  determined in  $\text{UCo}_{5.3}$  may be justified.

We mention that the spin fluctuation model is supported also by negative paramagnetic Curie temperatures evidenced in the composition range  $x < 0.5$ . Negative  $\theta$  values were observed in all typical spin fluctuation compounds as  $UAl_2$  [14] or  $ACo_2$  ( $A = Y, Lu, Sc$ ) [6,13]. For higher cobalt content than  $x = 0.5$ , the paramagnetic Curie temperatures are positive, but smaller than  $T_C$  values. When cobalt content is increasing the exchange interactions increase. They superpose on the typical spin fluctuations behaviour characteristic for nearly ferromagnetic alloys. As a consequence, the  $\theta$  values are gradually changed being more close to  $T_C$  values when cobalt content increases.

In addition, the effective moments are very close to those expected for  $Co^{2+}$  ions. The data may be well described by the spin fluctuations model.

#### R E F E R E N C E S

1. A.Dommann, H.Brandle and F.Hulliger, *J.Less Common Met.* **158**, 287(1990).
2. V.Sechovsky and L.Havela in *Handbook of Ferromagnetic Materials*, ED. E.P.Wohlfarth and K.H.J.Buschow, Vol 4, North Holland, 1990.
3. M.B.Brodsky and N.J.Bridger, *AIP Conf. Proc.* **18**(1974).
4. L.Havela, J.Strebik and A.V.Andreev, *Acta Phys. Slovaca* **36**, 182(1986).
5. A.V.Deryagin and A.V.Andreev, *Sov. Phys. JETP* **44**, 610(1976).
6. E.Burzo, E.Gratz and V.Pop, *J.Magn. Magn. Mat* **119**(1993) in press.
7. E.Burzo and H.R.Kirchmayr in *Handbook on Physics and Chemistry of Rare Earth*, Vol 12, chapter 82, North Holland Publ. Comp., 1989.
8. S.Vonsovski, *Magnetizm*, Nauka, Moscow, 1971.
9. T.Moriya and A.Kawabata, *J.Phys. Soc. Jpn* **34**, 639(1973), **35**, 660(1973).
10. T.Moriya, *Solid. State Commun.* **26**, 483(1978).
11. Y.Takahashi and T.Moriya, *J.Phys. Soc. Jpn* **46**, 3451(1979).
12. T.Moriya, *J.Magn. Magn. Mat.* **14**(1979) 1.
13. E.Burzo and R.Lemaire, *Solid State Commun.* **84**, 1145(1992).
14. R.J.Trainor, M.B.Brodsky and H.V.Culbert, *Phys. Rev. Lett.* **34**, 1019(1975).





THE INFLUENCE OF THE VITREOUS MATRIX ON THE  $\text{Cu}^{2+}$   
EPR ABSORPTION SPECTRA

M. PETEANU\*, L. COCIU\*, I. ARDELEAN\*

Received 6 04.1992

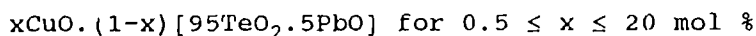
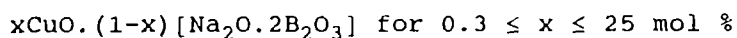
**ABSTRACT.** - EPR absorption spectra of  $\text{Cu}^{2+}$  were investigated in vitreous matrices [ $\text{Na}_2\text{O}\cdot 2\text{B}_2\text{O}_3$ ] and [ $95\text{TeO}_2\cdot 5\text{PbO}$ ]. The structure of the sodium-borate matrix appears as much stable when rising the impurities content than the tellurite one. The form of the absorption spectra and the values of the EPR parameters are strongly dependent on the matrix composition and the concentration of the paramagnetic ions. Fluctuations in the ligand field in the  $\text{Cu}^{2+}$  ion environment were evidenced.

**1. Introduction.** Several papers concerning tellurite glasses revealed their special properties largely used in microelectronics [1,2]. EPR of paramagnetic ions was successfully used for their structure investigation. Some structural details were revealed by our previous studies concerning the EPR of  $3d^5$  ions in tellurite vitreous matrices [3-9]. For further information about these glasses we investigated their structure by means of the  $\text{Cu}^{2+}$  EPR measurements. For a better understanding of the absorption spectra, and the revealed structural details of the host matrix, we proceeded in comparison with EPR absorptions of the  $\text{Cu}^{2+}$  ions in a sodium-borate vitreous matrix, corresponding to a system more studied, and better understood [10,11]. The range of the paramagnetic ions concentration was large enough for obtaining interesting results about the  $\text{Cu}^{2+}$  ions distribution in the host vitreous matrix, the microstructural details of their environment, the ligand field effects on their state, etc.

---

\* "Babeș-Bolyai" University, Faculty of Physics, 3400 Cluj-Napoca, Romania

**2. Experimental.** Series of samples were prepared, representing vitreous matrices containing  $\text{Cu}^{2+}$  as paramagnetic ions. The investigated systems were



Samples were prepared by melting the oxide mixtures corresponding to the given compositions, in an electrically heated furnace at  $1000^\circ\text{C}$ . After an hour of homogenising the melt at this temperature, by means of thermal convection, the molten material was quenched on a stainless steel plate at room temperature. Typical glasses were obtained, having the gradual darkening in colour, corresponding to the paramagnetic ions' accumulation along the investigated concentration range. Thus, the sodium-borate samples' color varies from light blue to black, and that of the tellurite ones, from light green to black.

EPR measurements were performed at room and liquid nitrogen temperature, by using a JES-3B spectrometer in the X frequency band and a 100 kc/s field modulation.

**3. Experimental results.** The EPR absorption spectra recorded for the  $x\text{CuO} \cdot (1-x) [\text{Na}_2\text{O} \cdot 2\text{B}_2\text{O}_3]$  samples were asymmetric and characteristic for  $\text{Cu}^{2+}$  ions in axial symmetric environment, along the whole investigated concentration range. They show the hyperfine structure (hfs) due to the unpaired electron interaction with the nuclear spin  $I = 3/2$  of the  $\text{Cu}^{2+}$  ion, well resolved in both parallel and perpendicular band. The hfs of the obtained spectra is given in Fig.1.

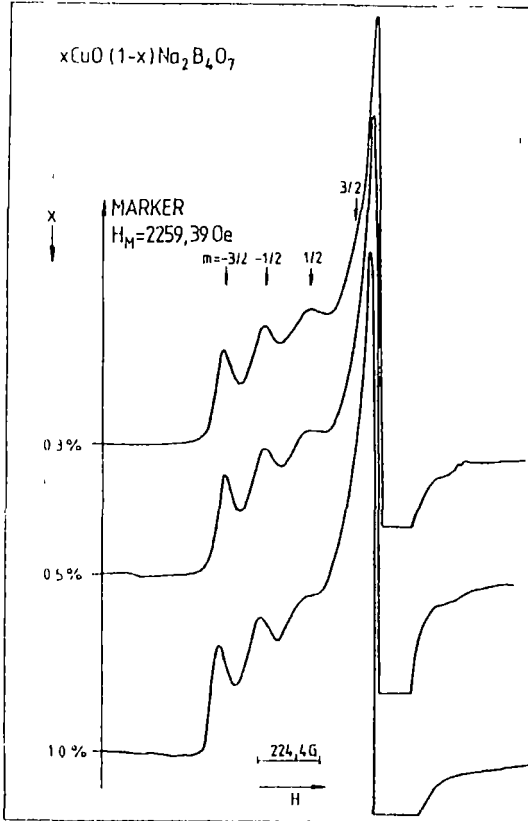


Fig 1 a

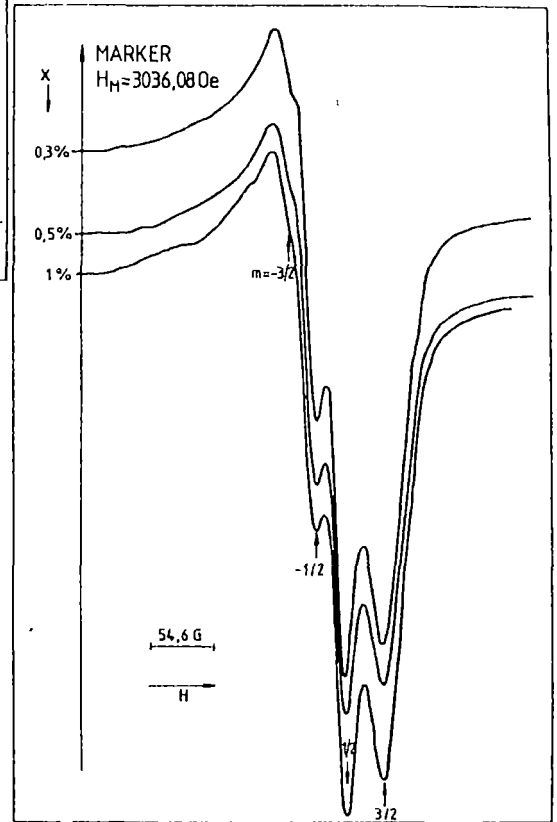


Fig 1 b

Fig.1. EPR absorption spectra of the  $\text{Cu}^{2+}$  ions in  $x\text{CuO} \cdot (1-x)[\text{Na}_2\text{O} \cdot 2\text{B}_2\text{O}_3]$  glasses revealing the hyperfine structure resolved in the parallel band (a), and that resolved in the perpendicular one (b).

The spectral resolution is optimal in the low impurities concentration range. Due to the lines broadening, as rising concentration, the hfs becomes less resolved. The hf constants were approximated as separation between the central peaks of hfs for parallel and perpendicular band of the absorption spectrum, and the corresponding  $g$  factor values were calculated at the middle point of this. The EPR parameters corresponding to the best resolved spectra are presented in Table 1.

x	$A_{\parallel} \pm 5.6$ (Gs)	$g_{\parallel}$ $\pm 0.0045$	$A_{\perp} \pm 1.4$ (Gs)	$g_{\perp}$ $\pm 0.0008$
0.3	151.58	2.3324	25.25	2.0536
0.5	147.03	2.3304	25.25	2.0552
1.0	145.90	2.3286	25.25	2.0513
2.0	145.91	2.3262	24.69	2.0479
3.0	144.88	2.3219	25.25	2.0464

Table 1. The EPR parameters of the  $\text{Cu}^{2+}$  absorptions in  $x\text{CuO} \cdot (1-x)[\text{Na}_2\text{O} \cdot 2\text{B}_2\text{O}_3]$  glasses with  $0.3 \leq x \leq 3$  mol %.

The separation between the hfs peaks increases as the magnetic field increases. For the  $0.003\text{CuO} \cdot 0.997[\text{Na}_2\text{O} \cdot 2\text{B}_2\text{O}_3]$  sample, the estimated values of the field separations between the parallel peaks were 219.07 Gs, 151.58 Gs, 179.58 Gs and those between the perpendicular ones were 19.64 Gs, 25.25 Gs and 33.67 Gs. This effect imposes second order approaches in the theoretical treatment of the EPR absorption.

Another characteristic of these absorptions is the progressive broadening of the parallel hf peaks in m order, the nuclear magnetic quantum number corresponding to each transition of the hfs. The peak-to-peak width of the hfs lines recorded for

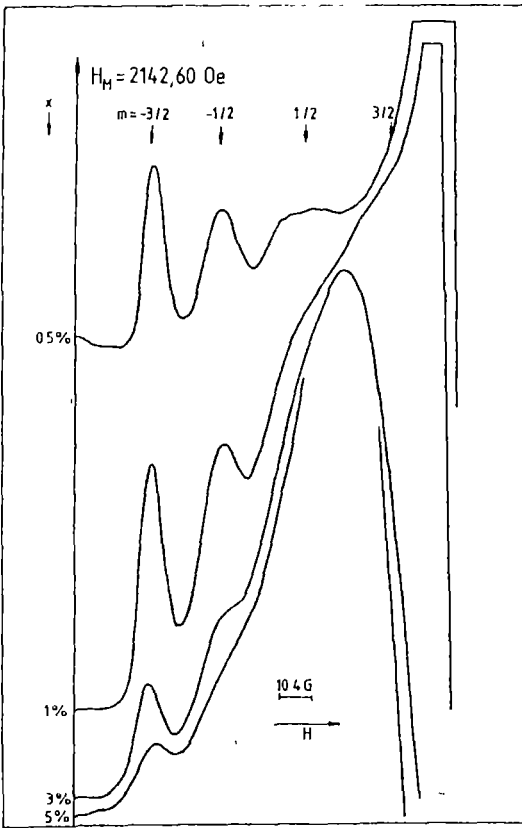


Fig 2 a

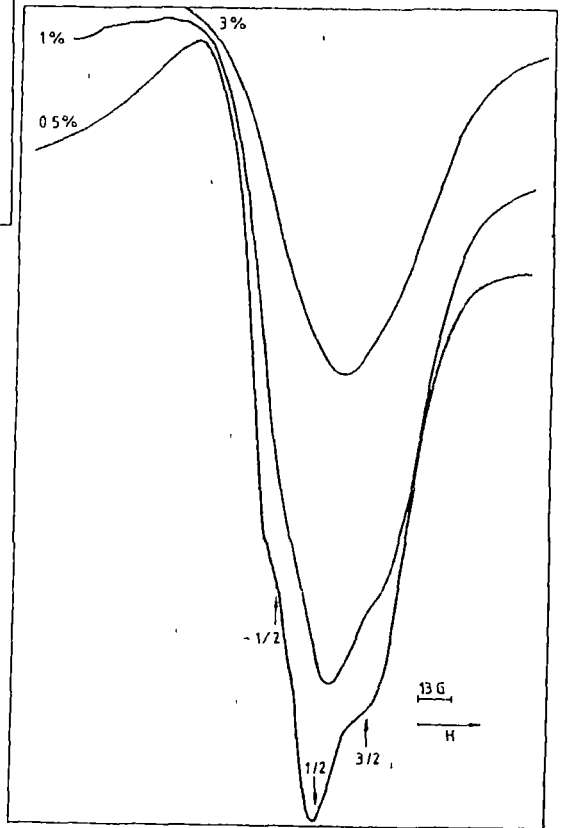


Fig 2 b

Fig.2. EPR absorptions of  $\text{Cu}^{2+}$  ions in the  $x\text{CuO} \cdot (1-x)[95\text{TeO}_2 \cdot 5\text{PbO}]$  glasses with  $0.5 \leq x \leq 5$  mol % for both parallel (a) and perpendicular (b) absorption bands.

the  $0.003\text{CuO} \cdot 0.997[\text{Na}_2\text{O} \cdot 2\text{B}_2\text{O}_3]$  samples, varies as 65.09 Gs, 89.79 Gs and 112.24 Gs. Together with the dipolar broadening, this effect reduced the spectral resolution, so as for  $x > 9$  mol % a large envelope superimposes the spectrum.

For glasses corresponding to the  $x\text{CuO} \cdot (1-x)[95\text{TeO}_2 \cdot 5\text{PbO}]$  system the concentration range for  $\text{Cu}^{2+}$  ions in axial symmetric environments is much more restricted. The spectral resolution is optimal only at the lowest limit of the investigated concentration range ( $x = 0.5$  mol %). The parallel hfs is partially resolved, but the perpendicular one has a weak resolution. As rising concentration, the broadening of the hfs components results in a nonresolved absorption line and for  $x > 5$  mol %, the spectrum is reduced to the characteristic large envelope. The features of these spectra are given in Fig.2. This compositional dependence of the spectral resolution affect the accuracy of the determined EPR parameters. The calculated  $g$  values are presented in Table 2.

$x$	$g_{\parallel}$	$g_{\perp}$
0.5	2.2724	2.0467
1.0	2.2383	2.0520
3.0	2.2845	2.0566
5.0	2.2844	2.0751

Table 2. EPR parameters of the  $\text{Cu}^{2+}$  spectra in  $x\text{CuO} \cdot (1-x)[95\text{TeO}_2 \cdot 5\text{PbO}]$  glasses with  $0.5 \leq x \leq 5$  mol %.

The spectral resolution was optimal for the  $0.005\text{CuO} \cdot 0.995[95\text{TeO}_2 \cdot 5\text{PbO}]$  sample, the corresponding separation between the resolved parallel hf peaks was estimated as 112.27 Gs, and 150.91 Gs and their peak-to-peak width as 41.77 Gs, 62.66

Gs, and 99.218 Gs.

For  $10 \leq x \leq 20$  mol % the EPR absorption spectrum for tellurite glasses changes essentially. Its features are presented in fig. 3.

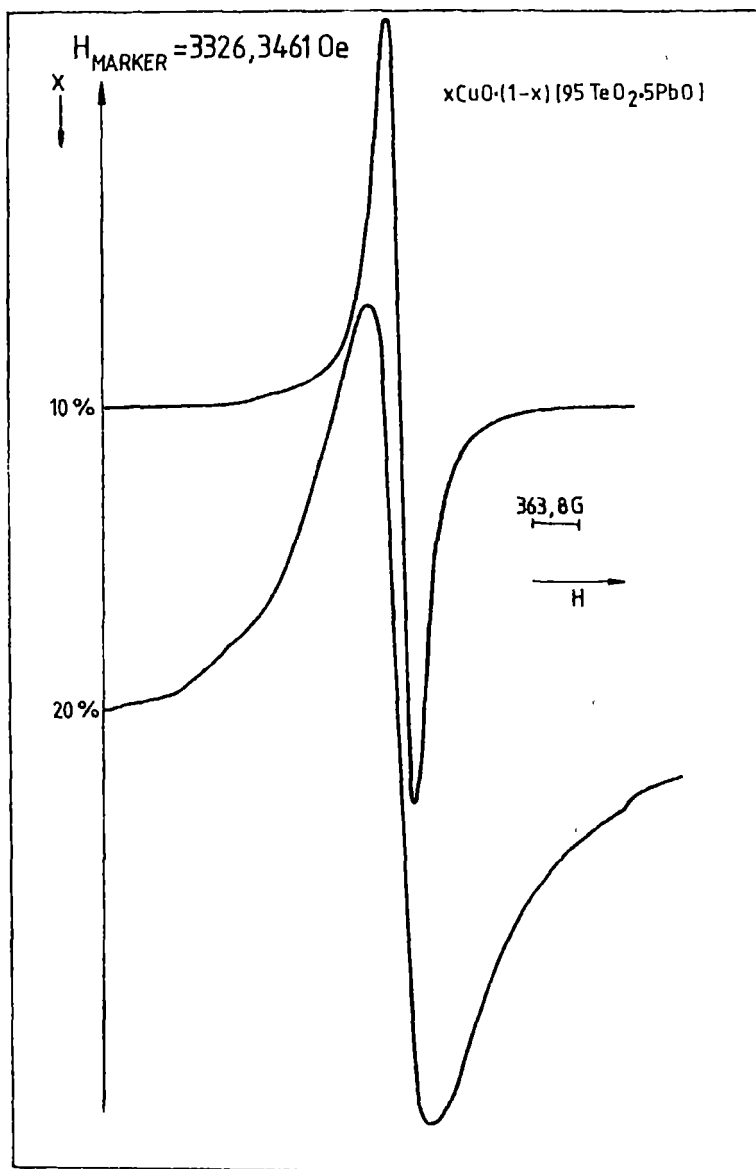


Fig.3. EPR absorptions of  $\text{Cu}^{2+}$  ions in the  $x\text{CuO} \cdot (1-x)[95\text{TeO}_2 \cdot 5\text{PbO}]$  glasses with  $10 \leq x \leq 20$  mol %.

The EPR parameters, that is the line amplitude  $I$ , the line width  $\Delta H$ , and the intensity of the absorption approximated as  $J = I \cdot \Delta H^2$ , are presented in

Fig 3

Table 3. The absorption line becomes a symmetric one as the results of the great degree of disorder which characterises now

the structure of the vitreous matrix.

x	I (arb.units)	$\Delta H$ (Gs)	J (arb.units)	g
10	54.67	247.43	334.71	2.1927
15	30.59	302.01	279.03	2.0821
20	12.67	542.17	372.47	2.0638

Table 3. The parameters of the  $\text{Cu}^{2+}$  absorptions for  $x\text{CuO} \cdot (1-x)[95\text{TeO}_2 \cdot 5\text{PbO}]$  glasses with  $10 \leq x \leq 20$  mol %.

**4. Discussions.** For both types of glasses, at low impurities content, the shape and structure of the EPR absorption line are typical for isolated  $\text{Cu}^{2+}$  ions in predominantly axial symmetric environment. Usually, these spectra are analysed in terms of the spin hamiltonian:

$$\mathcal{H} = g_1 \beta H_z S_z + g_1 \beta (H_x S_x + H_y S_y) + A_1 S_z I_z + A_L (S_x I_x + S_y I_y) \quad (1)$$

where z is the symmetry axis of the individual  $\text{Cu}^{2+}$  centers. Two series of lines, each consisting in four peaks, are designated as parallel hf peaks, respectively perpendicular ones, because they originate in the resonance of those centra maintaining their axis of symmetry parallel, respectively perpendicular to the static magnetic field.

The spin hamiltonian (1) gives generally, a satisfactory approximation for the line shape of the EPR spectra. There are some features of the experimental spectra, pointed out in the previous paragraph, which impose a refined theoretical treatment. For obtaining the hfs peaks position, related to the principal values of the g and A tensors, one uses the solution of the above spin hamiltonian (1), in the second order approach, which may explain the lack of equidistancy of the hfs peaks on the



experimentally obtained absorptions. These are:

$$h\nu = g_{\parallel}\beta H + mA_{\parallel} + \left(\frac{15}{4} - m^2\right) \frac{A_{\parallel}^2}{2g_{\parallel}\beta H} \quad (2)$$

for the parallel peaks, and

$$h\nu = g_{\perp}\beta H + mA_{\perp} + \left(\frac{15}{4} - m^2\right) \frac{A_{\perp}^2 + A_{\parallel}^2}{4g_{\perp}\beta H} \quad (3)$$

for the perpendicular ones. Relations (2) and (3) give the theoretical values for  $g$  and  $A$ , calculated from positions of the best resolved hfs peaks.

Being better resolved and extended on a larger field range the parallel hfs offers more possibilities to investigate the effects of the vitreous matrix composition on the resonance phenomenon and, therefore, more experimental informations than the perpendicular one. The perpendicular hfs is more sensitive to the matrix composition and the content of paramagnetic ions and consequently its resolution is overpassed by the  $|A_{\perp}|$  values.

The calculated  $g_{\parallel}$  and  $g_{\perp}$  values satisfy the relation  $g_{\parallel} > g_{\perp} > g_e \approx 2.0023$  which characterises the  $\text{Cu}^{2+}$  ions coordinated by six ligand atoms in a distorted octahedron, elongated along one axis. This configuration allows a LCAO MO analysis of the EPR absorption spectra [12]. By estimating the covalency effects in the field of ligands, the possibility of revealing its changes determined by the chemical composition of the vitreous matrix is obtained. The correlation between the covalency degree of the bonds involving  $\text{Cu}^{2+}$  ions and the glass composition allow to compare the strength of bondings between the oxygen ligands and the network forming cation in its neighbourhood, and the ligand bonds acting as an electron donor upon the cupric ion. Because the  $\text{Cu}^{2+}$  ion is a network modifier, there is a competition in the  $\text{Cu}^{2+}$ -O-X bonds, between  $\text{Cu}^{2+}$  and the neighbouring network forming

cations X, in attracting the isolated oxygen ions pairs available in their vicinity (X = B, Si, P, etc.). In the sodium-borate glasses the convalency of Cu<sup>2+</sup>-O bonds increases when the strength of B-O bonds diminishes.

A characteristic of the Cu<sup>2+</sup> ions EPR spectra in the investigated sodium-borate and tellurite matrices, is that of the gradual broadening of the parallel hf peaks along the recorded spectrum. Therefore, the theoretical treatment has to take into account the ligand field fluctuations from a cupric complex to another in the amorphous matrix, as a predominant factor in the line broadening [10]. The fluctuations of the field in which resonate the parallel complexes may be expressed having in view the fluctuation of g<sub>⊥</sub> and A<sub>⊥</sub>, as:

$$dH = -\frac{1}{g_{\perp}\beta} \left[ hv \frac{dg_{\perp}}{g_{\perp}} + mA_{\perp} \left( \frac{dA_{\perp}}{A_{\perp}} - \frac{dA_{\parallel}}{A_{\parallel}} \right) \right] \quad (4)$$

The peak width ΔH(m) is related to the variation δg<sub>⊥</sub> of the g<sub>⊥</sub> values by:

$$\Delta H(m) = \delta g_{\perp} \frac{hv + m(g_{\perp}P - A_{\perp})}{g_{\perp}^2\beta} \quad (5)$$

where P = 2γββ<sub>N</sub><r<sup>-3</sup>> is 0.036 cm<sup>-1</sup>.

In the studied vitreous systems xCuO.(1-x)[Na<sub>2</sub>O.2B<sub>2</sub>O<sub>3</sub>] and xCuO.(1-x)[95TeO<sub>2</sub>.5PbO] the A<sub>⊥</sub> values calculated for the best resolved spectra, show preponderent ionic bondings of the paramagnetic ion with the neighbour ligand atoms. There is a little increasing in covalency of these bonds, as a result of rising the Cu<sup>2+</sup> content in the vitreous matrix. In the sodium-borate glasses, the Δg<sub>⊥</sub> values decrease from 0.3301 as the CuO content in the sample increases along the range 0.3 ≤ x ≤ 3 mol% and those of Δg<sub>⊥</sub> from 0.0513 to 0.0441 on the same concentration

range. The unpaired electron becomes more and more delocalized and the interaction with the nuclear spin  $I = 3/2$  becomes more intense. The fluctuations in the ligand field determine the progressive broadening of the hfs peaks.

Despite of these features, a great stability of the sodium-borate matrix structure at the impurities accumulation over the investigated concentration range, may be ascertained. The EPR absorption show  $\text{Cu}^{2+}$  ions in predominantly axial symmetric vicinities. There are distortions of the structural aggregates involving the paramagnetic ions, inherent to the amorphous state but these distortions do not affect essentially the  $\text{Cu}^{2+}$  ions neighbourhood.

The ligand field fluctuations are much more pronounced in the tellurite matrices where the broadening of the individual peaks of hfs appear at a relatively low  $\text{Cu}^{2+}$  ions content, the bonding with the ligands is more covalent, and the long range interactions become stronger. At concentrations over 10 mol %  $\text{CuO}$ , the axial vicinity of the paramagnetic ion is destroyed, the absorption line symmetrizes and the g factor's value becomes closer to the  $g_e$ . All these spectral features show a high disorder degree characterising the glass structure. The  $\text{Cu}^{2+}$  ions are involved in distorted aggregates having a predominantly octahedral coordination.

**5. Conclusion.** The EPR absorption spectra due to  $\text{Cu}^{2+}$  ions in the  $x\text{CuO} \cdot (1-x)[\text{Na}_2\text{O} \cdot 2\text{B}_2\text{O}_3]$  glasses, for  $0.3 \leq x \leq 25$  mol % revealed well resolved hfs for both centers, having parallel and perpendicular spin, typical for isolated  $\text{Cu}^{2+}$  in axial symmetric

vicinities. These characteristics are more pronounced at low  $\text{Cu}^{2+}$  ions content. Second order effects have to be taken into account in order to explain the increasing of separation between the hfs peaks. Fluctuations of the ligand field in the  $\text{Cu}^{2+}$  ion environment cause the progressive broadening of the parallel hf peaks.

The EPR absorptions due to  $\text{Cu}^{2+}$  ions in the tellurite system  $x\text{CuO} \cdot (1-x)[95\text{TeO}_2 \cdot 5\text{PbO}]$  for  $0.5 \leq x \leq 20$  mol % revealed a strong dependence of their structure, and the values of EPR parameters, on glass composition. At low  $\text{CuO}$  content, resonances due to isolated  $\text{Cu}^{2+}$  in axially distorted environment were detected, having the hfs better resolved in the parallel band than in the perpendicular one of the EPR spectrum. The pronounced fluctuations in the ligand field broaden the absorption lines so that the hfs is rapidly smeared out as rising concentration. In the high concentration range the absorption line becomes a symmetric one, corresponding to  $\text{Cu}^{2+}$  in distorted octahedral environment. The matrix is now characterised by a high degree of disorder.

The structure of the sodium-borate matrix is more stable than that of the tellurite one at the impurities'accumulation in its composition.

The bonds of  $\text{Cu}^{2+}$  with the ligand atoms are predominant ionic in both glasses. A small increasing of their convalency was observed as rising concentration of  $\text{Cu}^{2+}$  ions in the matrix.

R E F E R E N C E S

1. V.S.Kozhouharov, M.P.Marinov, G.Grigorova, *J.Non-Cryst. Solids* **28**, 429 (1973).
2. V.S.Kozhouharov, M.P.Marinov, T.Troev, *Mat. res. Bull.* **14**, 735 (1979).
3. Al.Nicula, M.Peteanu, I.Ardelean, *Studia Univ. "Babeş-Bolyai", Physica* **2**, 65 (1979).
4. I.Ardelean, Gh.Ilonca, M.Peteanu, D.Pop, *Solid State Commun.* **33**, 653 (1980).
5. I.Ardelean, M.Peteanu, Gh.Ilonca, *Phys. Stat. Sol. (a)* **V58**, K33 (1980).
6. I.Ardelean, Gh.Ilonca, M.Peteanu, *J. Non-Cryst. Sol.* **51**, 389 (1982).
7. M.Peteanu, I.Ardelean, Al.Nicula, *Rev. Roum. Phys.* **28**, 47 (1983).
8. M.Peteanu, E.Trif, Al.Nicula, *Materiale de construcții* **14** (4), 211 (1984).
9. M.Peteanu, I.Ardelean, *Studia Univ. "Babeş-Bolyai"* **26**(2), 79 (1990).
10. H.Imagawa, *Phys. Stat. Sol.* **30**, 469 (1968).
11. H.Kawazoe, H.Hosono, H.Hokumai, *J.Non-Cryst. Solids* **40**, 291 (1980).
12. D Kivelson, R.Neiman, *J.Chem. Phys.* **35**, 149 (1961).



MAGNETIC FIELD-RELATED HYSTERETIC EFFECTS IN THE  $1/f$  NOISE  
OF THE  $\text{YBa}_2\text{Cu}_3\text{O}_{7-x}$  BULK SUPERCONDUCTORS

A. STEPANESCU\*, P. MAZZETTI\*, A. MASOERO\*\*, I. STIRBAT\*\*\*, I. POP\*\*\*\*, G. CONE\*\*\*\*

Received: 15 06 1992

**ABSTRACT.** - Experimental results about the hysteretic behaviour of the current noise in  $\text{YBa}_2\text{Cu}_3\text{O}_{7-x}$  specimens, having a low critical current, obtained by increasing or decreasing of magnetic field at liquid-nitrogen temperature are presented. A qualitative statistical model, based on the percolation theory, which could explain this new hysteretic effect on current noise, is proposed.

**1. Introduction.** A periodic function of time  $F_c(t)$  can be expanded into a Fourier series. Let  $F_c$  be its average value. The component of  $F_c(t) - F_c$ , at frequency  $f$ , has a constant amplitude  $a_r$ , independent of time. If  $F_c(t)$  is not a periodic function, it cannot be expanded into a Fourier series, but can be expanded into a Fourier integral. Its component at frequency  $f$  (within small bandwidth  $\delta f$ ) has in that case a constant amplitude  $a_r$ .

Let us consider a random function  $F_r(t)$ , of average value  $F_r$ . In that case,  $F_r(t) - F_r$  can be expanded into a Fourier-Stieltjes integral, and its component at frequency  $f$ , within the band with  $\delta f$ , is now a random function of time  $a_r(t)$ . The average amplitude, or its square average is

$$S_r(f) \delta f = \overline{|a_f(t)|^2} = \overline{a_f(t) a_f^*(t)} \quad (1)$$

where (\*) means complex conjugate.  $S_r(f)$  is the noise spectral density of  $F_r(t)$ .

---

\* Dipartimento di Fisica del Politecnico di Torino, Corso Duca degli Abruzzi 24, Torino, Italy.

\*\* Istituto Elettrotecnica Nazionale "Galileo Ferraris", C.so Massimo D'Azeglio 42, Torino, Italy.

\*\*\* Institute of Electrotechnical Researches, Bucharest, Romania

\*\*\*\* Polytechnic Institute of Bucharest, Physics Department, Splaiul Independenței 313, Bucharest, Romania.

Filtering at frequency  $f$  within the bandwidth  $\delta f$  gives

$$|a_f(t)|^2 \quad (2)$$

and finally an integration gives an output signal proportional to

$$|\overline{a_f(t)}|^2 \quad (3)$$

that is proportional to  $S_r(f)$ .

The occurrence of  $1/f$  type noise generally indicates the presence of hot spots, defects, failures in the technology [1]. The study of  $1/f$  noise is very important because its universal character and its direct relations to practical applications.  $1/f$  noise measurements have been performed by several groups of researchers on various copperoxide superconductors [2-6]. To date, the mechanism of  $1/f$  noise in this materials have not been identified, but various speculative models have been proposed [7].

The purpose of this paper is to present the experimental data of the current noise in the (1:2:3) high  $T_c$  superconductors submitted to a variable magnetic field, to discuss its hysteretic behaviour and its possible origin.

**2. Experimental results and discussions.** We report the results of the measurements of the current noise in the bulk sintered samples of  $YBa_xCu_3O_{7-x}$ . These were prepared by mixing  $BaO$ ,  $Y_2O_3$  and  $CuO$  powders in the stoichiometric proportions. This mixture was grounded and heated at  $925^\circ C$  in air for 24 h and after that regrounded. This process was repeated for three times under identical conditions. The substance prepared was then pressed into pellets, sintered at  $950^\circ C$  in flowing  $O_2$  for 72 h



and slowly cooled in the furnace to the room temperature.

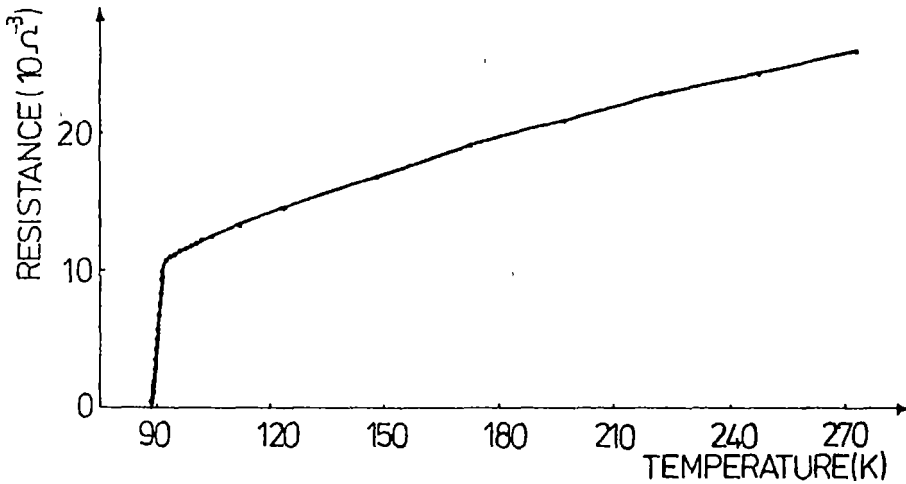


Fig. 1. The electrical resistance vs. the temperature for YBa<sub>2</sub>Cu<sub>x</sub>O<sub>7-x</sub>.

The electrical resistivity vs. temperature was measured using the standard DC four-probe technique. The probing current was of 1 mA and the electrical contacts were made with silver paste. The noise spectral density was measured in the frequency range (0,125 - 300) Hz using a cross-correlation method [8] and injecting in sample a current of 5 mA. The spectrum was obtained by using a two channel signal analyzer, taking the cross spectrum at the outputs of two noise amplifiers, whose inputs were connected with the voltage contacts of the probe. The measurements in the superconducting state were performed by immersing the sample in liquid-nitrogen.

In Figure 1 it is represented the electrical resistance vs temperature. At the room temperature this resistance is about

$25 \cdot 10^{-3}$  Ohm and at 92 K (onset of the superconducting state) is  $104 \cdot 10^{-4}$  Ohm. The superconducting critical temperature, determined by the resistivity measurement is 91 K with a transition width of about 1.6 K. The sample has a metallic quasi-linear temperature dependence above the value 92K of the temperature. The critical current density of the sample is about  $29 \cdot 10^2 \text{A} \cdot \text{m}^{-2}$ .

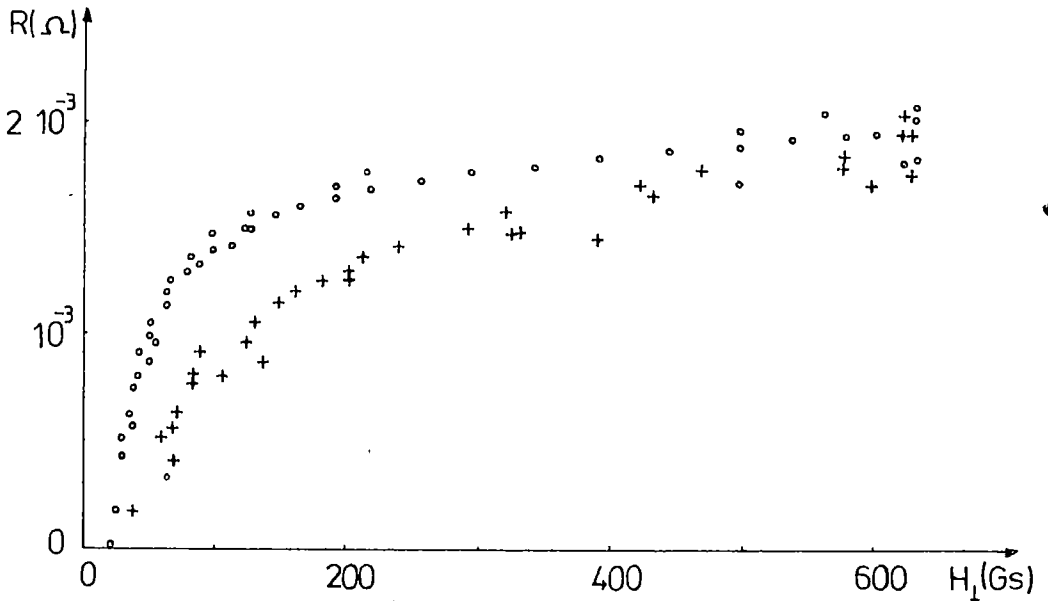


Fig.2. The electrical resistance vs. the increasing and decreasing magnetic field for  $\text{YBa}_2\text{Cu}_x\text{O}_{7-x}$ . It is evident the hysteretical behaviour.

The shape of the noise power-spectrum in normal state and in the superconducting state was of the  $1/f$  type, with  $\alpha$  in the 0.87-1.15 range as in [6,9]. This shape, close to the  $1/f$  type, is influenced very little by the presence of the magnetic field, this suggesting that the  $1/f$  type noise power-spectrum is an intrinsic property of these materials.

In Figure 2 it is shown the behaviour of the resistance value, which has been measured on the same sample immediately after the noise spectra measurement, when the magnetic field was looped between 20 Gs and 630 Gs. It can be seen that the same value of the resistance is obtained for two different values of the magnetic field, depending on whether the magnetic field is being increased or decreased.

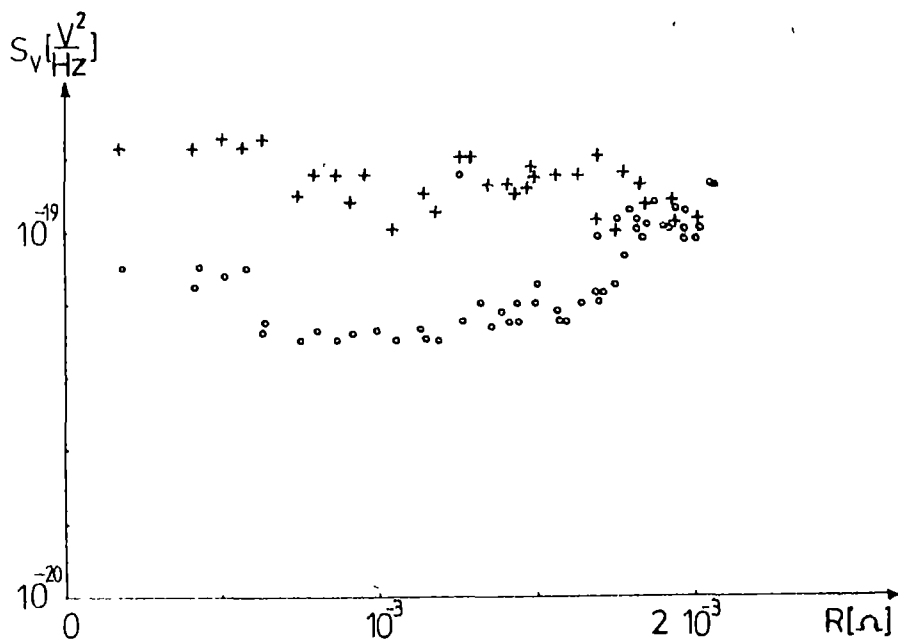


Fig. 3. The current-noise spectral density vs. the increasing and decreasing magnetic field for  $\text{YBa}_2\text{Cu}_x\text{O}_{7-x}$ . It is evident the effect of hysteresis.

Figure 3 shows the results of the noise spectral density at 30 Hz vs. electrical resistance for both an increasing (lower branch) and a decreasing (upper branch) magnetic field. The hysteretic behaviour of the noise shows that the same value of the electrical resistance corresponds, in the two cases, to a different physical situation of the conduction. It can be

observed that the intensity of the spectral density depends on the way that this resistance value has been obtained.

The possible origin of this observable hysteretical behaviour lies in the heterogeneous nature of this material. To the liquid nitrogen temperature and minimum magnetic field the sample is completely in the superconducting state. By increasing the applied magnetic field the material starts to pass to a mixed state. We can say that the material is composed of grains of superconductor embedded in a nonsuperconducting host that can be of a variety of materials: insulator, semiconductor, normal metal, or superconductor with a lower transition temperature, all of this having a resistive nature. Between the superconductor grains there are weak couplings that are partially destroyed when a magnetic field is applied and a thin layer beginning at the grains surface transits to the mixed state. The fluxoids which begin to penetrate the both type of regions have a different mobility in these. So, the fluxoids which penetrate in the weak superconducting regions are weakly trapped by the pinning strength and a little current density is necessary to give rise to the movement of the fluxoids, which is a source of dissipative effects. The fluxoids which penetrate in the strongly superconducting regions are trapped inside these regions by strong pinning strength, at the high magnetic fields. Consequently, below the percolation threshold, this material presents an equivalent resistance owing to the fluxoids mobility and the noise is a result of the fluctuations of the mobility and/or of the density of this mobile fluxoids from the weak superconducting regions. From this point of view there exists a

certain similarity with the noise generated in discontinuous thin films [10-12] for which it has been found that for the same resistance value and the same current density a structure of large islands was more noisy than other structures characterized by little islands.

When the intensity of the magnetic field is decreasing the real field inside the superconductor is the sum of the applied field and the demagnetizing field created by the trapped fluxoids in the strongly superconducting regions. In this way there are large regions where the resulting field is close to zero and the resistance decreases more rapidly than in the situation when the applied field was increasing and producing the hysteretical behaviour of the electrical resistance. At the same time this induces some larger superconducting regions with a more irregular boundaries, on the another directions as that of the applied field. Therefore, even the weak superconducting regions become more irregular. This influences the mobility of the fluxoids and in this way the intensity of the noise. The observed hysteresis of the current noise spectral density, depending whether the magnetic field is increasing or decreasing, seems to be the result of the structure modification of the superconducting islands and of their boundaries. In this way the noise measurements can be a good method for the observation of the islands modification and so a test for making evident the internal sample demagnetizing effects.

**3. Conclusions.** Our measurements on  $\text{YBa}_x\text{Cu}_x\text{O}_{7-x}$  reconfirmed a hysteresis of the noise vs. the electrical resistance

analogical with that reported in [6] in the samples that present a critical current more little.

This hysteretic effect is possible due to the inhomogeneous structure of the material and the noise measurements may be a good investigation tool for obtaining important informations about the modification of this structure when the applied magnetic field is varied.

It can be anticipated that our experimental results are useful for the development of a percolation model for the high temperature superconductors.

#### R E F E R E N C E S

1. J.P.Nougier, *Microelectronics*, Preprinted from European Materials Research Society Monograph, vol.2, 185 (1991).
2. J.A..Testa, Y.Song, X.D.Chen, J.Golbe, S.I.Lee, B.R.Patton and J.R.Gainnes, *Phys. Rev.*, B 38, 2922 (1989).
3. A.Maeda, J.Nakayama, S.Takebayashi and K.Uchinokura, *Physica*, C 160, 443 (1989).
4. Y.Song, A.Misra, Y.Cao, A.Querubin Jr.X.D.Chen, P.P.Crooker and J.R.Gainnes, *Physica*, C 172, 1 (1990).
5. Y.Song, A.Mistra, P.P.Crooker and J.R.Gainnes, *Phys. Rev. Lett.*, 66, 825 (1991).
6. M.Celasco, A.Masoero, P.Mazzetti and A.Stepanescu, *Phys. Rev.*, B 44, 5366 (1991).
7. L.Wang, Y.Zhen, H.Zhao and S.Feng, *Phys. Rev. Lett.*, 64, 3094 (1990).
8. F.Abbattista, C.Appino, A.Masoero, P.Mazzetti, A.Stepanescu and M.Vallino, *Phys. Stat. Sol.(b)*, 164, 253 (1991).
9. K.Takagi, T.Mizunami, H.Okayama and S.Yang, *IEEE Trans. Comp. Hybrids Manuf. Technol.*, 13, 2, 303 (1990).
10. M.Celasco, A.Masoero, P.Mazzetti and A.Stepanescu, *Phys. Rev.*, B 17, 2564, 3040 (1978).
11. D.A.Rudman, J.J.Calabrese and J.C.Garland, *Phys. Rev.*, B 33, 1456 (1986).
12. J.W.Mantese, W.I.Goldeburg, D.H.Darling, H.G.Craighead, U.J.Gibbson, R.A.Buchrman and W.W.Webb, *Solid State Comm.*, 37, 353 (1981).

THE GHINZBURG-LANDAU THEORY AND THE SUPERCONDUCTIVITY  
AT HIGH TEMPERATURE

I. POP\*, I. STIRBAT\*\*, G. CONE\*, I. M. POPESCU\*, A. STEPANESCU\*\*\*

Received: 7 03.1992

**ABSTRACT.** - The analysis of the Ginzburg-Landau theory and of the superconductivity at high temperature are made in terms of the thermodynamic fluctuations. For comparing the theory with experiment, the results about the paraconductivity of  $\text{YBa}_2\text{Cu}_3\text{O}_{7-x}$  specimens are presented.

**1. Introduction.** The experimental results obtained in the least years for high temperature superconductors (HTSC) show two relevant aspects: the insufficient knowledge of the physical phenomenon and, consequently, the absence of an adecvated theory.

In the absence of a more complete theory, it is necessary to test the phenomenological theories which try to explain certain properties of ceramic superconductors. The Ginzburg-Landau (G-L) theory is considered as a successfull in understanding the properties of classical superconductors. The motivation of the present work is to study if the limits of this theory may be admissible in the analysis of superconductivity at high temperature.

**2. The limits of Ginzburg-Landau theory.** In the G-L theory [1] one assumes that the free-energy density may be expanded in therms of the order parameter  $\psi$ :

$$f = \alpha |\psi|^2 + \frac{1}{2} \beta |\psi|^4 + \frac{1}{2m} \left| \left( \frac{\hbar}{i} \nabla - \frac{2e\bar{A}}{c} \right) \psi \right|^2 + \frac{H_1^2}{8\pi} \quad (1)$$

where  $\alpha$  and  $\beta$  are regular functions of temperature  $T$ ,  $m$  is the

---

\* Polytechnic Institute of Bucharest, Physics Department, Splaiul Independenței 313, Bucharest, Romania

\*\* Institute of Electrotechnical Researches, Bucharest, Romania.

\*\*\* Politecnico di Torino, Dipartimento di Fisica, Corso Duca degli Abruzzi 24, Torino, Italy.

electronic mass,  $e$  is the electrical charge,  $\vec{A}$  is the vector potential and  $H_i$  is the internal magnetic field. The coefficients  $\alpha$  and  $\beta$  have also been deduced from the microscopic theory, in the similar conditions with that will be discussed further on. For pure materials, Gorkov obtained

$$\alpha(T) = \alpha_0 \left( \frac{T - T_{CO}}{T_{CO}} \right) = 1.83 \frac{\hbar^2}{2m} \frac{1}{\xi_0^2} \left( \frac{T - T_{CO}}{T_{CO}} \right) \quad (2)$$

$$\beta = 0.35 \frac{1}{N(0)} \left[ \frac{\hbar^2}{2m\xi_0^2} \right]^2 \frac{1}{(K_B T_{CO})^2} \quad (3)$$

with

$$\xi^2(T) = -\frac{\hbar^2}{2m\alpha(T)} \quad (4)$$

where  $\xi$  is the coherence length,  $N(0)$  is the density of the states on the Fermi level and  $T_{CO}$  represent the critical temperature [2].

By minimizing the free energy for variation of the order parameter  $\psi$  and of the magnetic field  $\vec{H}_i$ , one obtains the two equations of G-L theory, with a local relation between the current and the vector potential  $\vec{A}$ . These approximations will be valid only if  $\vec{H}_i$  and  $\vec{A}$  are slowly varying functions over distances of the order of  $\xi_0$  and is equivalent with:

$$\lambda(T) \gg \xi_0 \quad (5)$$

Actually, in pure metallic superconductors, at a constant  $|\psi|$  and at a small value of  $\vec{H}_i$ , the current  $\vec{J}(\vec{r})$  depends on  $\vec{A}(\vec{r}')$  for distances  $|\vec{r} - \vec{r}'| \sim \xi_0$ . The limit expressed by eq. (5) may be evaluated using the Gorkov expression for  $\alpha$  and  $\beta$  in the G-L penetration depth  $\lambda_{GL}$ . The condition (5) may be written as:



$$\frac{|T-T_{co}|}{T_{co}} < 1 \quad (6)$$

A similar limit is obtained if one analyzes the variation of the order parameter. In the G-L theory,  $\psi$  must be a slowly varying function over distance of the order of  $\xi_0$ . Such a necessary condition for the validity of the theory is

$$\xi(T) \gg \xi_0 \quad (7)$$

which leads to the same restriction, expressed by eq.(6).

The main limit introduced in the G-L theory consists in the "rigidity" of the order parameter; more precisely, one assumes that  $|\psi|$  is constant and one neglects the fluctuation effects. However, the fluctuations can be treated approximately, as long as they are small, [3]. If the fluctuation in the superconducting order parameter is large, compared with itself, the G-L theory is not expected to be valid in a narrow range of temperature, very close to  $T_c$ , defined by the Ginzburg criterion [4].

In the absence of magnetic field, this criterion is:

$$\frac{|T-T_{co}|}{T_{co}} < \frac{1}{32\pi^2} \frac{\beta^2}{\alpha_0} \left[ \frac{2m}{h^2} \right]^3 (K_B T_{co})^2 \quad (8)$$

This equation may be evaluated for superconducting materials by using the G-L theory results for  $H_c(T)$ ,  $H_{c2}(T)$ ,  $k_{GL}$  (ratio of the penetration depth to the coherence length),  $\xi(T)$  and the expression of superconducting flux quantum:

$$|T - T_{co}| < 10^{-9} \frac{k_{GL}^4 T_{co}^3}{H_{c2}(0)} \quad (9)$$

with  $T_{co}$  measured in kelvin and  $H_{c2}(0)$  in G. Typical values for classical superconductors are  $|T - T_{co}| < 10^{-6}K$ . In the case of an anisotropic material,  $k_{GL}$  and  $H_{c2}(0)$  are replaced by their geometric means in this expression of critical region.

The strong dependence of the temperature interval on  $T_{CO}$ , defined by eq. (9), suggests that HTSC have wider critical regions than conventional superconductors. The extrapolation of experimental results situates  $H_{c2}(0)$  in the domain 500 kG - 1500 kG and  $k$  in the interval 50 - 200 [5,6]. For the mean values  $H_{c2}(0) = 1000$  kG,  $k = 125$  and  $T_{CO} = 100$  K one obtains  $|T - T_{CO}| \approx 0.26$ . If there are used the extreme values indicated above, one obtains the limits for critical region as 1.96 K and 8 mK respectively.

**3. Paraconductivity in HTSC materials.** The study of the temperature dependence of the electrical resistivity, particularly near  $T_c$  and  $T > T_c$  provides useful informations about some of the fundamental aspects of the superconducting materials. The rounding of the resistivity curve close to  $T_c$  may be explained, also for high HTSC, in terms of thermodynamic superconducting fluctuations. In this analysis  $T_c$  represents the experimental value of critical temperature.

Because of their higher transition temperatures, compared to the conventional superconductors, the effect of the thermodynamic fluctuations is manifested more strongly for the physical properties of ceramic superconductors as diamagnetism, electrical conductivity, specific heat or thermoelectric power, [7,8,9].

The thermodynamic fluctuation effects on the electrical conductivity of HTSC have been reported by several groups, [9,10], but the conclusions about dimensionality seem to be highly controversial. Ambiguous values of the temperature

dependence of the excess conductivity result from the absence of an unified model for the temperature dependence of the resistivity in the normal phase. The choice and the imprecise location of critical temperature modify the conclusions about the dimensionality of the fluctuations also.

Aslamazov and Larkin [11] predicted that the excess of conductivity  $\Delta\sigma$  above  $T_c$ , due to the electron pairing, is:

$$\frac{\Delta\sigma}{\sigma_0} = C\varepsilon^\lambda \quad (10)$$

where  $\Delta\sigma = \sigma_{\text{measured}} - \sigma_{\text{background}}$ ,  $\sigma_a$  is the room temperature conductivity,  $\varepsilon = (T - T_c)/T_c$ . The critical exponent  $\lambda$  and the constant  $C$  depend on the dimensionality of the fluctuations: for the threedimensional system (3D)  $\lambda = -1/2$ ,  $C = e^2/(32h \xi(0)\sigma_0)$  and for bidimensional system (2D)  $\lambda = -1$ ,  $C = e^2/(16hd\sigma_0)$  with  $d$  being a characteristic length.

In the absence of a more complete theory for critical phenomena in HTSC, Lobb, [12], uses the physical arguments (analogy with the normal conductivity above the lambda normal-superfluid transition in liquid He) and the dynamic theory ideas. On suggests that, for 3D, eq.(10) may be a reasonable approximation for  $\Delta\sigma$  in the so called mean field ( $\lambda = -1/2$ ), cross over ( $\lambda = -1/2$ ), cross over ( $\lambda = -2/3$ ) and full critical ( $\lambda = -1/3$ ) regions closer to  $T_c$ . Now, these critical regions are accesible experimentally for HTSC. For a fixed  $T_c$ , from  $\ln(\Delta\sigma/\sigma_0)$  vs  $\ln(\varepsilon)$  one gets both  $\lambda$  and  $C$  and one can draws conclusions about the dimensionality of the fluctuations.

The excess electrical conductivity may be estimated using the metallic behaviour at  $T > T_c$  for variation of the resistivity

with T:

$$\rho(T) = a + bT \quad (11)$$

or Anderson-Zou [13] relation (A-Z)

$$\rho(T) = AT + \frac{B}{T} \quad (12)$$

which takes care of the metallic conductivity in the Cu-O planes and the semiconducting behaviour for conduction process between planes and across the grain boundaries. In both methods, the background conductivity is estimated from the extrapolation at temperatures  $T_c < T < 2T_c$ .

**4. Experimental results.** We have studied the fluctuation effects on samples of  $YBa_2Cu_3O_{7-x}$  which were prepared by the standard ceramic method using constituent oxides of 99.99% purity with identical starting conditions for grinding, pelletising and intermediate heat-treatments.

The variation of the electrical resistivity with temperature was measured using the four - probe d.c. method. The experiments were performed having precaution for precise temperature control (measured with Omega Pt-100) and for minimizing the heat losses (vacuum better than  $10^{-4}$  torr and radiation shields). In all cases the resistivity of the contacts were stable in the range  $10^{-4} - 10^{-5}$  ohm\*cm<sup>2</sup>. The resolution in  $\Delta\sigma/\sigma_c$  was better than 1 part in  $10^3$ .

The temperature dependences of the electrical resistivity of  $YBa_2Cu_3O_{7-x}$  samples are shown in fig.1. All these data show sharp resistive transition to superconducting state. Different values of  $T_c$ , width of the transition and room temperature

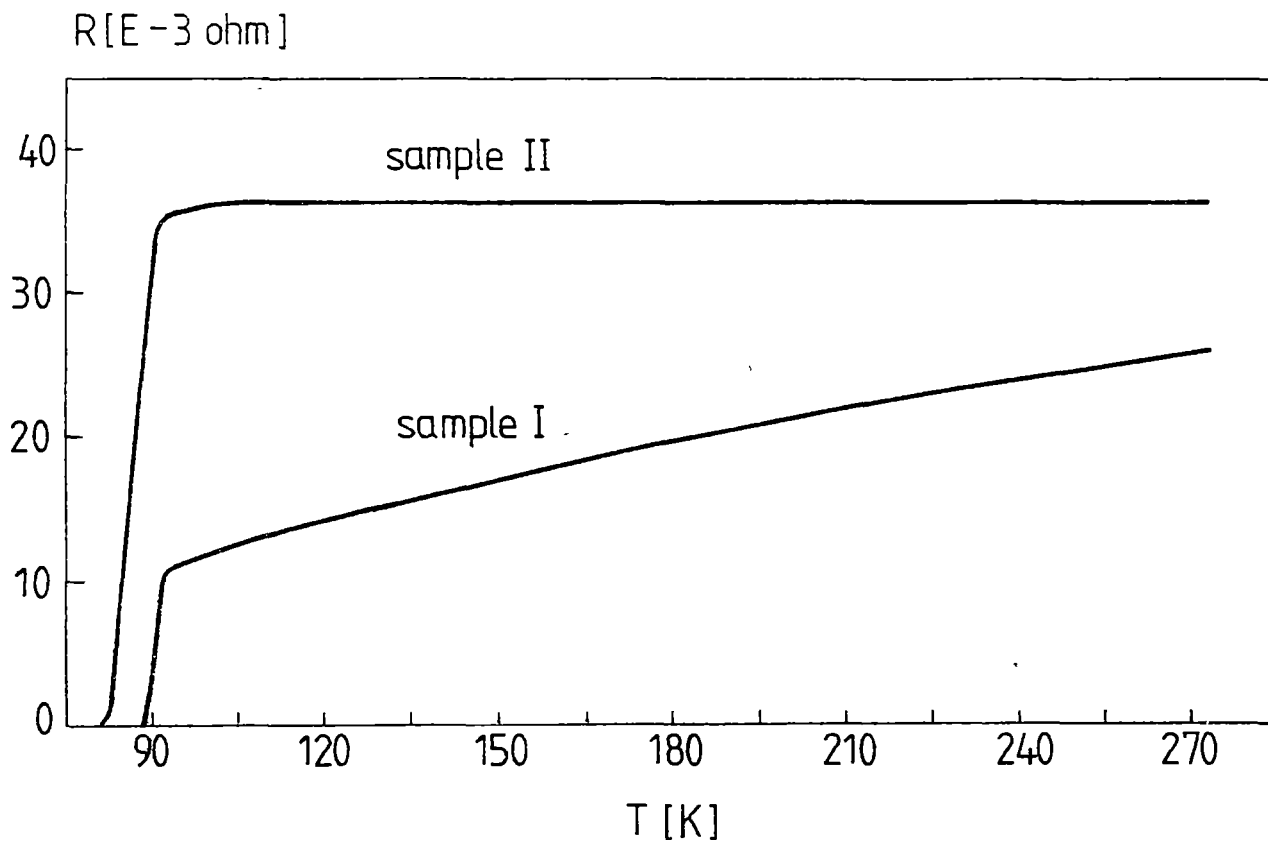


Fig.1 Temperature dependence of the resistance for samples I and II

resistivity result from different conditions of sintering, [14]. Sample I presents a linear (metallic) temperature dependence from at least  $2T_c$  to room temperature, but for sample II the metallic trend of the resistivity changes to a "semiconducting" one. This modification, accompanying the decrease of  $T_c$  and the increase of transition width, may be associated with different oxygen content in the samples or with the conduction process between the planes and across the grain boundaries, [15].

We determine  $\Delta\sigma$  by taking the difference between the experimental value at temperature  $T$  and the value for the same temperature obtained from an extrapolation at  $T < 2T_c$  of metallic or A-Z behaviour. After normalizing by the room temperature conductivity  $\sigma_c$ , we have plotted  $\ln(\Delta\sigma/\sigma_c)$  vs  $\ln\epsilon$ . In our analysis,  $T_c$  was defined by the peak position in  $\partial R/\partial T$  with respect to temperature. In order to observe the regions below the mean-field it is necessary to go well below  $\ln(\epsilon) < -4$ ; for  $\ln(\epsilon) < -6$ , in the "full critical" region, our data become unreliable.

Figure 2 shows plots of the metallic or AZ fits for sample I. For both fits the plots look roughly the same. This behaviour is similar to those found in [10,16], with a deviation from  $-1/2$  coming closer to  $T_c$ . In the mean-field region our critical exponents are  $-0.49$  (linear fit) or  $-0.51$  (A-Z fit) and in the crossover region  $-0.65$  or  $-0.55$  respectively. The choice of the extrapolation method may modify the conclusions about the critical regions, particularly for  $\ln(\epsilon) < -4$ .

The excess conductivity for sample II has been calculated as a function of the reduced temperature for both methods of finding the normal state conductivity. As a result, the

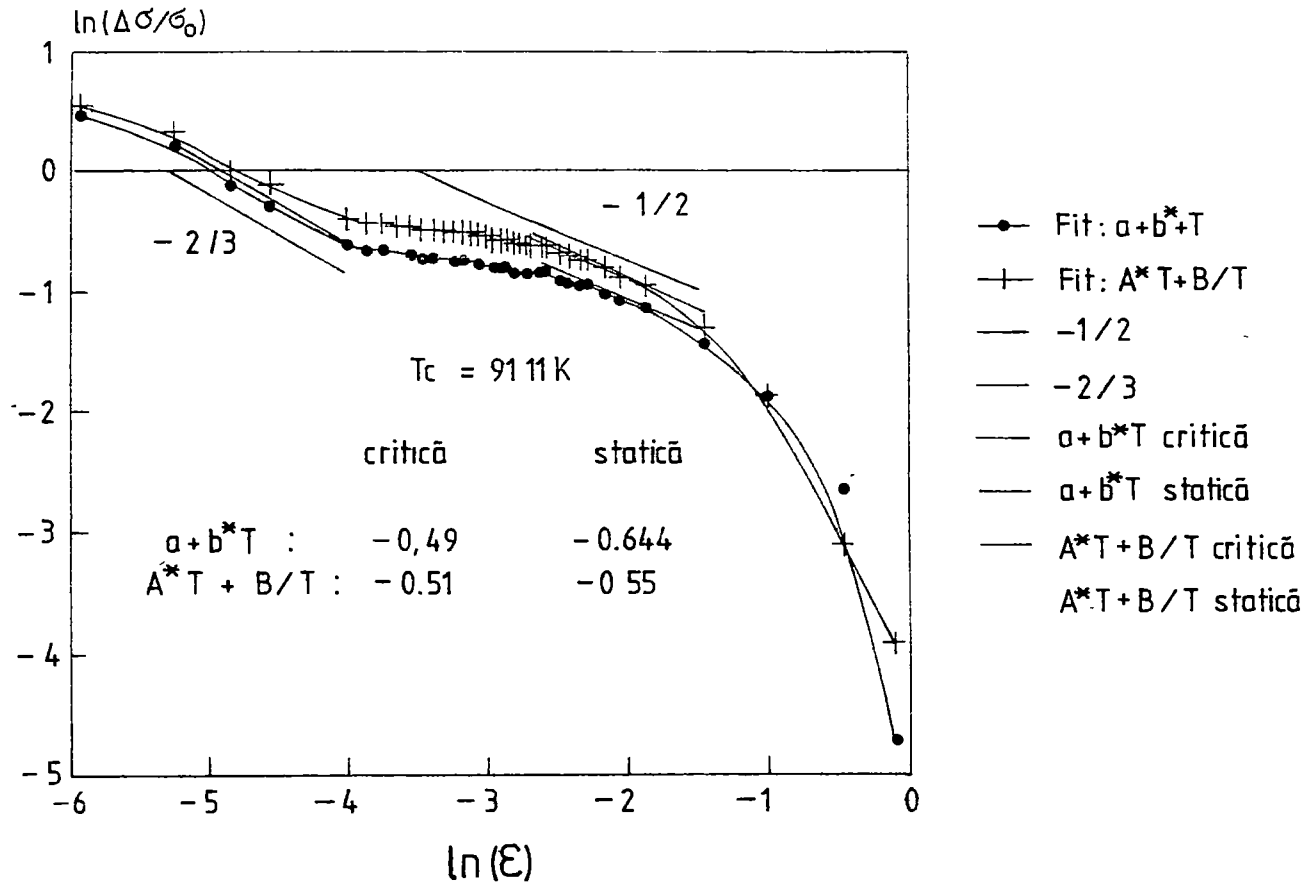


Fig.2. Plot of  $\ln(\Delta\sigma/\sigma_0)$  against  $\ln(\epsilon)$  for sample I; linear and hyperbolic fits.

estimation of the  $\sigma_b$  and hence of the excess conductivity becomes totally unphysically in the region between  $T_c$  and  $2T_c$ , if it used the linear fit. Our data for sample II cannot permit to make the difference between A-Z or exponential models.

**5. Conclusions.** The analysis of resistivity data above  $T_c$  and the study of critical fluctuation through excess conductivity measurements have evidenced that the thermodynamic fluctuations play an important role for HTSC. In this case, near the transition temperature, the thermodynamic fluctuations not may be assumed small and treated approximately. The high values for critical temperature and for penetration depth, associated with a small value for coherence length, should cause the G-L theory to break down within 0.1 K or more of the transition temperature.

## R E F E R E N C E S

1. V.L.Ginzburg, L.D.Landau, Zh.Eksperim. i Teor. Fiz. **20**, 1064 (1950).
2. L.P.Gorkov, Sh.Eksperim. i Teor. Fiz. **36**, 1918 (1959) and **37**, 833 (1959).
3. M.Tinkham, Introduction to superconductivity, McGraw-Hill, New York, 1975.
4. V.L.Ginzburg, Fiz. Tverd. Tela **2**, 2031 (1960).
5. D.R.Harshman, G.Aeppli, E.J.Ansaldo, B.Batlogg, J.H.Breuer, J.F.Carolan, R.J.Cava, M.Celio, A.C.D..Chaklader, W.N.Hardy, S.R.Kreitzman, G.M.Luke, D.R.Noakes, M.Senba, Phys. Rev. **B36**, 2386 (1987).
6. O.Labore, J.L.Tholence, P.Monceau, H.Noel, P.Gougeon, J.Padiou, J.C.Lebet, M.Potel, Solid State Comm. **69**, 513 (1989).
7. T.K.Dey, K.Radha, H.K.Barik, D.Bhattacharya, K.L.Chopra, Solid State Comm. **74**, 1315 (1990).
8. P.Clippe, Ch.Laurent, S.K.Patapis, M.Ausl66s, Phys. Rev. **B42**, 8611 (1990).
9. P.P.Freitas, C.C.Tsuei, T.S.Plaskett, Phys. Rev. **B36**, 833 (1987).
10. F.Vidal, J.A.Veira, J.Maza, J.J.Ponte, J.Amador, C.Cascales, M.T.Casais, I.Rasines, Physica C **156**, 165 (1988).
11. L.G.Aslamazov, A.I.Larkin, Phys. Lett **26A**, 238 (1968).
12. C.J.Lobb, Phys. Rev. **B36**, 3930 (1987).
13. P.W.Anderson, Z.Zou, Phys. Rev. Lett **60**, 132 (1988).
14. P.Mazzetti, A.Stepanescu, A.Masoero, G.Cane, I.Pop, I.Stirbat, in Proc.



- of the Fifth Asia Pacific Physics Conference, Kuala Lumpur, Malaysia, (1992), (in press).
15. K.R.Krylov, A.I.Ponomarev, I.M.Tsidilkovski, V.I.Tsidilkovski, G.V.Bazuev, V.L.Kozhevnikov, S.M.Cheshnitski, Physics Letters A131, 203 (1988).
  16. N.Sudhakar, M.K.Pillai, A.Banerjee, D.Bahadur, A.Das, P.K.Gupta, S.V.Sharma, A.K.Mojumdar, Solid State Comm. 77, 529 (1991).



MAGNETIC PROPERTIES OF  $\text{YBa}_2(\text{Cu}_{1-x}\text{Zn}_x)_3\text{O}_{7-\delta}$   
SUPERCONDUCTING MATERIALS

E. BURZO\*, V. POP\*

Received. 20 12.1991

**ABSTRACT.** - The results of magnetic measurements performed on  $\text{YBa}_2(\text{Cu}_{1-x}\text{Zn}_x)_3\text{O}_{7-\delta}$  superconducting materials with  $x \leq 0.1$ , in the temperature range 5-300 K and fields up to 70 kOe are reported. The rate of induction of  $\text{Cu}^{2+}$  ions, as compared to the number of Zn ones, is 1:1 for  $x \leq 0.05$ . For higher zinc content the number of  $\text{Cu}^{2+}$  ions is smaller than that of  $\text{Zn}^{2+}$  ions. The reciprocal of critical temperatures  $T_c^{-1}$  and of critical current densities,  $j_c^{-1}$  are linearly dependent on  $\text{Cu}^{2+}$  content.

The great reduction of superconducting transition temperatures,  $T_c$ , by zinc substitution in  $\text{YBa}_2\text{Cu}_3\text{O}_{7-\delta}$  has stimulated a large number of experimental studies in order to understand the changes of electronic properties induced by zinc. It is known from other works that zinc doping induces  $\text{Cu}^{2+}$  ions [1-4]. According to Alloul et al.[4], the major effect of zinc substitution in  $\text{YBa}_2\text{Cu}_3\text{O}_{7-\delta}$  is the appearance of local moments in the  $\text{CuO}_2$  planes associated with the disorder induced by the zinc, substituted on the Cu(2) sites. The same site occupation by zinc is suggested by Lin et al.[5]. A linear dependence is evidenced between the discontinuity in the specific heat at the transition temperature,  $T_c$ , as well as the coefficient of linear term in specific heat and the number of  $\text{Cu}^{2+}$  ions in  $\text{YBa}_2\text{Cu}_3\text{O}_{7-\delta}$  lattice [6].

In this note, by using magnetic measurements, we determined the number of  $\text{Cu}^{2+}$  ions induced by zinc,  $n_{\text{Cu}^{2+}}$ , in  $\text{YBa}_2(\text{Cu}_{1-x}\text{Zn}_x)_3\text{O}_{7-\delta}$  system and we correlated these values with critical current densities  $j_c$  and superconducting transition temperatures,  $T_c$ .

---

\* "Babeș-Bolyai" University, Faculty of Physics, 3400 Cluj-Napoca, Romania

Linear relations between  $j_c^{-1}$  and  $T_c^{-1}$  as function of  $n_{Cu^{2+}}$  are evidenced.

The samples were prepared by solid state reaction. A mixture of  $Y_2O_3$ ,  $CuO$ ,  $ZnO$  and  $BaCO_3$ , in the required proportions, was homogenized, finely ground and calcined in the temperature range 920-950°C, in oxygen atmosphere. After calcination, the structure of the samples was checked by X-rays. The formation of perovskite type structure is evidenced for all compositions. The calcined samples were finely ground and then compacted at a pressure of 3 tcm<sup>-2</sup>. Sintering was performed in the temperature range 930-960°C in oxygen atmosphere. The samples were then slowly cooled.

The density of sintered materials was around 90% from theoretical density. The final X-ray analysis show the presence of the orthorhombic-type structure.

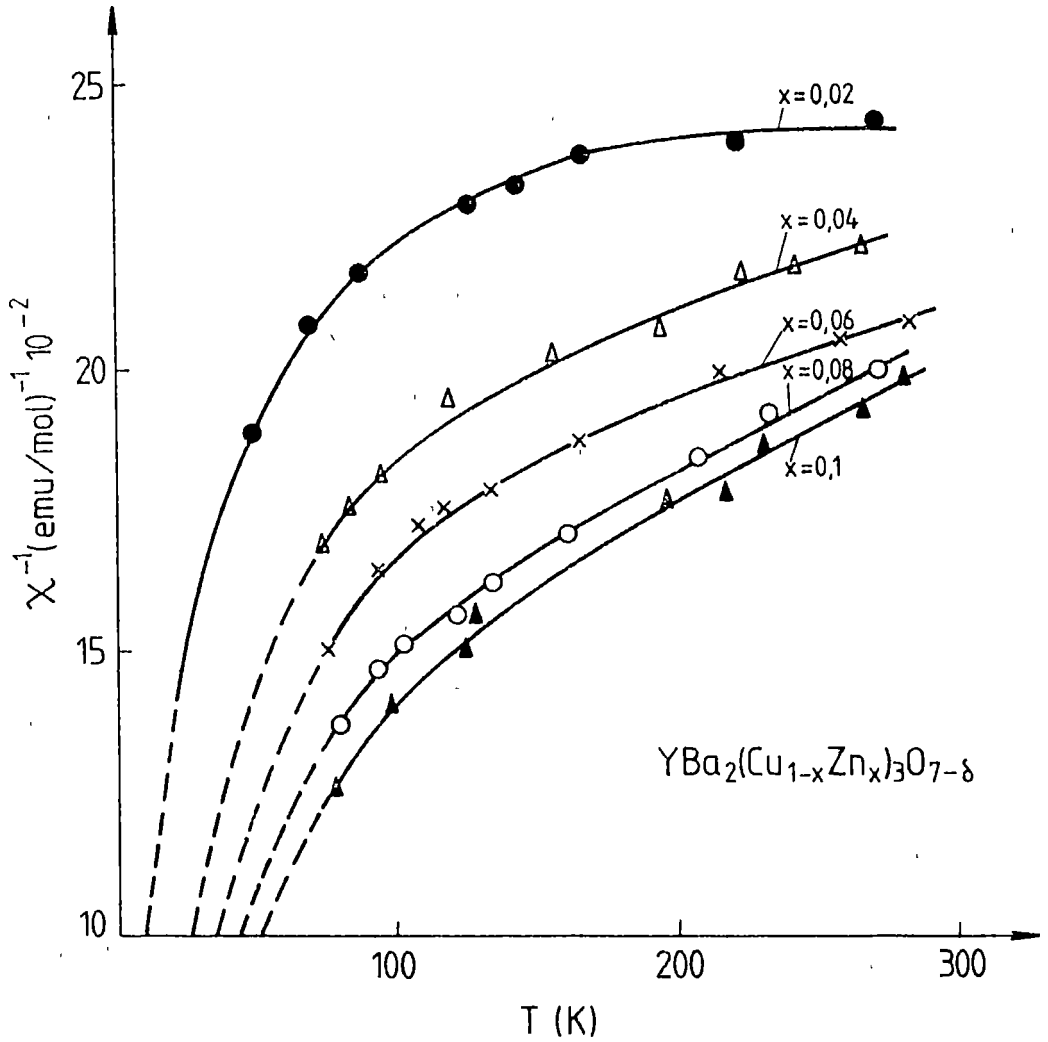
The magnetic measurements were performed in temperature range 5-300 K and external field up to 70 kOe. In addition electrical resistivities and EPR studies were performed.

The thermal variations of reciprocal susceptibilities at temperatures greater than  $T_c$ , are plotted in figure 1. The experimental data may be analysed according to a modified Curie-Weiss law

$$\chi = \chi_0 + C(T - \theta)^{-1} \quad (1)$$

We denoted by  $\chi_0$  a temperature independent contribution to susceptibility,  $\theta$  is the paramagnetic Curie temperature and  $C$  is the Curie constant.

The temperature independent contributions,  $\chi_0$ , increase

Fig.1. Thermal variations of reciprocal susceptibilities at  $T > T_c$

little when increasing the zinc content - figure 2a. This variations may be connected with the differences in the diamagnetic susceptibilities of zinc and copper ions, the last one being greater in absolute magnitude. The paramagnetic Curie temperatures,  $\theta$ , are nearly nil, showing that the exchange interactions between localized moment are small.

The Curie constants are plotted in figure 2b. The C values increase nearly linear up to  $x = 0.05$  when zinc content increase. For  $x > 0.05$  the composition dependence of the Curie constants deviate from linearity.

The EPR measurements on  $\text{YBa}_2(\text{Cu}_{1-x}\text{Zn}_x)_3\text{O}_{7-\delta}$  show the presence of resonance lines of  $\text{Cu}^{2+}$  ions, having  $g = 2.00$ . These suggest spin contribution only. The corresponding effective moment is  $1.73\mu_B$ . Taking the above into account, we determined the number of  $\text{Cu}^{2+}$  ions present in the system. The variation of the number of  $\text{Cu}^{2+}$  ions as function of the zinc content is plotted in figure 2c. By thin line is plotted the prediction corresponding to an induction rate of one  $\text{Cu}^{2+}$  ion for each zinc ion introduced in lattice. This behaviour is fulfilled up to a composition  $x < 0.05$ . Then, the increase of the number of  $\text{Cu}^{2+}$  ions is smaller then that of zinc ones.

Magnetic measurements were also performed, in the low temperature range, in the superconducting state, respectively.

The magnetization curves of  $\text{YBa}_2(\text{Cu}_{1-x}\text{Zn}_x)_3\text{O}_{7-\delta}$  samples obtained at 5 K are plotted in figure 3. The hysteresis loops constrict as the zinc content increases. The hysteresis curves are also narrower when increasing temperature, as evidenced in

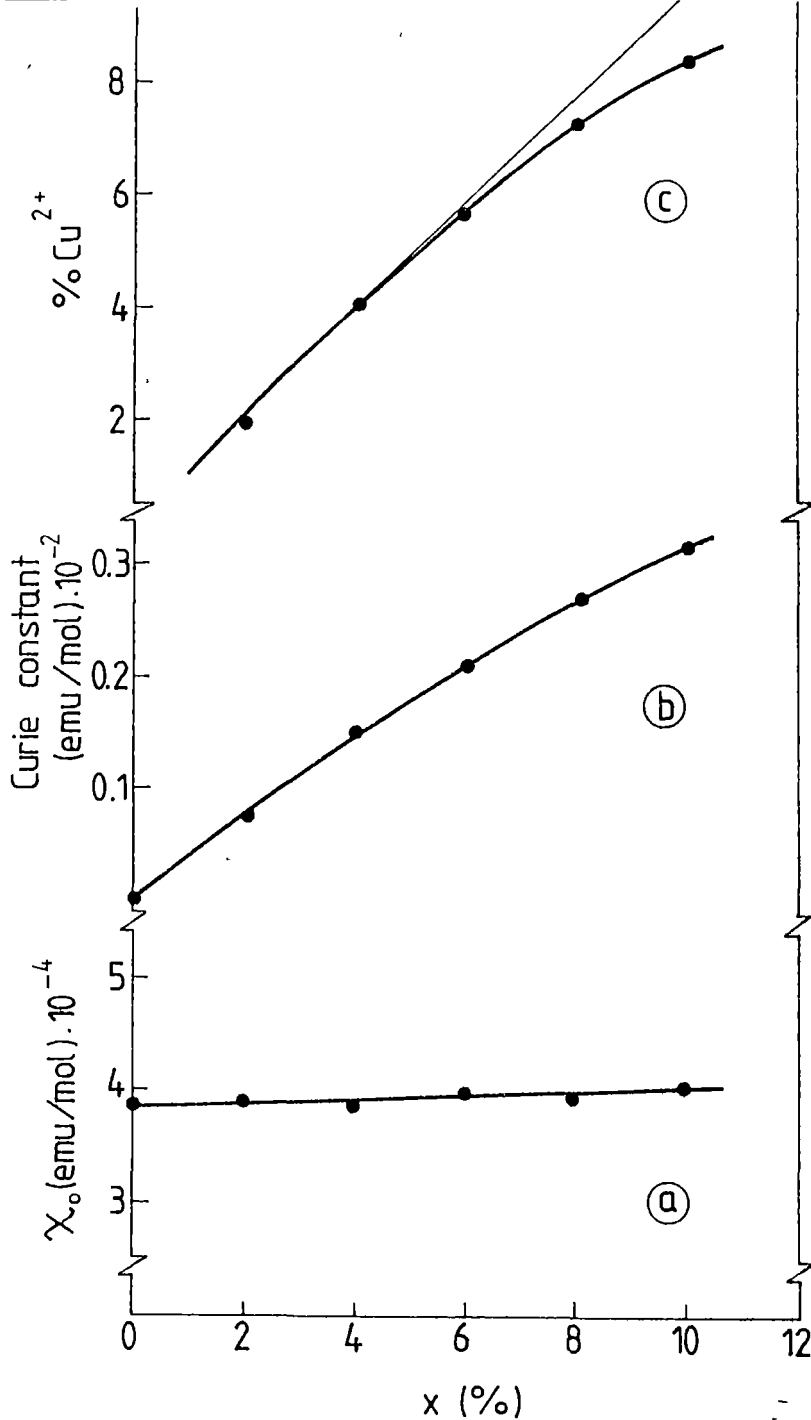


Fig.2. Composition dependence of the temperature independent contributions to susceptibilities (a), Curie constants (b), and of the relative number of  $\text{Cu}^{2+}$  ions (c).

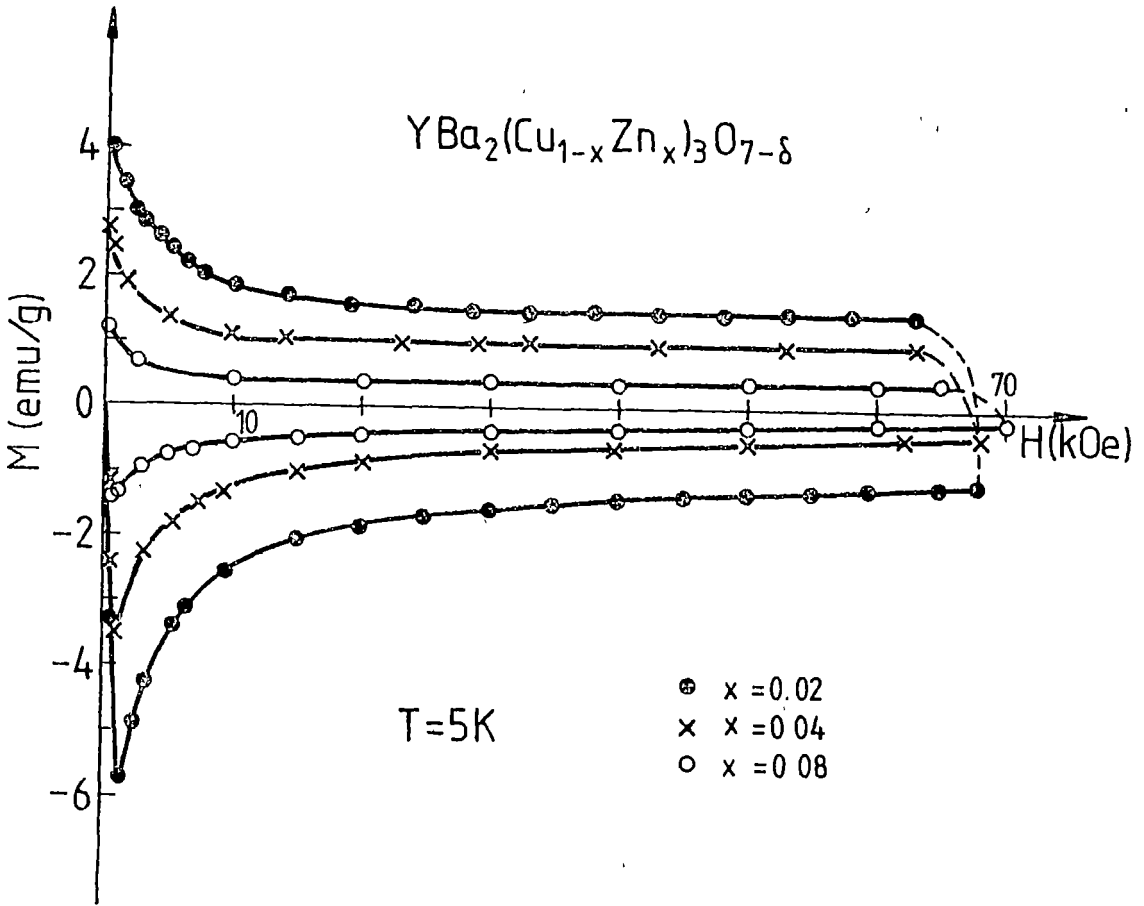


Fig.3. Magnetizations isotherms at 5K for  $\text{YBa}_2(\text{Cu}_{1-x}\text{Zn}_x)_3\text{O}_{7-\delta}$  with  $x=0.02; 0.04$  and  $0.06$ .

figure 4.

From the magnetic hysteresis loops, the critical current densities,  $j_c(T,H)$  were determined. According to critical state model [7,8], the  $j_c(T,H)$  values within a grain of radius  $r$  are given by



$$j_c(T, H) = \frac{15}{r} [M_{\downarrow}(T, H) - M_{\uparrow}(T, H)] \quad (2)$$

where  $r$  is given in cm, the magnetization,  $M$ , in  $\text{emu}\cdot\text{cm}^{-3}$  and  $j_c(T, H)$  in  $\text{Acm}^{-2}$ .  $M_{\downarrow}(T, H) - M_{\uparrow}(T, H)$  is the distance between the direct and returning of the magnetic cycle.

The mean values,  $r$ , of grain sizes were determined by electron microscope studies. Because of their distribution function, the grain size is typical known only within a factor of 10 [9]. Since our samples have the same distribution function of the grains, the trends of the composition and temperature dependences of  $j_c(T, H)$  values are correct.

From the relation (2) we determined the critical current densities  $j_c(H, x, T)$ . As example, in figure 5 we plotted the field and temperature dependences of the  $j_c$  values for  $YBa_2(Cu_{1-x}Zn_x)_3O_{7-\delta}$  samples. The critical current densities decrease strongly, in the region  $T < 20$  K, when increasing temperature.

We analysed in what extent the critical current densities,  $j_c$ , and transition temperatures,  $T_c$ , show a regular trend as function of the number of  $\text{Cu}^{2+}$  ions,  $n_{\text{Cu}^{2+}}$ . Thus, in figure 6 we plotted the  $j_c^{-1}$  at 5 K and  $T_c^{-1}$  as function of  $n_{\text{Cu}^{2+}}$ . Linear dependences are evidenced. The transition temperatures as well as critical current densities decrease when the number of  $\text{Cu}^{2+}$  ion increase. Thus, is possible to establish a quantitative correlation between macroscopic data and the microscopic behaviour.

We conclude that the major effect of the zinc substitution in  $YBa_2Cu_3O_{7-\delta}$  system is the appearance of local moments on copper. The rate of induction of local moment is 1:1 for  $x < 0.05$ .



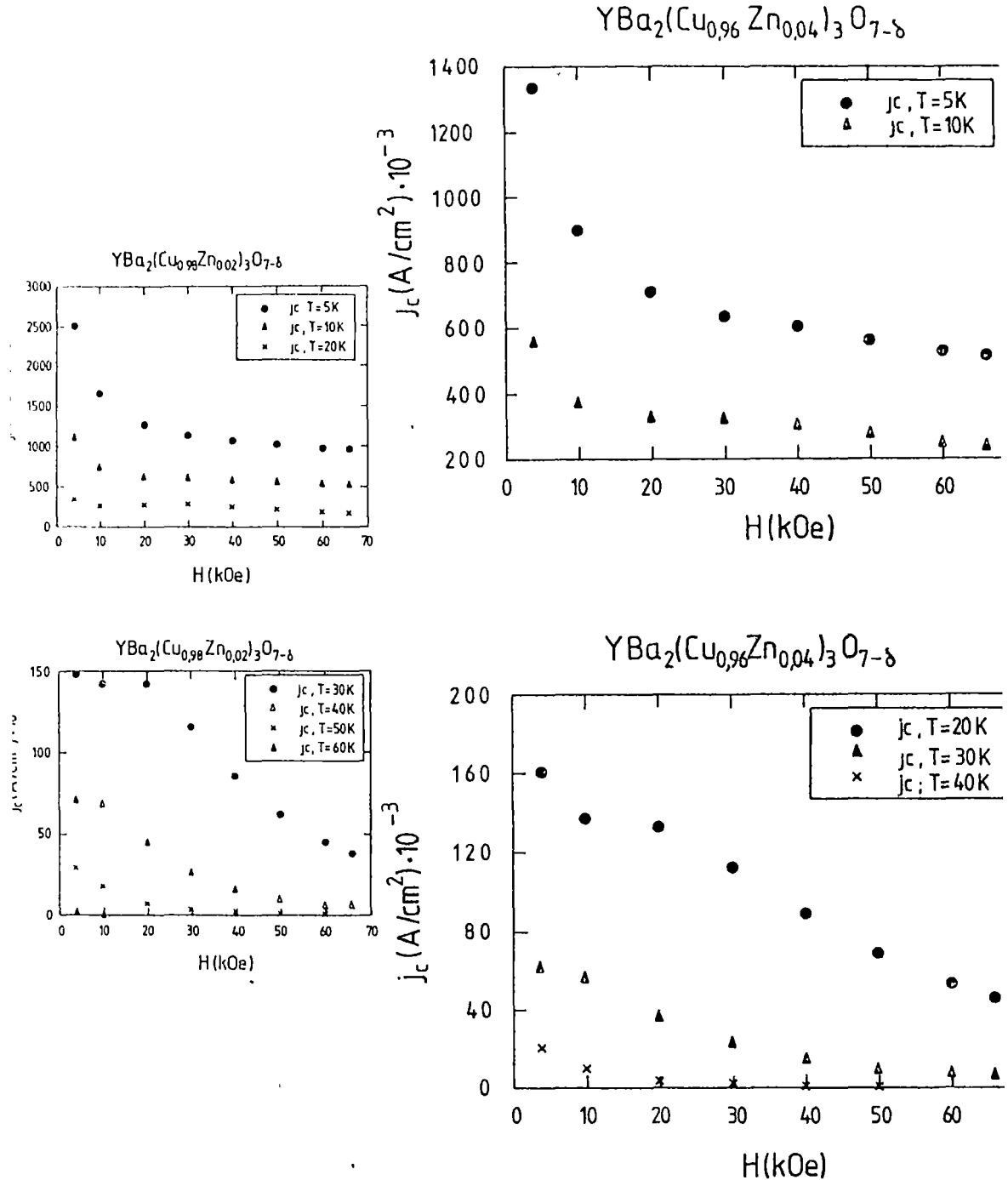


Fig. 5. Temperature and field dependences of the critical current densities for  $\text{YBa}_2(\text{Cu}_{1-x}\text{Zn}_x)_3\text{O}_{7-\delta}$  with  $x = 0.02$  and  $0.04$ .

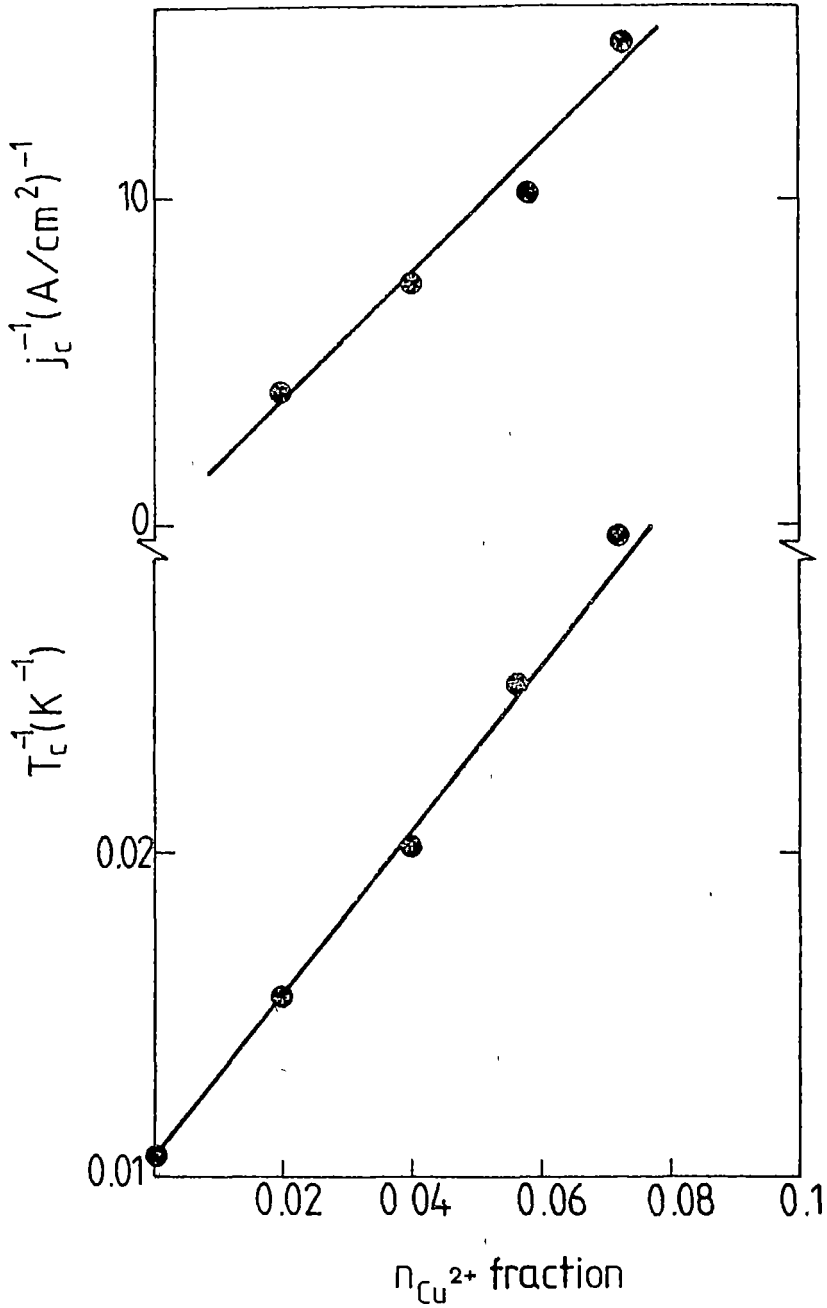


Fig.6. The dependence of transition temperatures  $T_c$  and critical current density on the fraction of  $\text{Cu}^{2+}$  ions

This rate decrease as compared to above behaviour when increasing zinc content. The critical current densities and critical temperatures are strongly correlated with the fraction of  $Cu^{2+}$  ions in lattice. Both  $j_c^{-1}$  and  $T_c^{-1}$  show a linear dependence, as function of  $n_{Cu^{2+}}$ .

## R E F E R E N C E S

1. G.Xiao, A.Bakhshai, M.Z.Cieplak, Z.Tesanovic and C.L.Chien, Phys. Rev. **B39**, 315 (1989).
2. M.Z.Cieplak, G.Xiao, A.Bachshai and C.L.Chien, Phys. Rev. **B39**, 4222 (1989).
3. C.S.Jee, D.Nichols, A.Kebede, S.Rahman, J.E.Grow, A.M.Ponte Goncalves, T.Mihalisin, G.H.Nyen, L.Perez, R.E.Salomon, P.Schlottmann, S.H.Bloom, M.V.Kuric, Y.S.Yao and R.P.Guertin, J.Supercond. **1**, 63 (1988).
4. H.Alloul, P.Mendels, H.Casalta, J.F.Marucco and J.Arabski, Phys. Rev. Lett. **67**, 3140 (1991).
5. C.Lin, Z.X.Liu and J.Lan, Phys. Rev. **B42**, 2554 (1990).
6. N.E.Phillips and R.A.Fisher, J.Magn. Magn. Mat. **90-91**, 589 (1990).
7. C.P.Bean, Phys. Rev. Lett. **8**, 250 (1962).
8. C.P.Bean, Rev.Med. Phys. **36**, 31 (1964).
9. O.D.Stancil, T.E.Schlesinger, A.R.Stamper and D.Wong, J.Appl. Phys. **64**, 5899 (1988).



THE THERMAL TREATMENT INFLUENCE ON SOME CHARACTERISTIC  
PARAMETERS OF THE Y123 SUPERCONDUCTORS

N. REZLESCU\*, R. ANGHELACHE\*, D.P. POPA\*, C. BUZEA\*

Received. 27 05.1992

**ABSTRACT.** - In order to optimize the superoxidation treatment we detailed some aspects of the dependence of normal resistivity versus oxidation temperature in the Y123 superconductors. We found two significant temperatures directly related to the structure of this class of superconductors and to the oxygen in and out-diffusion processes.

1. **Introduction.** In the field of the high-T<sub>c</sub> superconductors, the influence of the thermal treatment acting on their start composition is recognized as being essential [1/. This fact is due to the effect of the thermal treatment on the final resistive, magnetic, thermodynamic and structural properties of the superconductors. Consequently, the importance of the thermal treatment was signaled since the discovery of the ceramic superconductors and returned into present together with the discovery of some new classes of superconductors (Y,Bi,Tl), having in view the optimization of their characteristic parameters, and creating, in the same time, the possibility of repeatability in the process of getting superconductors with the desired parameters.

The best studied class, among the up-to-date discovered high-T<sub>c</sub> superconductor classes, is the one described by the base formula, briefly noted Y123 (YBa<sub>2</sub>Cu<sub>3</sub>O<sub>x</sub>). One of the reasons for which the physicists focused on that one, is the fact that the Y123 offers a single superconducting stable phase above the nitrogen liquefying temperature, with the corresponding critical

---

\* Institute of Technical Physics, Iași, Romania

temperature value ( $T_c$ ) being of about 90K. This feature of the Y123 class justifies the studies that are pointing to the causes of the superconductors specific phenomena, unlike the Bi and Tl classes, which, being multiphase compounds, characterized by critical temperatures ( $T_c=110\div 125K$ ) greater than that of the Y123 class, encourage the technological studies and applications of their physical properties.

In the frame of the Y123 class, the conclusions related to the occurrence of the superconducting transition developed from the simple presence of the Y or Cu atoms in the final structure to the presence of the Cu-O chains /2/. These structures appear only after an adequate treatment that changes the structure of the cell from tetragonal (non-superconducting) to orthorhombic. It can be asserted that the orthorhombic cell proportions within the compound is directly related to the presence of the Cu-O chains, the latter resulting from the supplementary introducing of the oxygen atoms in the initial composition ( $YBa_2Cu_3O_{6.5} \rightarrow YBa_2Cu_3O_{6.5+\delta}$ ).

It's well known that the T123 class samples don't become superconducting if they are simply quenched from the sintering temperature down to the room temperature, because the Cu-O chains, which are responsible for the occurrence of the superconducting transition, don't have enough time to grow /3/. Consequently, the ordinary superoxidation method consists of sufficiently slow cooling the samples from about 400-500°C, to the room temperature.

Starting with the idea that "slow enough" cooling achieves the superoxidation for a "long enough" time at a certain value,



or for a certain narrow interval of interest of the treatment temperature, we intend to study this interval, in order to optimize the superoxidation treatment. In the same time, the existence of some determined values (representative for their effects on the superconductor final properties) of the oxidation temperature may be the macroscopic effect of the binding energy of the oxygen atoms within the Cu-O chains, as well as their interactions with the neighbouring atoms, providing state information. The influence of treatment's length at certain temperatures on the parameters of the compound may provide data concerning the way which the oxygen atoms arrive from the medium within the respective chains, namely process information.

**2. Experimental procedure.** The start composition of the samples was obtained by homogenizing a mixture of dry powders of  $Y_2O_3$ ,  $Ba(NO_3)_2$  and  $CuO$ . The mixture was then pressed into cylindrical pellets (10x5mm). They were warmed (500deg/h) up to 900°C, maintained in this state for 12h and then quenched down to the room temperature. This process gave off the  $NO_2$  from the samples. The thermal treated pellets were then milled and pressed into prismatic samples (3x3x11mm). The resulting samples were warmed up to 930°C (500deg/h) and kept at this temperature ( $T_r$ ) during a period of time ( $t_r$ ) between 6 and 36h and then quenched down to the room temperature. Then, followed the superoxidation at different temperatures ( $T_o$ ) and periods of time ( $t_o$ ).

There have been obtained several series of samples. In the frame of a single series, the samples were sintered or oxidated simultaneously (sim) or successively (sc).

The six series of samples are showed in the table 1, together with their thermal treatment details, and using the above notations. All samples exhibit zero resistive transitions about the temperature of 90K. For illustration, we give in fig.1 and 2 the resistivity-temperature plots for the series of samples 5 and 6, respectively, round about the critical temperature.

The samples resistivities were measured by using the classical 4 - probe method, in alternative current, in order to eliminate

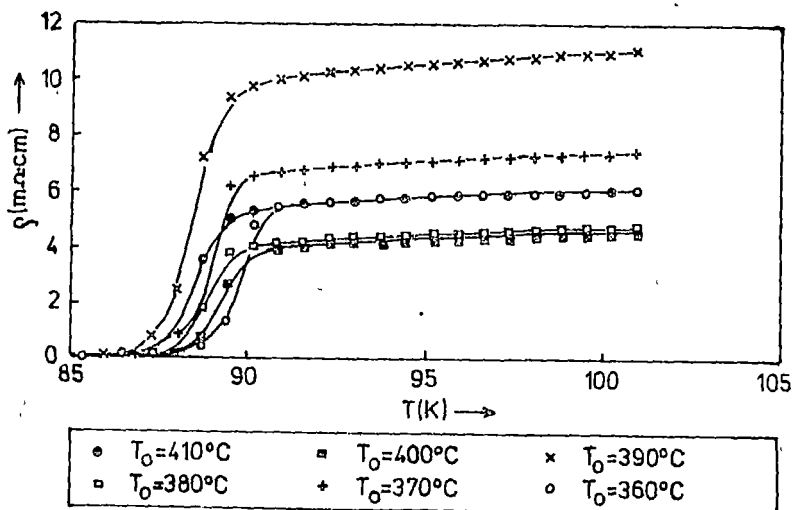


Fig.1. The R vs.T plot for the 5-th series.

from the final data the possible presence of a continuous, electrochemically nature potential, which could appear between the sample and the terminal. The sample temperature was measured by using a standardized termoresistance, made of a Cu wire (20μm in diameter) wound in two opposite directions to eliminate any magnetic interaction with the sample, during the measurements. The potential and the resistance measurements were made automatically, using two digital multimeters MERATRONIK Type V545, and a computer data acquisition system, designed in our laboratory /4/.

Note that, the usual method of obtaining the superconducting phase within an  $YBa_2Cu_3O_{6.5}$  compound consists in slow cooling it from the

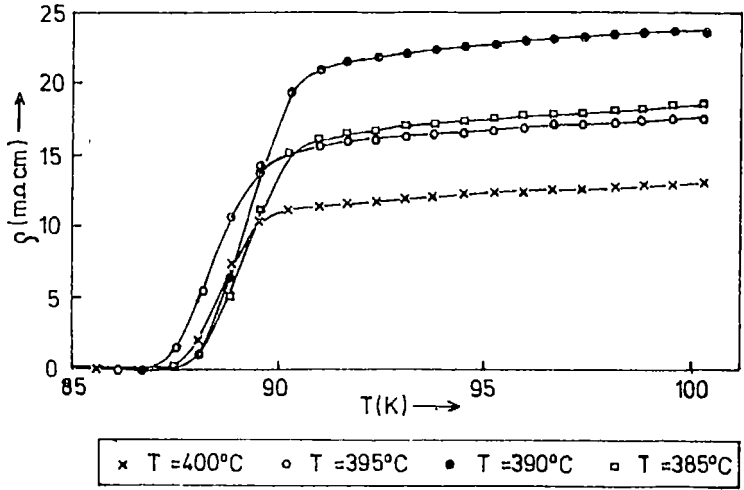


Fig.2. The R vs. T plot for the 6-th series.

sintering temperature down to the room temperature. Another way is to warm the sintered unoxidated sample from the room temperature up to a temperature value about 350-450<sup>0</sup>C and keeping it in this state during a long enough time. These situations, more often met in the literature, ignore the existence of certain values for the superoxidation temperature, specific to the Y123 compounds.

In order to give emphasis to these values, along the series of experiments we performed, we use a superoxidation method at fixed values of temperature, the samples warming or cooling time being practically negligible compared to the superoxidation time. Thus, we got a straightforward relation between the specific to the compound parameters and the temperature values fixed by us.

This method is imposed because, during the superoxidation, essential structural changes occurs, which can depend on the initial degree of superoxidation and can influence the speed of the in-diffusion/ex-diffusion process of the oxygen atoms within

the compound and also, their final equilibrium concentration /5/, /6/.

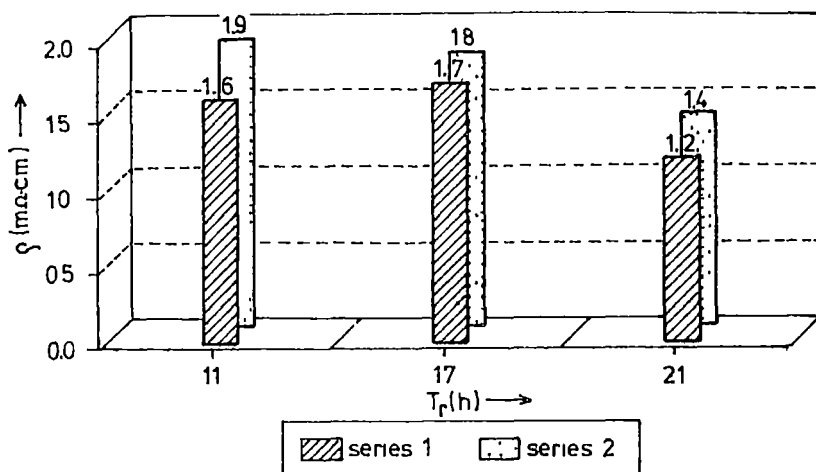


Fig.3. Resistivities measured at  $T=180^{\circ}\text{C}$  for the series no.1-2.

**3. Results and discussion.** In fig.3 we show the resistivity values of the 1 and 2 series samples, picked at the temperature  $T = 180\text{K}$ , for different times of sintering. It can be noticed that samples oxygenated at  $400^{\circ}\text{C}$  (series 1) have a resistivity that is smaller than that of the samples oxygenated at  $430^{\circ}\text{C}$  (series 2), this comparative result being, as it must be, independent on the samples sintering time, inscribed on the abscise axis.

In fig. 4 we plot the 180K resistivities which correspond to the other four series of samples. One can notice that samples oxygenated for 18h (series 3) exhibit resistivity values close to those corresponding to the 1 and 2 series. Then, is obvious that, the resistivity obtained after oxygenation at  $400^{\circ}\text{C}$  is relatively smaller that those corresponding to  $420^{\circ}\text{C}$  and  $380^{\circ}\text{C}$ .

In order to detail the dependence of the normal resistivity on the superoxidation temperature there have been im-

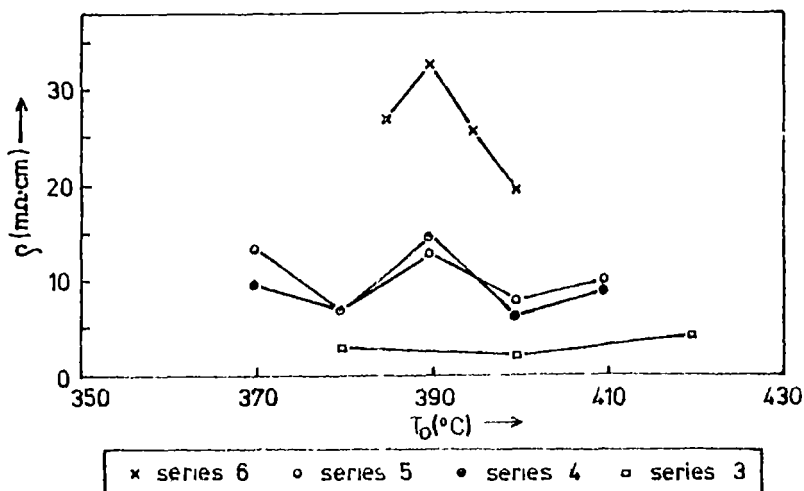


Fig. 4. Resistivities measured at T=180°C for the series no. 3-6.

posed a revise of the experiment by decreasing the measurement intervals for the latter. The 4 and 5 series, plotted in fig. 4, were treated in the same conditions (sintered and superoxidated together). One can notice an increase in the relative difference of the resistivities, obtained by oxidation on 10 degree steps, and a relative maximum at 390°C.

To check around the 390°C zone, we repeated the experiment this time between 385-395°C, in 5 degree steps (series 6). The relative differences between the resistivity values are even greater than those obtained in the 4 and 5 series, imposing a relative maximum in the sample resistivities for an oxidation temperature of 390°C. Besides, we note that the absolute resistivity values also, are greater than those referring to the 3, 4 and 5 series. This fact is due to the accidental appearance of a bigger proportion of structural defects within the samples.

The increase in the relative difference of resistivities with the superoxidation time represents, in fact, the increase in

the concentration of those oxygen atoms which give rise to the Cu-O chains and implies the conclusion that the thermodynamic equilibrium between the medium and sample's oxygen atoms has not yet been reached in the 1 to 5 series.

The maximum in resistivity, obtained at an oxidation temperature of 390°C, corresponds to a minimum in the oxygen concentration within the compound.

It's well known that oxidation treatments above 440°C, results in a decrease onto annulling of the concentration in the supplementary oxygen atoms. In other words, the ex-diffusion of these prevails on the in-diffusion, with the increase of the oxidation temperature, resulting in a complete destruction of the Cu-O chains from the structure of the compound.

Series no	T <sub>0</sub> (°C)	t <sub>0</sub> (h)	t <sub>r</sub> (h)	sinter. / oxidat.	Present in fig.
1	400	5	6	scc/sim	3
2	430	5	6	scc/sim	3
3	-	18	12	sim/scc	4
4	-	72	24	sim/scc	4
5	-	72	24	sim/scc	1, 4
6	-	84	36	sim/scc	2, 4

Table 1. Experimental details of the thermal treatment for the six series of the manufactured samples.

Consequently, the data impose the interpretation of the discovered value for the resistivity, which resulted from oxygenation at 400°C, as a relative minimum. The latter corresponds to a relative maximum in the oxygen concentration.

The concentration minimum from 390°C and the maximum from 400°C, can be explained through the existence of a well-defined value for the binding energy of the oxygen atoms within the chains responsible for superconductibility, if taking into account the moving mechanism of the oxygen atoms during the concurrent in-diffusion and ex-diffusion processes, as well /7/.

A better conclusion can be outlined only after a more detailed research on the behaviour of the resistivity versus oxidation temperature, using a larger range of temperatures.

R E F E R E N C E S

1. Shamrai V.F., Efimov Yu.V., Karpinskii O.G., Babareko A.A., Leitus G.M., Frolova T.M., Myasnikova E.A., Postnikov A.M., Savelyeva M.E. and Lipikhin Yu.L., "Phase equilibria, structure and properties of Y-Ba ceramics", in *J. Less- Comm. Met.*, **162**, 181 (1990).
2. Kubo Y. and Igarashi H., "Significance of the Cu-O chain and a percolation model for superconductivity in  $\text{YBa}_2\text{Cu}_3\text{O}_{7-\delta}$ ", in *Phys. Rev. B*, vol. **39**, **1**, 725 (1989).
3. Fujimori A., "Character of doped oxygen holes in high-Tc Cu oxides", in *Phys. Rev. B*, vol. **39**, **1**, 793 (1989).
4. Rezlăscu N., Anghelache R., Popa P.D. and Buzăa C., "Data acquisition system for the study of the high-Tc superconductors" in *An. Univ. "Al.I.Cuza" Iași*, 1992 (to be published).
5. Tu K.N., Yeh N.C., Park S.I. and Tsuei C.C., "Diffusion of oxygen in superconducting  $\text{YBa}_2\text{Cu}_3\text{O}_{7-\delta}$  ceramic oxides", in *Phys. Rev. B*, vol. **39**, **1**, 304 (1989).
6. Wille L.T., Berera A. and Fontaine D. de, "Thermodynamics of oxygen ordering in  $\text{YBa}_2\text{Cu}_3\text{O}_x$ ", in *Phys. Rev. Lett.*, vol **60**, **11**, 106 (1988).
7. Poulsen H.F., Andersen N.H., Andersen J.V., Bohr H. and Mouritsen O.G., "Dynamical scaling of oxygen ordering in  $\text{YBa}_2\text{Cu}_3\text{O}_{7-\delta}$ ", in *Phys. Rev. Lett.*, vol. **66**, **4**, 465 (1991).



2

4

7





ASPECTS OF THE SUBSTITUTION FOR  
GALLIUM IN THE Y Ba Cu O SYSTEM

Teodor-Radu REDAC\*

Received. 5 12 1991

**ABSTRACT.** - The influence of gallium, partly or totally substituting the yttrium, in a  $Y_1Ba_2Cu_3O_{7-\delta}$  system, that is a representative ceramic system of the superconducting transition temperature ceramic materials, is discussed. The prepared samples of two systems show a significant transition near the liquid nitrogen temperature. The  $GaBa_2)_3O_{7-\delta}$  sample shows a semiconductive behaviour, the increasing of the thermic treatment temperature leading to a superconductive behaviour.

1. **Introduction.** The  $Y_1Ba_2Cu_3O_{7-\delta}$  system is a representative ceramic system of the superconducting transition temperature ceramic materials.

The value of the transition critical temperature is influenced by both the stoichiometry of the system and the substitutions of some chemical elements of the system.

Substitutions of copper with silver are known as well as for zinc or other elements, these leading to the diminuation of the critical temperature value while the substitution of yttrium for rare-earth metals modified at a certain degree the critical temperature, [1-4].

In the present work we tried to emphasize the influence of gallium in the system, the latter partly or totally substituting the yttrium, [5].

The following values have been chosen as compounds of the new  $Y_{1-x}Ga_xBa_2Cu_3O_{7-\delta}$  system:  $x = 0,2; 0,3; 0,5$  and  $x = 1$ , respectively the samples being codified Ga [1-4].

---

\* "Aurel Vlaicu" University of Arad, C.P. 41, Arad 1, 2900 Arad, Romania

2. **Sample Preparation.** The oxides and carbonates of p.a. purity have been desed in micro-samples weighting 10 gr., the mesurements realisated with an accuracy of 0,1 gr.

The homogenization was achieved in the presence of the izopropyl alcohol during eight hours. A sample was chosen from the Ga 4 sample in order to be investigated by thermogravimetry, together with another sample taken from the  $Y_1Ba_2Cu_3O_{7-\delta}$  composition prepared in identical conditions.

After homogenization, the dry blends were calcined in air at 800°C for 4 hours by three times, the sample being weighted after each calcination.

The resultant powder was cold pressed in the shape of pills with a diameter of 10 mm using a manual press at the some pressure controled by a dynamometer.

The pills have been sintered in air at 900, 950 and 1000°C.

After a first measurement of the samples sintered at 950°C, all the samples were sintered at 950°C for four hours, in oxygen atmosphere afterwards the temperature decreases with 3°C on minute, until 500°C, the sample remaining at this temperature for one hour. After this final period, the sample was furnace cooled, mantaining the oxygen atmosphere.

The results of the X-ray analysis have been shown in (5) and they have emphasized the orthorhombic structure as far the first three samples are concerned and also the presence of a tetragonal structure along with the former in the case of the fourth sample. The analysis have been made for calcined powders.

A second group of four compositions have been additionally calcined at 1000°C, the resultant powder being pressed in the

shape of pills with a diameter of 10 mm; afterwards they have been sintered in oxygen together with the others.

In order to accomplish the electric measurements the samples were introduced between the plates of a capacitor connected in a series circuit to the quartz of an oscillator.

The junction of a copper-constantan thermocouple was placed beside the sample; afterwards they were both closed in a plastic casing in order to diminish the effects of water condensing.

**3. Measurements and results.** In order to accomplish the measurements we have created a screw device permitting a controlled introduction of the sample in the liquid nitrogen container.

The sample is fixed to the end of a bifilar line, fixed together with the thermocouple to a glassfibre rod that is fixed to the screw nut. In this way the sample can be maintained at any level till the stabilization of temperature.

In fig. 1 a) and b) are shown the derivatogrammes of the sample  $Y_1Ba_2Cu_3O_{7-\delta}$ . They have been obtained in air, up to 1200°C for 100 minutes.

The results of the electric measurements are shown in fig.2.

In fig.2 a) is presented the behaviour of a sample, noted B 3, which belongs to the system  $Y_{1+x}Ba_{2+x}Cu_3O_{7-\delta}$ , in some measurement conditions.

Frequency was measured with a frequencymeter of type E0204 and the temperature with a galvanometer.

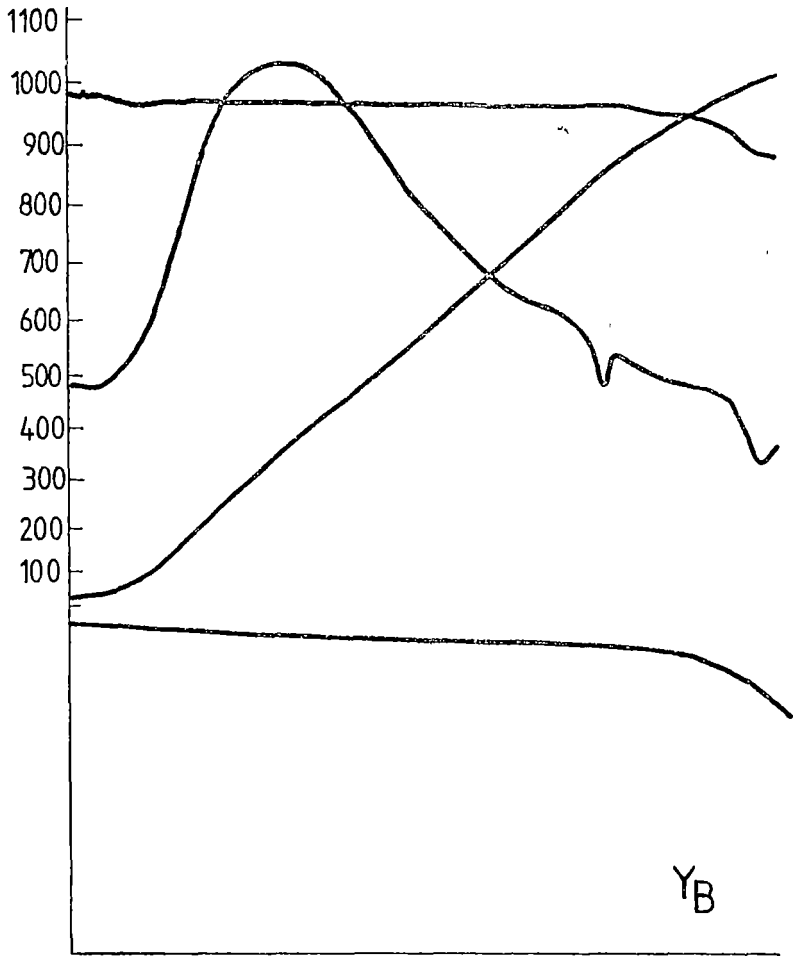


Fig.1a. Derivatogramme of the sample  
 $Y_1Ba_2Cu_3O_{7-\delta}$

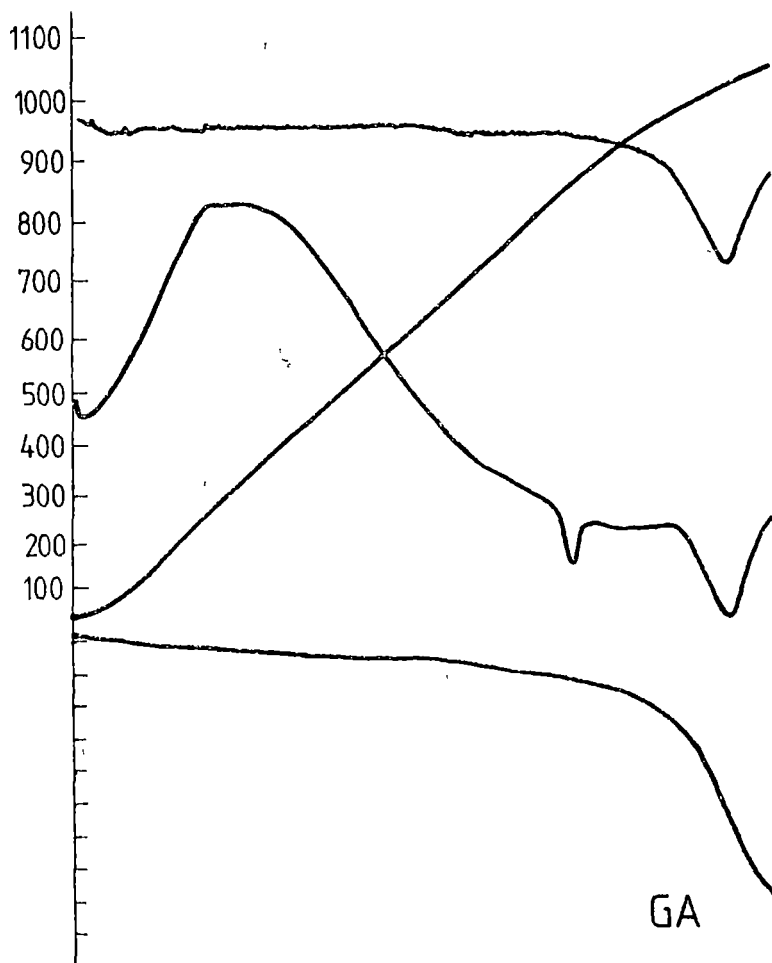


Fig.1b. Derivatogramme of the sample  
 $\text{Ga}_1\text{Bo}_2\text{Cu}_3\text{O}_{7-\delta}$

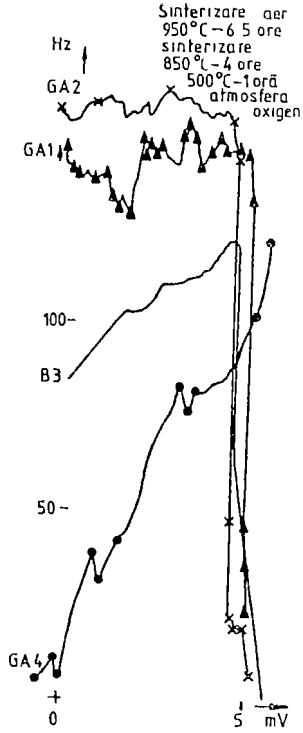


FIG 2a THE B<sub>3</sub>-SAMPLE BEHAVIOUF

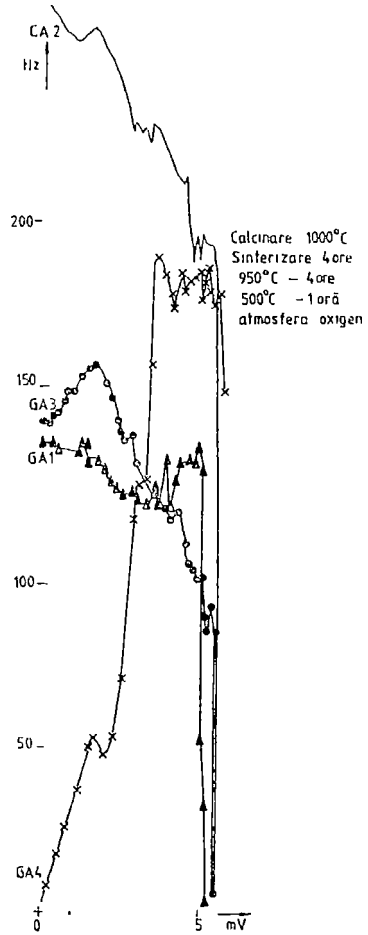


FIG 2c THE B<sub>3</sub>-SAMPLE BEHAVIOUR

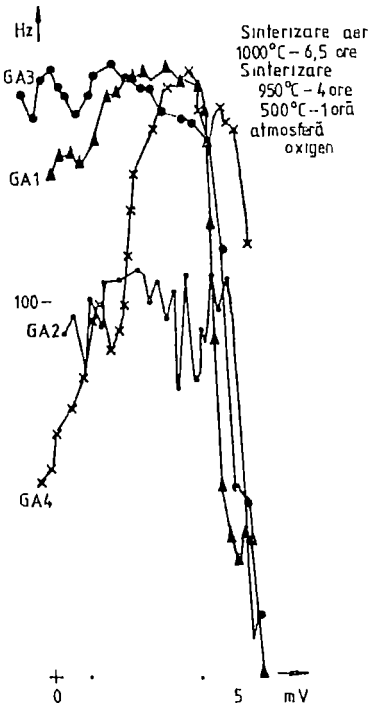


FIG 2b THE B<sub>3</sub>-SAMPLE BEHAVIOUR

The quartz oscillator works on a 10,69 MHz frequency and it has proved a good stability. In order to study the behaviour of the oscillator when the circuit is introduced in liquid nitrogen, it was compacted a capacitor without sample to which it had been attached the thermocouple and which proved a good frequency stability similarly to the sample sunk in liquid nitrogen.

**4. Conclusions.** The study of the  $Y Ba_2Cu_3O_{7-\delta}$  and  $Ga Ba_2Cu_3O_{7-\delta}$  samples by means of derivatograph did not emphasize relevant differences between the two samples, the significant values of the temperatures being close.

The samples have shown a significant transition near the liquid nitrogen temperature.

The  $Ga Ba_2Cu_3O_{7-\delta}$  sample shows a semiconductive behaviour, the increasing of the thermic treatment temperature leading to a superconductive behaviour as soon as the thermic treatment temperature is increasing. The sample behaviour is shown in fig. 2 by the Ga 4 curve.

## REFERENCES

1. D.Cahen, M.Schwartz, S.Reich, I.Felner, Characterization of  $Y, Ba_2(Ca, Ag)_2O_{7-\delta}$  Superconductors - Inorganic Chemistry Vol. 26, Nr.22(1987).
2. Yu Mei, S.M.Green, G.G.Reynolds, T.Wiczynski, H.L.Luo and C.Politis - Magnetic Properties of  $Gd, Ba_2Cu_3O_{7-\delta}$  in the Normal and Superconducting States, Z. Phys, B-Condensed Matter 67, 3033, 305(1987).
3. C.Jiang, Yu Mei, S.M.Green, H.L.Luo and C.Politis, Magnetic Proper of Superconducting  $Eu Ba_2Cu_3O_{7-\delta}$ , Z.Phys B-Condensed Matter 68, 15-18, (1987).
4. P Knoll, C.Thomsen, M.Cardova and P.Murugara, Temperature dependent lifetime of spin excitation in  $RE Ba_2Cu_3O_{7-\delta}$  ( $RE=Eu, Y$ ) Phys. Rev. B 42, 4842 (1990).
5. I.Pop, T.R.Redac, Gh.Borod1, S.Simon, Influența galiului asupra compusului ceramic  $Y, Ba_2Cu_3O_{7-\delta}$ , Sesiunea de comunicări științifice a Universității "Aurel Vlaicu" din Arad, mai 1992.
6. S.Simon, I.Barbur, I.Ardelean, R.Redac, Seminars on HIGH -  $T_c$  Superconductors, Cluj, 1989.
7. S.Simon, Gh.Ilonca, I.Barbur, I.Ardelean, R.Redac, EPR on Y - ceramics doped with a stata paramagnetic ions, International Conference MMSH , TS'S, Stanford(1989).





In cel de al XXXVII-lea an (1992) *Studia Universitatis Babeş-Bolyai* apare în următoarele serii:

matematică (trimestrial)  
fizică (semestrial)  
chimie (semestrial)  
geologie (semestrial)  
geografie (semestrial)  
biologie (semestrial)  
filosofie (semestrial)  
sociologie-politologie (semestrial)  
psihologie-pedagogie (semestrial)  
ştiinţe economice (semestrial)  
ştiinţe juridice (semestrial)  
istorie (semestrial)  
filologie (trimestrial)  
teologie ortodoxă (semestrial)

In the XXXVII-th year of its publications (1992) *Studia Universitatis Babeş-Bolyai* is issued in the following series:

mathematics (quarterly)  
physics (semesterily)  
chemistry (semesterily)  
geology (semesterily)  
geography (semesterily)  
biology (semesterily)  
philosophy (semesterily)  
sociology-politology (semesterily)  
psychology-pedagogy (semesterily)  
economic sciences (semesterily)  
juridical sciences (semesterily)  
history (semesterily)  
philology (quarterly)  
orthodox theology (semesterily)

Dans sa XXXVII-e année (1992) *Studia Universitatis Babeş-Bolyai* paraît dans les séries suivantes:

mathématiques (trimestriellement)  
physique (semestriellement)  
chimie (semestriellement)  
géologie (semestriellement)  
géographie (semestriellement)  
biologie (semestriellement)  
philosophie (semestriellement)  
sociologie-politologie (semestriellement)  
psychologie-pédagogie (semestriellement)  
sciences économiques (semestriellement)  
sciences juridiques (semestriellement)  
histoire (semestriellement)  
philologie (trimestriellement)  
théologie orthodoxe (semestriellement)